Differential Geometric Aspects of Discrete and Semi-discrete surfaces

安本，真士

(Degree)
博士（理学）

(Date of Degree)
2015-03-25

(Date of Publication)
2016-03-01

(Resource Type)
doctoral thesis

(Report Number)
甲第6319号

(URL)
https://hdl.handle.net/20.500.14094/D1006319

博　士　論　文

Differential Geometric Aspects of
Discrete and Semi-discrete surfaces
(離散曲面・半離散曲面の
微分幾何学的様相)

平成27年1月

神戸大学大学院理学研究科

安本　真士

Contents

Acknowledgements

I would like to express my deepest gratitude to my advisor Professor Wayne Rossman for his invitation to the fascinating world of differential geometry, for many discussions on my work, and for his encouragement. In particular, without his constant support, I would not have discovered the ideas here about singularities of discretized surfaces. I am equally grateful to Professors Udo Hertrich-Jeromin and Tim Hoffmann for numerous essential comments on discrete surfaces, and in particular about how to treat cross ratios on those surfaces properly. I also thank the postdoctoral fellows Christian Mueller and Erhan Güler for discussing the topics I treat in this thesis with me. I would like to express my appreciation to Professors Shoichi Fujimori, Yoshihiro Ohnita, Kentaro Saji, Yoshihiko Suyama, Masaaki Umehara, Kotaro Yamada and postdoctoral fellow Kosuke Naokawa for their many suggestions. Many thanks should go to my fellow graduate students Shotaro Konnai and Yuta Ogata for collaborating with me, and to the staff in the department of mathematics of Kobe University for providing me with a comfortable and pleasant environment for studying mathematics.

I was partly supported by the Grant-in-Aid for JSPS Fellows Number 26-3154 and JSPS/FWF bilateral joint project "Transformations and Singularities" between Austria and Japan. I am grateful for this support.

Overview of this thesis

This paper is concerned with smooth, discrete and semi-discrete surfaces with certain special curvature conditions. In particular, we will primarily focus on discretized surfaces with singularities given by Weierstrass-type representations. Smooth surfaces have been studied for many centuries, and in the last two decades or so, discrete surfaces have been carefully studied. Only in the most recent half a decade have semi-discrete surfaces been investigated, and they have the promise to be a bridge between the theories of smooth and discrete surfaces, helping us to recognize the similarities and differences between smooth and discrete surfaces.

In the smooth case, when we study surfaces, we do not necessarily need to focus on the aspect of integrable systems. For example, a surface is CMC if and only if its Gauss map is harmonic, which is an aspect coming rather from variational principals. This does not seem to have an immediate need for integrable systems techniques, and we have other choices for how to study CMC surfaces. In fact, Kenmotsu [**43**] gave a Weierstrass-type representation for CMC surfaces in Euclidean 3-space $\mathbb{R}^3$, Akutagawa, Nishikawa [**6**] gave a Weierstrass-type representation for CMC surfaces in Minkowski 3-space $\mathbb{R}^{2,1}$, and Aiyama, Akutagawa [**2**], [**3**], [**4**], [**5**] gave representation formulas for CMC surfaces in spherical 3-space $\mathbb{S}^3$, hyperbolic 3-space $\mathbb{H}^3$, de Sitter 3-space $\mathbb{S}^{2,1}$ and anti de Sitter 3-space $\mathbb{H}^{2,1}$ in terms of harmonicity of the Gauss maps.

However, in the realm of discrete differential geometry, it is hard to realize discretizations that still maintain all the properties that smooth surfaces have. In fact, two important ways to discretize surfaces are as follows: One way is to discrete surfaces based on only variational principles, and the second is to discretize based on only integrable systems techniques.

In the former approach, primarily discretizations of minimal and CMC surfaces in $\mathbb{R}^3$ have been investigated, because they have typical variational characterizations (in fact, they are critical for area amongst continuous piecewise linear variations). In this direction, Pinkall, Polthier [**59**] and Polthier, Rossman [**60**] studied discrete surfaces. Though this approach is interesting, as for other classes of surfaces, there are few typical variational characterizations like the ones minimal and CMC surfaces have.

On the other hand, in the latter approach, we can discretize so-called "integrable surfaces". In the realm of discrete surface theory based on integrable systems techniques, we can expect that, if smooth surfaces have some relations with the theory of integrable systems, we will be able to discretize them. In fact, in this direction, not only minimal and CMC surfaces but also constant negative Gaussian surfaces

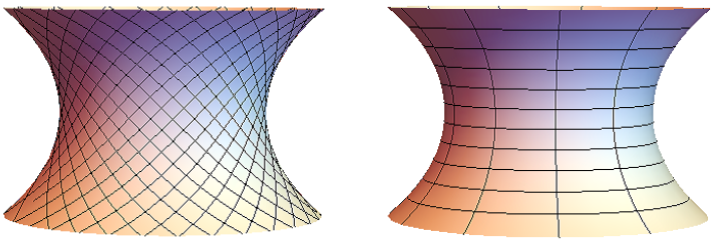

FIGURE 1. The same surface parametrized with different coordinate systems

were discretized. All of these discretizations are governed by some integrable equations, and the transformation theories of these surfaces are preserved. In order to derive such integrable equations, we have to choose special coordinates for each class of surfaces. For constant negative Gaussian curvature surfaces, we should consider Chebyshev nets, as summarized in Bobenko [**11**]. This has a less direct relation to the discretizations that we will consider, and we only mention that the discretization of constant negative Gaussian curvature surfaces was done by Bobenko, Pinkall [**12**].

There are two important points when we discretize surfaces based on integrable systems techniques, the first being which coordinate we choose, and the second being what the role of the transformations of surfaces is.

Like in Figure 1, even when we discretize the same surface, taking different coordinates gives us different results (the left picture in Figure 1 is a combination of rhombi, and the right picture in Figure 1 is a combination of isosceles trapezoids). So we need to pay attention to the special choice of coordinate when discretizing surfaces.

As isothermic surfaces have conformal curvature line coordinates, we can think of isothermic surfaces as being divided into infinitesimal squares. After dividing smooth surfaces into infinitesimal quadrilaterals, we can characterize smooth isothermic surfaces by use of quaternic cross ratios. Focusing on this point, Bobenko, Pinkall [**13**] discretized isothermic surfaces and minimal surfaces in $\mathbb{R}^3$, and investigated analytic descriptions of discrete isothermic surfaces, and their work became a turning point in the discretization of surfaces in terms of integrable systems techniques. Subsequently Bobenko, Pinkall [**14**] discretized CMC surfaces using Lax representations, and Hoffmann [**35**] described Weierstrass-type representations for them using a discretized version of a matrix factorizing method called the DPW method.

Bobenko, Suris [**18**] showed that discrete isothermic surfaces in $\mathbb{R}^3$ have metric functions, and showed that a discrete surface is discrete isothermic in the sense of [**13**] if and only if it is a circular Koenigs net, that is, it possesses a Christoffel dual, which is another characterization of discrete isothermic surfaces. Then Christoffel duals were defined using the metric functions for the discrete isothermic surfaces. Focusing on conformality of smooth isothermic surfaces, Mueller, Wallner [**54**] described semi-discrete isothermic surfaces in $\mathbb{R}^3$. In the realm of semi-discrete surface theory, we cannot consider cross ratios of semi-discrete surfaces directly, so

the characterization above (that isothermicity of discrete surfaces is equivalent to dualizability) is important. In fact, they showed that a semi-discrete surface is semi-discrete isothermic if and only if it possesses a Christoffel dual. Furthermore, they described semi-discrete minimal surfaces in $\mathbb{R}^3$. After that, the author and Rossman [**64**] gave a Weierstrass representation for semi-discrete minimal surfaces in $\mathbb{R}^3$, and Mueller [**52**] described semi-discrete CMC surfaces in $\mathbb{R}^3$. In both [**53**] and [**52**], the primary considerations were on theoretical aspects of semi-discrete surfaces, so there were few explicit examples of semi-discrete minimal or semi-discrete CMC surfaces included.

On the other hand, when we discretize surfaces based on integrable systems techniques, obviously we cannot use derivatives, so in order to discretize integrable surfaces, transformations theory becomes a very useful alternate tool. As already mentioned, transformations characterize minimal and CMC surfaces, and what is more, Weierstrass-type representations can be obtained from the transformation theory of the surfaces. For example, the Weierstrass representation for isothermic minimal surfaces can be obtained by considering when Christoffel transforms of isothermic surfaces lie in $\mathbb{S}^2$, and the Bryant representation for CMC 1 surfaces in $\mathbb{H}^3$ can be obtained by considering when Darboux transforms of isothermic surfaces are inscribed in the ideal boundary of $\mathbb{H}^3$. In both cases, permutability theorems of transformations play important roles. In all of this, instead of differentiating, we are characterizing some integrable surfaces using transformation theory.

Hertrich-Jeromin, Hoffmann, Pinkall [**34**] defined Darboux transformations for discrete isothermic surfaces. They defined CMC surfaces as the discrete isothermic surfaces for which Christoffel duals are also Darboux transforms. In [**34**], they showed permutability of Darboux transformations and between Christoffel and Darboux transformations, like as hold for smooth isothermic surfaces. They gave necessary and sufficient conditions for determining discrete CMC surfaces - as discrete isothermic surfaces with Christoffel duals being parallel surfaces of distance the inverse of their mean curvatures, which is the same geometric property as smooth isothermic CMC surfaces have. Hertrich-Jeromin [**33**] defined Calapso transforms of discrete isothermic surfaces and gave the Weierstrass-type representation for discrete CMC 1 surfaces in $\mathbb{H}^3$. Furthermore, Burstall, Hertrich-Jeromin, Rossmann, Santos [**23**] described discrete CMC surfaces in all 3-dimensional Riemannian space forms.

0.1. Weierstrass-type representations. It is well-known that any smooth minimal surface can be described using a pair consisting of a meromorphic function and a holomorphic 1-form, as follows:

THEOREM 0. Let $\mathbb{D}$ be a domain in the complex plane $\mathbb{C}$. Then any conformal immersion f from $\mathbb{D}$ to $\mathbb{R}^3$ with mean curvature identically 0 can be described by

$$f = \int (1 - g^2, i(1 + g^2), 2g)\omega, \tag{1}$$

where (g, ω) is a pair consisting of a meromorphic function g and a holomorphic 1-form ω.

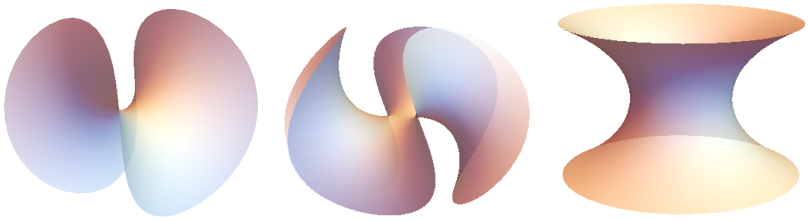

FIGURE 2. Classical isothermic minimal surfaces in $\mathbb{R}^3$

Equation (1) is called the Weierstrass representation for minimal surfaces in $\mathbb{R}^3$.

There are several other kinds of Weierstrass-type representations as well, for surfaces in Riemannian and Lorentzian space forms: For example, there is a representation formula for spacelike conformal immersions with mean curvature identically 0 in $\mathbb{R}^{2,1}$, and those surfaces are called maximal surfaces (Kobayashi [**47**]). For timelike conformal immersions with mean curvature identically 0, which are called timelike minimal surfaces, in $\mathbb{R}^{2,1}$, there is also a Weierstrass-type representation (Magid [**51**]). We have other such representations for conformal CMC 1 surfaces in $\mathbb{H}^3$ (Bryant [**16**]), for conformal spacelike CMC 1 surfaces in $\mathbb{S}^{2,1}$ (Aiyama, Akutagawa [**1**]), for intrinsically flat surfaces in $\mathbb{H}^3$ (Gálvez, Mártinez, Mìlan [**29**]), and for surfaces with other special curvature conditions in $\mathbb{H}^3$ and $\mathbb{S}^{2,1}$ (Gálvez, Mártinez, Mìlan [**28**], Aledo, Espinar [**7**]) as well. Weierstrass-type representations are useful for describing these surfaces and their elegant analytic behaviors.

0.2. Surfaces with singularities given by Weierstrass-type representations. Unlike the case of minimal surfaces, surfaces given by Weierstrass-type representations generally have singularities, making it is natural and interesting to investigate their singularities. Here we introduce some classes of surfaces with singularities given by Weierstrass-type representations.

Gálvez, Martínez, Milàn [**29**] described a Weierstrass-type representation for intrinsic flat surfaces in $\mathbb{H}^3$, and considered only immersed parts of the surfaces. After [**29**], a work by Kokubu, Rossman, Saji, Umehara, Yamada [**44**] gave criteria for a singular point on a front to be a cuspidal edge or a swallowtail. Applying these criteria, [**44**] gave necessary and sufficient conditions for a singular point on a flat front (surface) to be a cuspidal edge or a swallowtail, using the Weierstrass data, and Umehara, Yamada [**69**] expanded upon this. Furthermore, Fujimori, Saji, Umehara, Yamada [**27**] gave criteria for a singular point on a frontal to be a cuspidal cross-cap, and applying this criteria, they gave a necessary and sufficient condition for a singular point on a maxface in $\mathbb{R}^{2,1}$ and a CMC 1 face in $\mathbb{S}^{2,1}$ to be a cuspidal cross-cap, using the Weierstrass data.

In addition, Gálvez, Martínez, Milàn [**28**] described a Weierstrass-type representation for linear Weingarten surfaces with special curvature conditions, which are called linear Weingarten surfaces of Bryant type, and which will be discussed in Chapter 5 here. Applying criteria given in [**44**], we can recognize which singular points will appear on a linear Weingarten front of Bryant type in $\mathbb{H}^3$.

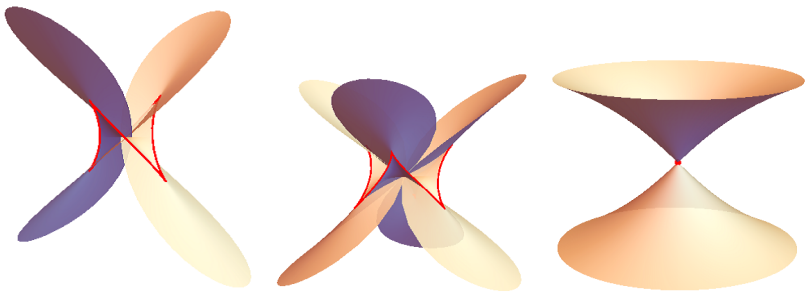

FIGURE 3. Isothermic maximal surfaces in $\mathbb{R}^{2,1}$. Unlike the case of minimal surfaces, maximal surfaces generally have singularities. The red curves and points in these figures are singular sets.

Linear Weingarten surfaces of Bryant type are linear Weingarten surfaces which lie in a deformation family between flat surfaces and CMC 1 surfaces and constant harmonic mean curvature 1 surfaces in $\mathbb{H}^3$. There are various ways to choose those deformations, but the essential point is that they all have Weierstrass-type representations. Thus we have a unified description for flat surfaces, CMC 1 surfaces and constant harmonic mean curvature 1 surfaces. Furthermore, their normal vector fields (normal surfaces, for short) are also linear Weingarten surfaces with special curvature conditions in $\mathbb{S}^{2,1}$, which are then called linear Weingarten surfaces of Bianchi type. Izumiya, Saji [**41**] showed that a surface in $\mathbb{S}^{2,1}$ is a linear Weingarten surface of Bianchi type if and only if its normal surface in $\mathbb{H}^3$ is a linear Weingarten surface of Bryant type. Thus we can investigate linear Weingarten surfaces of both Bryant and Bianchi type simultaneously.

We should remark that Aledo, Espinar [**7**] described a Weierstrass-type representation for linear Weingarten surfaces of Bianchi type. Like linear Weingarten surfaces of Bryant type in $\mathbb{H}^3$, they lie in a deformation family between flat surfaces, CMC 1 surfaces and constant harmonic mean curvature 1 surfaces in $\mathbb{S}^{2,1}$.

0.3. Isothermic surfaces. In the classical differential geometry of surfaces, surfaces with conformal curvature line coordinates, which are called isothermic surfaces, have been studied. Isothermic surfaces include many important classes of surfaces. For example, quadrics, minimal surfaces, constant mean curvature (CMC, for short) surfaces lie in the class of isothermic surfaces. We will consider only isothermic minimal and CMC surfaces. Here we assume that the coordinates are isothermic, and then we can derive certain integrable equations for minimal and CMC surfaces. So it is natural to think about how integrable systems techniques can be applied to these surfaces. In fact, isothermic surfaces admit various transformations, such as Christoffel, Baecklund, Darboux and Calapso transformations.

Here we introduce several contributions of transformation theory for isothermic surfaces: Christoffel transforms of smooth isothermic minimal surfaces in $\mathbb{R}^3$ are their own Gauss maps, Christoffel transforms of smooth CMC surfaces in $\mathbb{R}^3$ are parallel surfaces of constant distance equal to the inverse of the mean curvature.

Baecklund transforms of smooth CMC surfaces in $\mathbb{R}^3$ become different CMC surfaces in $\mathbb{R}^3$ and are special cases of Darboux transforms. Calapso transforms of CMC surfaces in $\mathbb{R}^3$ become CMC surfaces in $\mathbb{H}^3$, and in particular, the Calapso transformation for smooth CMC surfaces in $\mathbb{R}^3$ is the Lawson correspondence. When proving these properties, "permutability theorems" of various transformations are the most essential tools to describe isothermic surfaces in space forms. Transformation theory plays an important role in the discretization of surfaces.

0.4. Singularities of discrete and semi-discrete surfaces. Hoffmann, Rossman, Sasaki, Yoshida [**38**] described discrete flat surfaces and discrete linear Weingarten surfaces of Bryant type using Weierstrass-type representations. Because smooth counterparts generally have singularities, we can expect that, in the discrete case, they have also have certain singularities. [**38**] defined (implicitly) certain singularities of discrete flat surfaces in $\mathbb{H}^3$ using discrete caustics. We call singularities of flat surfaces the singular vertices. This comes from an idea based on the good geometric properties which singularities of smooth flat surfaces have. However, singularities of discrete linear Weingarten surfaces of Bryant type were not defined, and also singularities of general discrete surfaces had not yet been considered, previous to this thesis.

Independently of [**38**], this author [**70**] described discrete maximal surfaces in $\mathbb{R}^{2,1}$, which will again be introduced in Section 2. In [**70**], we also described singularities of discrete maximal surfaces called singular faces. In the smooth case, when singularities of smooth maximal surfaces appear, tangent planes at the images of singular points are not spacelike. With awareness of this, we defined singular faces of discrete maximal surfaces. It is a natural definition not only in the geometric sense, but also in the complex analytic sense, because we can recognize where singular faces appear by only focusing on the position of faces in $\mathbb{C}$ given by the holomorphic Gauss maps. In addition, with the same approach, the author [**71**] described semi-discrete maximal surfaces with certain singularities in $\mathbb{R}^{2,1}$, which will be introduced here again in Chapter 3. However, in [**70**] and [**71**], the singularities of general discretized surfaces still had not yet been defined.

Because we cannot take derivatives in the realm of discrete differential geometry, describing singularities of general discrete surfaces becomes less direct. But for several classes of smooth surfaces with Weierstrass-type representations, we can recognize where singularities appear by focusing on the behavior of the principal curvatures. When singularities appear, typically one of the principal curvatures blows up and the other one is finite. (We should remark that, when we focus on only cuspidal edges, Teramoto [**66**] showed that this fact holds for general surfaces with cuspidal edges of type 3/2 in $\mathbb{R}^3$.) Casting a spotlight on this fact, the author and Rossman [**63**] gave a tentative definition of singularities of general discrete surfaces. In particular, we investigated the singular vertices and singular faces, and the interrelation between them.

0.5. Contents of this thesis. Let us briefly introduce the topics that are treated in this paper: In Chapter 1, we give a Weierstrass type representation for

semi-discrete minimal surfaces in $\mathbb{R}^3$. We then give explicit parametrizations of various smooth, semi-discrete and fully-discrete catenoids, determined from either variational or integrable systems principles. Finally, we state the shared properties that those various catenoids have. In Chapter 2, we describe discrete maximal surfaces with singularities in $\mathbb{R}^{2,1}$ and give a Weierstrass type representation for them. As already mentioned, in the smooth case, maximal surfaces in $\mathbb{R}^{2,1}$ generally have certain singularities. We give a criterion that naturally describes the "singular set" for discrete maximal surfaces, including a classification of the various types of singularities that are possible in the discrete case. In Chapter 3, we investigate semi-discrete maximal surfaces with singularities. In this chapter, we describe semi-discrete maximal surfaces with singularities in $\mathbb{R}^3$ and give a Weierstrass type representation for them determined from integrable system principles. We also give a criterion that naturally describes the "singular set" for these semi-discrete surfaces. Finally, we compare smooth, discrete and semi-discrete maximal surfaces of revolution. In Chapter 4, we give explicit parametrizations for Bour type surfaces in various 3-dimensional space forms, using Weierstrass-type representations. We also determine classes and degrees of some Bour type zero mean curvature surfaces in $\mathbb{R}^{2,1}$. In Chapter 5, we outline some preliminary recent work by the author on singularities of linear Weingarten surfaces with Weierstrass-type representations in Riemannian and Lorentzian space forms. We define singularities of general discrete Legendre immersions, and in particular, we analyze singularities of discrete linear Weingarten surfaces of Bryant type in $\mathbb{H}^3$ and discrete linear Weingarten surfaces of Bianchi type in $\mathbb{S}^{2,1}$. Finally in Appendix A, we introduce the discrete DPW method for discrete CMC surfaces in any Riemannian space form. Hoffmann had already presented a matrix factorizing method for discrete CMC surfaces in $\mathbb{R}^3$. Our result is an extension of this.

CHAPTER 1

Weierstrass representation for semi-discrete minimal surfaces, and comparison of various discretized catenoids

1. Introduction

The well known minimal surface of revolution in $\mathbb{R}^3 = \{(x_1, x_2, x_3)^t \mid x_j \in \mathbb{R}\}$ called the catenoid, which we refer to as the *smooth catenoid* here and which can be parametrized by

$$x(u,v) = \begin{pmatrix} \cosh u \cos v \\ \cosh u \sin v \\ u \end{pmatrix}, \ v \in [0, 2\pi), \ u \in \mathbb{R}, \tag{2}$$

has a number of discretized versions. A fully discretized version can be found in [**60**] by Polthier and the first author, which is defined using a variational approach, that is, those surfaces are triangulated meshes that are critical for area with respect to smooth variations of the vertex set. A different approach for defining fully discrete catenoids, using quadrilateral faces and based on integrable systems methods, was found by Bobenko and Pinkall [**13**], [**14**]. Both approaches apply to much wider classes of surfaces.

One can also consider semi-discrete catenoids, that is, catenoids that are discretized in only one of the two parameter directions corresponding to u and v in (2). There are now four choices for how to proceed with this, by choosing either the u direction or v direction to discretize, and by choosing to use either variational principles or integrable systems principles to determine the discretizations. Again, these approaches apply to much wider classes of surfaces.

Here we compare these various smooth, semi-discrete and fully-discrete catenoids to see in what ways they do or do not coincide. For the smooth and fully-discrete catenoids, the parametrizations have already been determined, making comparisons between them elementary. However, for some of the semi-discrete cases, we will need to first establish those parametrizations here. In particular, we will provide a Weierstrass representation for determining semi-discrete minimal surfaces as defined by Mueller and Wallner [**54**], [**72**]. Construction of the semi-discrete catenoids in particular, via an integrable systems approach, can be done either with this Weierstrass representation, or without it (instead using the results by Mueller and Wallner). However, the usefulness of the Weierstrass representation comes when one wishes to consider the full class of semi-discrete minimal surfaces based on an integrable systems approach, as this representation gives a classification of such surfaces in terms of semi-discrete holomorphic functions. This Weierstrass representation can be regarded as a restatement of the definition of such surfaces (Definition 4), but in

	associated authors
smooth catenoid	(classically known surface)
$BP^{in}_{pd,rd}$-catenoid	Bobenko and Pinkall
$PR^{va}_{pd,rd}$-catenoid	Polthier and Rossman
$M^{va}_{pd,rs}$-catenoid	Machigashira
$MW^{in}_{pd,rs}$-catenoid	Mueller and Wallner
$MW^{in}_{ps,rd}$-catenoid	Mueller and Wallner
$M^{va}_{ps,rd}$-catenoid	(Machigashira analogue)

TABLE 1. Names of seven types of catenoids

a more explicit form that tells us how the surface is constructed from the given dual surface inscribed in a sphere.

Once we have established this representation for semi-discrete minimal surfaces (Theorem 2), we compare the various types of catenoids (Theorem 1).

To make semi-discrete catenoids based on variational principles, Machigashira [**50**] chose to discretize them in the u direction. He then classified these surfaces and studied their stability properties. The surfaces obtained by Machigashira will be seen (Proposition 2) to be limiting cases of the discrete catenoids found in [**60**].

From the point of view of architectural structures in the shape of a semi-discrete catenoid, Machigashira's catenoids would involve producing circular-shaped flat pieces that cannot be so efficiently made as cut-outs from planar sheets, since there would be a large amount of waste material. So from the architectural point of view, a more efficient use of materials would be to discretize in the v direction instead. Such semi-discrete catenoids are considered here as well.

To distinguish between various catenoids, we write the superscript va (resp. in) when the catenoid is constructed by a variational (resp. integrable systems) approach, and write the subscript pd (resp. ps) when the catenoid has a discrete profile curve (resp. smooth profile curve) and the subscript rd (resp. rs) when the catenoid is discrete (resp. smooth) in the rotational direction. Thus, in total, we consider the seven types of catenoids in Table 1.

For catenoids with discrete profile curves, we will assume them to have a "neck vertex". In other words, we assume there exists a plane of reflective symmetry of the catenoids that is perpendicular to the axis of rotation symmetry and also contains one vertex of each profile curve. We note that there do exist discrete catenoids that do not have this neck-vertex symmetry.

THEOREM 1. After appropriate normalizations, we have the following:

(1) $PR^{va}_{pd,rd}$-catenoid profile curves and $M^{va}_{pd,rs}$-catenoid profile curves are never the same, but $PR^{va}_{pd,rd}$-catenoid profile curves converge to $M^{va}_{pd,rs}$-catenoid profile curves as the angle of rotation symmetry approaches 0.
(2) $BP^{in}_{pd,rd}$-catenoids and $MW^{in}_{pd,rs}$-catenoids have the same profile curves.

(3) $BP^{in}_{pd,rd}$-catenoid ($MW^{in}_{pd,rs}$-catenoid) profile curves and $PR^{va}_{pd,rd}$-catenoid profile curves are never the same, and $BP^{in}_{pd,rd}$-catenoid ($MW^{in}_{pd,rs}$-catenoid) profile curves and $M^{va}_{pd,rs}$-catenoid profile curves are never the same.
(4) The smooth catenoid and $MW^{in}_{ps,rd}$-catenoid have the same profile curve.
(5) $M^{va}_{ps,rd}$-catenoid profile curves and the smooth catenoid's profile curve are never the same. $M^{va}_{ps,rd}$-catenoid profile curves converge to the smooth catenoid ($MW^{in}_{ps,rd}$-catenoid) profile curve as the angle of rotation symmetry approaches 0.
(6) For all types of catenoids, the profile curves have vertices lying on affinely scaled graphs of the hyperbolic cosine function.

2. Notation for semi-discrete surfaces

To consider semi-discrete minimal surfaces from an integrable systems approach, we set some notations in this section.

Let $x = x(k,t)$ be a map from a domain in $\mathbb{Z}\times\mathbb{R}$ to $\mathbb{R}^3$ ($k\in\mathbb{Z}$, $t\in\mathbb{R}$). We call x a *semi-discrete surface*. Set

$$\partial x = \frac{\partial x}{\partial t},\ \Delta x = x_1 - x,\ \partial\Delta x = \partial x_1 - \partial x,$$

where $x_1 = x(k+1,t)$. The following definitions can be found in [**54**], and are all naturally motivated by geometric properties found in previous works, such as [**13**], [**14**], [**15**], [**33**], [**34**], [**35**], [**53**], [**54**], [**72**].

Definition 1. Let x be a semi-discrete surface.

- x is a *semi-discrete conjugate net* if ∂x, Δx and $\partial\Delta x$ are linearly dependent.
- x is a *semi-discrete circular net* if there exists a circle $\mathscr{C}$ passing through x and x_1 that is tangent to ∂x, ∂x_1 there (for all k, t).

Remark. If x lies in $\mathbb{R}^2\cong\mathbb{C}$, circularity is equivalent to the following condition: there exists a non-zero-valued function s such that

$$\Delta x = \mathrm{i}s\left(\frac{\partial x}{\|\partial x\|} + \frac{\partial x_1}{\|\partial x_1\|}\right), \tag{3}$$

which follows from

$$\Delta x = \mathrm{i}s\frac{\partial x}{\|\partial x\|} - \left(-\mathrm{i}s\frac{\partial x_1}{\|\partial x_1\|}\right)$$

for some $s\in\mathbb{R}$, in the setting shown in Figure 1.

□

Definition 2. Suppose x, x^* are semi-discrete conjugate surfaces. Then x and x^* are *dual* to each other if there exists a function $\nu:\mathbb{Z}\times\mathbb{R}\to\mathbb{R}^+$ so that

$$\partial x^* = -\frac{1}{\nu^2}\partial x,\ \Delta x^* = \frac{1}{\nu\nu_1}\Delta x.$$

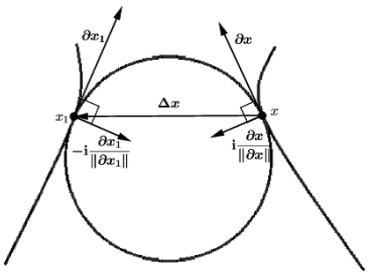

FIGURE 1. Sketch of the proof of Remark 3

DEFINITION 3. A semi-discrete circular surface x is *isothermic* if there exist positive functions $\nu,\ \sigma,\ \tau$ such that

$$\|\Delta x\|^2 = \sigma\nu\nu_1,\ \|\partial x\|^2 = \tau\nu^2,\ \text{with } \partial\sigma = \Delta\tau = 0.$$

Remark. For circular semi-discrete surfaces, dualizability and isothermicity are equivalent, by Theorem 11 in [**54**]. In particular, the ν, ν_1 in Definitions 2 and 3 are the same. □

DEFINITION 4. A semi-discrete isothermic surface x is *minimal* if its dual x^* is inscribed in a sphere.

3. Semi-discrete catenoids with discrete profile curve

Take the following parametrization for $MW^{in}_{pd,rs}$-catenoids:

$$x(k,t) = \begin{pmatrix} f(k)\cos t \\ f(k)\sin t \\ h\cdot k \end{pmatrix}$$

where $f = f(k)$ and h are positive. Then, with $f_1 = f(k+1)$,

$$\|\Delta x\|^2 = (f_1 - f)^2 + h^2,$$
$$\|\partial x\|^2 = f^2.$$

One can check that x is isothermic by taking

$$\nu = f,\quad \tau = 1\ \text{ and }\ \sigma = \frac{(\Delta f)^2 + h^2}{f\cdot f_1}.$$

We compute x^* by solving

$$x^* = -\frac{1}{\nu^2}\int \partial x dt = -\frac{1}{f}\begin{pmatrix}\cos t\\ \sin t\\ 0\end{pmatrix} + \overrightarrow{c}_k,$$

where $\overrightarrow{c}_k$ depends on k but not t. We now have

$$\Delta x^* = \frac{1}{f\cdot f_1}\begin{pmatrix}\Delta f\cdot\cos t\\ \Delta f\cdot\sin t\\ 0\end{pmatrix} + \overrightarrow{c}_{k+1} - \overrightarrow{c}_k.$$

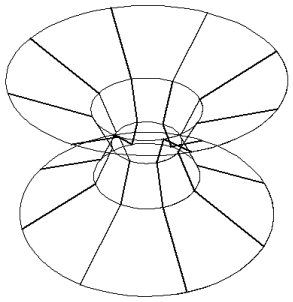

FIGURE 2. a semi-discrete $MW^{in}_{pd,rs}$-catenoid with discretized profile curve

Therefore, x^* is dual to x if

$$\overrightarrow{c}_{k+1} - \overrightarrow{c}_k = \frac{h}{f \cdot f_1} \begin{pmatrix} 0 \\ 0 \\ 1 \end{pmatrix}.$$

Without loss of generality, we can take $\overrightarrow{c}_k$ as $(0, 0, c(k))^t$ with

$$c(k+1) = c(k) + \frac{h}{f(k)f(k+1)}. \tag{4}$$

For x to be minimal, we wish to have

$$\|x^*\| \equiv \text{constant}$$

for some choice of $c(0)$. Substituting Equation (4) into the equation $\|x_1^*\| = \|x^*\|$, we obtain

$$f(k+1) = hc(k)f(k) + \sqrt{(hc(k)f(k))^2 + f(k)^2 + h^2}. \tag{5}$$

Then we can recursively solve the system of difference equations (4)-(5).

In order to compare the other catenoids with $MW^{in}_{pd,rs}$-catenoids, we wish to reduce the above system of difference equations to one equation.

LEMMA 1. We have

$$f(k+2) = \frac{f(k+1)^2 + h^2}{f(k)}. \tag{6}$$

Proof. By Equation (5),

$$c(k) = \frac{f(k+1)^2 - f(k)^2 - h^2}{2hf(k)f(k+1)}. \tag{7}$$

Inserting (7) into (4), we have

$$(f(k+2) + f(k))(f(k+2)f(k) - f(k+1)^2 - h^2) = 0,$$

which implies (6). □

Lemma 1 implies

$$f(1)f(-1) = f(0)^2 + h^2,$$

and then neck-vertex symmetry (in particular, $f(1) = f(-1)$) gives

$$f(1)^2 = f(0)^2 + h^2.$$

Then Equation (7) implies $c(0) = 0$. Without loss of generality, we can take $f(0) = 1$, and then the solution to Equation (6) is

$$f(k) = \cosh(\operatorname{arcsinh}(h) \cdot k).$$

4. Semi-discrete catenoids foliated by discrete circles

Take the following parametrization for $MW^{in}_{ps,rd}$-catenoids:

$$x(k,t) = \begin{pmatrix} f(t)\cos\alpha k \\ f(t)\sin\alpha k \\ t \end{pmatrix},$$

where $f(t)$ and α are positive. We assume

$$f(0) = 1 \text{ and } f'(0) = 0. \tag{8}$$

Then

$$\|\Delta x\|^2 = 4f(t)^2\sin^2\frac{\alpha}{2},$$

$$\|\partial x\|^2 = (f'(t))^2 + 1.$$

One can confirm that x is isothermic by taking

$$\nu = f(t), \quad \tau = \frac{(f'(t))^2 + 1}{(f(t))^2} \quad \text{and} \quad \sigma = 4\sin^2\frac{\alpha}{2}.$$

Now,

$$x^* = -\int \frac{1}{\nu^2}\partial x dt = \begin{pmatrix} -\cos\alpha k \int \frac{f'}{f^2}dt \\ -\sin\alpha k \int \frac{f'}{f^2}dt \\ -\int \frac{1}{f^2}dt \end{pmatrix}$$

$$= \begin{pmatrix} \frac{\cos\alpha k}{f} \\ \frac{\sin\alpha k}{f} \\ \ell(t) \end{pmatrix} + \overrightarrow{c}_k, \tag{9}$$

where $\overrightarrow{c}_k$ depends on k but not t, and $\ell(t) = -\int_0^t f(t)^{-2}dt$ depends on t but not k. We compute that

$$\Delta x^* = \frac{1}{f}\begin{pmatrix} \Delta\cos\alpha k \\ \Delta\sin\alpha k \\ 0 \end{pmatrix} + \overrightarrow{c}_{k+1} - \overrightarrow{c}_k.$$

Therefore, x^* is dual to x if $\overrightarrow{c}_k$ is a constant vector. For x to be minimal, x^* must be inscribed in a sphere and therefore we can choose $\overrightarrow{c}_0 = (0, 0, c_0)^t$ so that $\|x^*\|$ is constant. From (9) we have

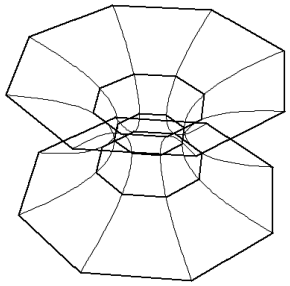

FIGURE 3. a semi-discrete $MW^{in}_{ps,rd}$-catenoid discretized in the direction of rotation

$$\frac{1}{f^2} + \left(\int_0^t \frac{1}{(f(t))^2} dt - c_0 \right)^2 = \text{constant}.$$

Differentiation gives that

$$\int_0^t \frac{1}{(f(t))^2} dt = \frac{f'}{f} + c_0$$

and

$$f'' f - (f')^2 = 1.$$

We find from (8) that

$$f(t) = \cosh t.$$

Thus semi-discrete catenoids with smooth profile curves and fixed α are unique up to homotheties. The picture in Figure 3 is such a semi-discrete catenoid. In fact, we have proven:

PROPOSITION 1. The profile curve of $MW^{in}_{ps,rd}$-catenoids is independent of choice of α.

5. Weierstrass representation for semi-discrete minimal surfaces

We now give a Weierstrass representation for semi-discrete minimal surfaces. First we define semi-discrete holomorphic functions.

DEFINITION 5. A semi-discrete isothermic surface g is a *semi-discrete holomorphic function* if the image of g lies in a plane.

Remark. Semi-discrete holomorphic maps have the following property: With σ and τ as in Definition 3 (with x replaced by g),

$$\frac{\|\Delta g\|^2}{\|g'\| \, \|g'_1\|} = \frac{\sigma}{\tau}, \tag{10}$$

where $g' = \partial g$. So we can think of τ and σ in the semi-discrete case as an analogy to the (absolute values of the) cross-ratio factorizing functions in the fully discrete case, see [**13**], [**14**], [**33**], [**34**], [**35**], [**61**]. □

We introduce the following recipe for constructing semi-discrete minimal surfaces.

THEOREM 2 (Weierstrass representation). Let g be a semi-discrete holomorphic function with data τ, σ, and ν as in Definition 3. Then we can construct a semi-discrete minimal surface by solving

$$\begin{aligned} \partial x &= -\frac{\tau}{2}\mathrm{Re}\left(\frac{1}{g'}\begin{pmatrix} 1-g^2 \\ \mathrm{i}(1+g^2) \\ 2g \end{pmatrix}\right), \\ \Delta x &= \frac{\sigma}{2}\mathrm{Re}\left(\frac{1}{\Delta g}\begin{pmatrix} 1-gg_1 \\ \mathrm{i}(1+gg_1) \\ g+g_1 \end{pmatrix}\right). \end{aligned} \tag{11}$$

Conversely, any semi-discrete minimal surface is described in this way by some semi-discrete holomorphic function g.

Proof. We start proving the first half of Theorem 2. Let g be a semi-discrete holomorphic function such that $|\Delta g|^2 = \sigma\nu\nu_1$, $|g'| = \tau\nu^2$ for some positive functions ν, σ, τ. Then

$$x^* := \frac{1}{1+\|g\|^2}\begin{pmatrix} 2g \\ -1+\|g\|^2 \end{pmatrix} \in \mathbb{S}^2 \subset \mathbb{C}\times\mathbb{R} = \mathbb{R}^3$$

is semi-discrete isothermic, because x^* is the image of g under the inverse of stereographic projection. Then

$$\begin{aligned} \partial x^* &= \frac{2}{(1+\|g\|^2)^2}\begin{pmatrix} g' - \overline{g'}g^2 \\ g'\bar{g} + \overline{g'}g \end{pmatrix}, \\ \Delta x^* &= \frac{2}{(1+\|g\|^2)(1+\|g_1\|^2)}\begin{pmatrix} \Delta g - \overline{\Delta g}gg_1 \\ \Delta g\bar{g}_1 + \overline{\Delta g}g \end{pmatrix}. \end{aligned}$$

It follows that

$$\begin{aligned} \|\partial x^*\|^2 &= \frac{4\|g'\|^2}{(1+\|g\|^2)^2} = \frac{4\tau\nu^2}{(1+\|g\|^2)^2}, \\ \|\Delta x^*\|^2 &= \frac{4\|\Delta g\|^2}{(1+\|g\|^2)(1+\|g_1\|^2)} = \frac{4\sigma\nu\nu_1}{(1+\|g\|^2)(1+\|g_1\|^2)}, \end{aligned}$$

so we can take the data τ^*, σ^*, ν^* for the isothermic surface x^* to be

$$\tau^* = \tau,\ \sigma^* = \sigma,\ \nu^* = \frac{2\nu}{1+\|g\|^2}.$$

Here σ^* depends only on k, and τ^* depends only on t. Then

$$\frac{-1}{(\nu^*)^2}\partial x^* = \frac{-1}{2\nu^2}\begin{pmatrix} g' - \bar{g}'g^2 \\ g'\bar{g} + \bar{g}'g \end{pmatrix} = \frac{-\tau}{2\|g'\|^2}\begin{pmatrix} g' - \bar{g}'g^2 \\ g'\bar{g} + \bar{g}'g \end{pmatrix}$$

$$= -\frac{\tau}{2}\begin{pmatrix} \mathrm{Re}\left(\frac{1-g^2}{g'}\right) + \mathrm{iRe}\left(\frac{\mathrm{i}(1+g^2)}{g'}\right) \\ \mathrm{Re}\left(\frac{2g}{g'}\right) \end{pmatrix} = \partial x,$$

where we have identified $\mathbb{C}\times\mathbb{R}$ and $\mathbb{R}^3$ in the final equality. Similarly,

$$\frac{1}{\nu^*\nu_1^*}\Delta x^* = \frac{\sigma}{2\|\Delta g\|^2}\begin{pmatrix} \Delta g - g g_1 \overline{\Delta g} \\ \overline{g_1}\Delta g + g\overline{\Delta g} \end{pmatrix}$$

$$= \frac{\sigma}{2}\begin{pmatrix} \mathrm{Re}\left(\frac{1-gg_1}{\Delta g}\right) + \mathrm{iRe}\left(\frac{\mathrm{i}(1+gg_1)}{\Delta g}\right) \\ \mathrm{Re}\left(\frac{g+g_1}{\Delta g}\right) \end{pmatrix} = \Delta x.$$

Thus if x solving (11) exists, x and x^* are dual to each other. A direct computation shows

$$\|\Delta x\|^2 = \sigma\left(\frac{1+\|g\|^2}{2\nu}\right)\left(\frac{1+\|g_1\|^2}{2\nu_1}\right),$$

$$\|\partial x\|^2 = \tau\left(\frac{1+\|g\|^2}{2\nu}\right)^2,$$

so x will be isothermic if it is circular. Since x^* is inscribed in a sphere, x must then be a semi-discrete minimal surface. Thus it remains to check existence and circularity of x.

To show existence of x, we need to show compatibility of the two equations in (11), and this amounts to showing that the two operators Δ and ∂ in (11) commute, that is,

$$\partial\left(\frac{\sigma}{2}\mathrm{Re}\begin{pmatrix} \frac{1-gg_1}{\Delta g} \\ \frac{\mathrm{i}(1+gg_1)}{\Delta g} \\ \frac{g+g_1}{\Delta g} \end{pmatrix}\right) = \Delta\left(-\frac{\tau}{2}\mathrm{Re}\begin{pmatrix} \frac{1-g^2}{g'} \\ \frac{\mathrm{i}(1+g^2)}{g'} \\ \frac{2g}{g'} \end{pmatrix}\right). \tag{12}$$

One can compute

$$\begin{aligned}
& \text{Left-hand side of (12)} \\
= \ & \frac{\sigma}{2}\mathrm{Re}\left(\frac{1}{(\Delta g)^2}\begin{pmatrix} g^2g' - g_1' - g'g_1^2 + g' \\ \mathrm{i}(g'g_1^2 + g' - g^2g_1' - g_1') \\ 2g'g_1 - 2gg_1' \end{pmatrix}\right) \\
= \ & \frac{\tau\|\Delta g\|^2}{2\|g'\|\|g_1'\|}\mathrm{Re}\left(\frac{1}{(\Delta g)^2}\begin{pmatrix} g^2g' - g_1' - g'g_1^2 + g' \\ \mathrm{i}(g'g_1^2 + g' - g^2g_1' - g_1') \\ 2g'g_1 - 2gg_1' \end{pmatrix}\right) \\
= \ & \frac{\tau}{2}\mathrm{Re}\left(\frac{\overline{\Delta g}}{\|g'\|\|g_1'\|\Delta g}\begin{pmatrix} g^2g' - g_1' - g'g_1^2 + g' \\ \mathrm{i}(g'g_1^2 + g' - g^2g_1' - g_1') \\ 2g'g_1 - 2gg_1' \end{pmatrix}\right) \\
= \ & -\frac{\tau}{2}\mathrm{Re}\left(\frac{1}{g'g_1'}\begin{pmatrix} g^2g' - g_1' - g'g_1^2 + g' \\ \mathrm{i}(g'g_1^2 + g' - g^2g_1' - g_1') \\ 2g'g_1 - 2gg_1' \end{pmatrix}\right). \\
= \ & \text{Right-hand side of (12).}
\end{aligned}$$

The last task is to check that x is circular. By a rotation and translation, we can assume that $\mathrm{span}\{\partial x, \partial x_1, \Delta x\} = \mathbb{C}\times\{0\}$ for one edge $\overline{xx_1}$. We fix $(k,t) = (k_0, t_0)$ arbitrarily, and write $x(k_0, t_0)$ simply as x. It suffices to show the existence of $s \in \mathbb{R}$ such that (3) holds. Now,

$$\frac{g}{g'},\ \frac{g_1}{g_1'},\ \frac{g+g_1}{\Delta g} \in \mathrm{i}\mathbb{R}.$$

Expressing g as $g = re^{\mathrm{i}\theta}$ in polar form, we have

$$r' = r_1' = 0,\ r_1e^{\mathrm{i}\theta_1} + re^{\mathrm{i}\theta} = \mathrm{i}\rho(r_1e^{\mathrm{i}\theta_1} - re^{\mathrm{i}\theta})$$

for some $\rho \in \mathbb{R}$. Taking the absolute value of

$$r_1(\mathrm{i}\rho - 1)e^{\mathrm{i}\theta_1} = r(\mathrm{i}\rho + 1)e^{\mathrm{i}\theta},$$

we find that $r = r_1$. The left and right hand sides of Equation (3) are real scalar multiples of

$$\begin{aligned}
\Delta g - gg_1\overline{\Delta g} &= r(1+r^2)(e^{\mathrm{i}\theta_1} - e^{\mathrm{i}\theta})\ , \\
\mathrm{i}\left(\frac{g' - \overline{g'}g^2}{|g' - \overline{g'}g^2|} + \frac{g_1' - \overline{g_1'}g_1^2}{|g_1' - \overline{g_1'}g_1^2|}\right) & \\
= \mathrm{i}\left(\frac{\mathrm{i}\theta' r(1+r^2)e^{\mathrm{i}\theta}}{|\mathrm{i}\theta' r(1+r^2)e^{\mathrm{i}\theta}|} + \frac{\mathrm{i}\theta_1' r_1(1+r_1^2)e^{\mathrm{i}\theta_1}}{|\mathrm{i}\theta_1' r_1(1+r_1^2)e^{\mathrm{i}\theta_1}|}\right) & \\
= \pm(e^{\mathrm{i}\theta} - e^{\mathrm{i}\theta_1}), &
\end{aligned}$$

respectively, where we used the following lemma in the final equality above. This lemma follows from Lemma 6 and Theorem 11 in [**54**], because g is isothermic.

Lemma 2. We have the following property:

$$\theta' \cdot \theta_1' < 0.$$

Therefore, we have

$$\arg\left(\Delta g - g g_1 \overline{\Delta g}\right) = \arg\left(\pm \mathrm{i}\left(\frac{g' - \overline{g'} g^2}{|g' - \overline{g'} g^2|} + \frac{g_1' - \overline{g_1'} g_1^2}{|g_1' - \overline{g_1'} g_1^2|}\right)\right),$$

which implies (3). Now we prove the final sentence of Theorem 2. Let x be a semi-discrete minimal surface and ψ be stereographic projection $\psi : \mathbb{S}^2 \to \mathbb{C}$. Then by definition, there exists a dual x^* that is semi-discrete isothermic and inscribed in $\mathbb{S}^2$. Take

$$g := \psi \circ x^*,$$

then g is a semi-discrete holomorphic function (see Example 1 of [**54**]). Setting

$$x^* = (X_1, X_2, X_3)^t,\ x_1^* = (X_{1,1}, X_{2,1}, X_{3,1})^t,$$

we have

$$g = \frac{X_1 + \mathrm{i}X_2}{1 - X_3},\ X_1^2 + X_2^2 + X_3^2 = X_{1,1}^2 + X_{2,1}^2 + X_{3,1}^2 = 1,$$
$$(X_1')^2 + (X_2')^2 + (X_3')^2 = \frac{\tau}{\nu^2},$$
$$1 - (X_1 X_{1,1} + X_2 X_{2,1} + X_3 X_{3,1}) = \frac{\sigma}{2\nu\nu_1}.$$

Using the above equations and Definition 2, computations give

$$-\frac{\tau}{2}\mathrm{Re}\begin{pmatrix} \frac{1-g^2}{g'} \\ \frac{\mathrm{i}(1+g^2)}{g'} \\ \frac{2g}{g'} \end{pmatrix} = -\nu^2 \begin{pmatrix} X_1' \\ X_2' \\ X_3' \end{pmatrix} = \partial x,$$

$$\frac{\sigma}{2}\mathrm{Re}\begin{pmatrix} \frac{1-gg_1}{\Delta g} \\ \frac{\mathrm{i}(1+gg_1)}{\Delta g} \\ \frac{g+g_1}{\Delta g} \end{pmatrix} = \nu\nu_1 \begin{pmatrix} X_{1,1} - X_1 \\ X_{2,1} - X_2 \\ X_{3,1} - X_3 \end{pmatrix} = \Delta x. \tag{13}$$

Thus g produces x via Equation (11), which completes the proof.

Because the computation of (13) in particular is rather laborious, we outline one part of that computation here: Since

$$\frac{\sigma}{\Delta g} = \nu\nu_1[X_{1,1}(1 - X_3) - X_1(1 - X_{3,1}) - \mathrm{i}\{X_{2,1}(1 - X_3) - X_2(1 - X_{3,1})\}],$$

we have

$$\begin{aligned}\frac{\sigma}{2}\mathrm{Re}\frac{1 - gg_1}{\Delta g} &= \frac{\nu\nu_1}{2(1 - X_3)(1 - X_{3,1})}\mathrm{Re}\,([X_{1,1}(1 - X_3) \\ &\quad - X_1(1 - X_{3,1}) - \mathrm{i}\{X_{2,1}(1 - X_3) - X_2(1 - X_{3,1})\}] \cdot \\ &\quad [(1 - X_3)(1 - X_{3,1}) - (X_1 + \mathrm{i}X_2)(X_{1,1} + \mathrm{i}X_{2,1})]) \\ &= \frac{\nu\nu_1}{2(1 - X_3)(1 - X_{3,1})}[\{X_{1,1}(1 - X_3) - X_1(1 - X_{3,1})\} \cdot \\ &\quad \{(1 - X_3)(1 - X_{3,1}) - X_1 X_{1,1} + X_2 X_{2,1}\} - \{X_{2,1}(1 - X_3)\end{aligned}$$

$$
\begin{aligned}
&-X_2(1-X_{3,1})\}\cdot(X_1X_{2,1}+X_{1,1}X_2)]\\
&=\frac{\nu\nu_1}{2(1-X_3)(1-X_{3,1})}\{(1-X_3)(1-X_{3,1})(X_{1,1}-X_1\\
&\quad -X_{1,1}X_3+X_1X_{3,1})-X_1(1-X_3)(X_{1,1}^2+X_{2,1}^2)\\
&\quad +X_{1,1}(1-X_{3,1})(X_1^2+X_2^2)\}\\
&=\frac{\nu\nu_1}{2(1-X_3)(1-X_{3,1})}\{(1-X_3)(1-X_{3,1})(X_{1,1}-X_1\\
&-X_{1,1}X_3+X_1X_{3,1})-(1-X_3)(1-X_{3,1})(1+X_{3,1})X_1\\
&\quad +(1-X_3)(1-X_{3,1})(1+X_3)X_{1,1}\}\\
&=\nu\nu_1(X_{1,1}-X_1).
\end{aligned}
$$

□

EXAMPLE 1. The semi-discrete minimal Enneper surface, has been given in [**54**]. We can also obtain that surface by taking $g(k,t)=k+\mathrm{i}t$ in Theorem 2.

EXAMPLE 2. The $MW^{in}_{pd,rs}$ (resp. $MW^{in}_{ps,rd}$) catenoid can be constructed via Theorem 2 with

$$g(k,t)=ce^{\alpha k+\mathrm{i}\beta t}\quad(\text{resp. }\ g(k,t)=ce^{\alpha t+\mathrm{i}\beta k}),$$

for the right choices of $c,\ \alpha,\ \beta\in\mathbb{R}\setminus\{0\}$.

6. Fully-discrete catenoids of Bobenko-Pinkall

The fully discrete catenoids of Bobenko and Pinkall [**13**] can be given explicitly by using the Weierstrass representation for discrete minimal surfaces (in the integrable systems sense), that is, we can use

$$x(q)-x(p)=\mathrm{Re}\left(\frac{a_{pq}}{g_q-g_p}\begin{pmatrix}1-g_qg_p\\ \mathrm{i}+\mathrm{i}g_qg_p\\ g_q+g_p\end{pmatrix}\right) \tag{14}$$

with the choice of g as $g_p=g_{n,m}=ce^{c_1n+ic_2m}$, where c, c_1, c_2 are nonzero real constants, and $p=(n,m)$ and $q=(n+1,m)$ or $q=(n,m+1)$, and a_{pq} is a cross ratio factorizing function for g. This formulation can be found in [**13**], [**14**], [**33**], [**35**], [**61**].

This choice of g has cross ratios

$$\mathrm{cr}(g_{n,m},g_{n+1,m},g_{n+1,m+1},g_{n,m+1})=\frac{-\sinh^2\frac{c_1}{2}}{\sin^2\frac{c_2}{2}}.$$

So we can take $a_{pq}=-\alpha\sinh^2\frac{c_1}{2}$ (resp. $a_{pq}=\alpha\sin^2\frac{c_2}{2}$), when $q=(n+1,m)$ (resp. $q=(n,m+1)$). The value $\alpha\in\mathbb{R}\setminus\{0\}$ can be chosen as we like.

Taking the axis of the surface to be

$$\left\{\begin{pmatrix}0\\0\\t\end{pmatrix}\,\middle|\,t\in\mathbb{R}\right\},$$

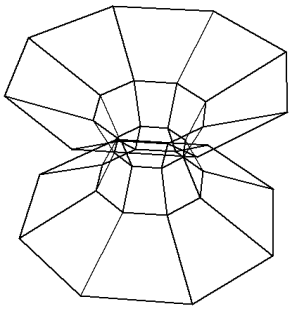

FIGURE 4. a (fully-discrete) $BP^{in}_{pd,rd}$-catenoid

and taking the vertex in the profile curve at the neck to be $f(0,0) = (1,0,0)^t$, we can propagate to find the discrete profile curve in the x_1x_3-plane. For this purpose, $\alpha = -2$ and $c = -1$ are suitable values. One can check that, for all $m \in \mathbb{Z}$,

$$x(0,m) = \begin{pmatrix} \cos(c_2 m) \\ \sin(c_2 m) \\ 0 \end{pmatrix}.$$

By (14), the discrete profile curve in the x_1x_3-plane is, for all $n \in \mathbb{Z}$,

$$x(n,0) = \begin{pmatrix} \cosh(c_1 n) \\ 0 \\ n \cdot \sinh c_1 \end{pmatrix}.$$

Again by (14), we obtain

$$x(n,m) = \begin{pmatrix} \cosh(c_1 n)\cos(c_2 m) \\ \cosh(c_1 n)\sin(c_2 m) \\ n \cdot \sinh c_1 \end{pmatrix}.$$

Setting $\ell = \sinh c_1$, one profile curve of the $BP^{in}_{pd,rd}$-catenoid is as written in the upcoming Section 9. Note that the profile curves do not depend on c_2.

7. Fully-discrete catenoids of Polthier-Rossman

The catenoids described in [**60**] are fully discrete and have discrete rotational symmetry, thus the symmetry group is a dihedral group. Taking the dihedral angle to be $\theta = 2\pi K^{-1}$ for a constant $K \in \mathbb{N}$ and $K \geq 3$, the vertices of a profile curve (when the x_3-axis is the central axis of symmetry) in the x_1x_3-plane can be taken to be points that are vertically equally spaced apart with height difference between adjacent vertices denoted as ℓ, and the x_1 coordinates of the vertices can be taken as $x(n) = r \cdot \cosh(r^{-1}a\ell n)$, where $a = r\ell^{-1}\text{arccosh}(1 + r^{-2}\ell^2(1+\cos\theta)^{-1})$. Here r is the waist radius of the interpolated hyperbolic cosine curve. Taking $r = 1$ without loss of generality, we can take one profile curve to be

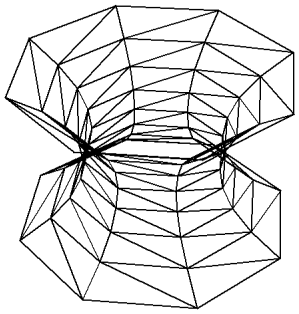

FIGURE 5. a (fully-discrete) $PR^{va}_{pd,rd}$-catenoid

$$\begin{pmatrix} \cosh(n \cdot \operatorname{arccosh}(1 + \ell^2(1+\cos\theta)^{-1})) \\ 0 \\ n \cdot \ell \end{pmatrix}, \; n \in \mathbb{Z}, \tag{15}$$

so when we take the limit as $\theta \to 0$, we have

$$\begin{pmatrix} \cosh(n \cdot \operatorname{arccosh}(1 + \frac{1}{2}\ell^2)) \\ 0 \\ n \cdot \ell \end{pmatrix}.$$

A direct computation, as in the proof of the next proposition, shows that this is exactly what was obtained by Machigashira [**50**], although it was not described in terms of the hyperbolic cosine function there, but rather by using Chebyshev polynomials and Gauss hypergeometric functions.

PROPOSITION 2. The $M^{va}_{pd,rs}$-catenoid equals the limiting case of the $PR^{va}_{pd,rd}$-catenoids as $\theta \to 0$, and no $PR^{va}_{pd,rd}$-catenoid (with positive θ) will ever have the same profile curve as the $M^{va}_{pd,rs}$-catenoid.

Proof. The vertices of an $M^{va}_{pd,rs}$-catenoid profile curve can be written as

$$\begin{pmatrix} T_n(1 + \frac{1}{2}\Lambda^2) \\ 0 \\ n \cdot \Lambda \end{pmatrix}, \tag{16}$$

where T_k can be defined by the recursion

$$T_0(z) = 1, \; T_1(z) = z, \; T_n(z) = 2zT_{n-1}(z) - T_{n-2}(z)$$

for $n \geq 2$. The T_n are called Chebyshev polynomials of the first kind, and are described in [**50**]. Suppose, for the vertex on the profile curve where $n = 1$, we

equate (15) and (16), i.e.

$$\begin{pmatrix} 1+\frac{1}{2}\Lambda^2 \\ 0 \\ \Lambda \end{pmatrix} = \begin{pmatrix} 1+\ell^2(1+\cos\theta)^{-1} \\ 0 \\ \ell \end{pmatrix} . \tag{17}$$

The third coordinate in (17) implies $\Lambda = \ell$, and then the first coordinate implies $\theta = 0$. Then we would need to check that all other corresponding vertices in (15) and (16) also become equal.

Letting x denote the first coordinate of the profile curve, the $M^{va}_{pd,rs}$-catenoid satisfies

$$x(n) = T_n(1+\tfrac{1}{2}\Lambda^2) = 2(1+\tfrac{1}{2}\Lambda^2)\cdot T_{n-1}(1+\tfrac{1}{2}\Lambda^2) \\ -T_{n-2}(1+\tfrac{1}{2}\Lambda^2).$$

For the limiting $PR^{va}_{pd,rd}$-catenoid ($\theta = 0$), we would like to see the same recursion for the first coordinate of the profile curve. That is, we wish to have

$$\cosh(n\cdot \operatorname{arccosh}(1+\tfrac{1}{2}\ell^2)) = \\ 2(1+\tfrac{1}{2}\ell^2)\cosh((n-1)\cdot\operatorname{arccosh}(1+\tfrac{1}{2}\ell^2)) \\ -\cosh((n-2)\cdot\operatorname{arccosh}(1+\tfrac{1}{2}\ell^2)) ,$$

and this is indeed true, which proves the proposition. □

8. Another type of semi-discrete catenoid

Consider the two discrete loops, for a constant $K \in \mathbb{N}$, $K \geq 3$,

$$\begin{pmatrix} \cos(2\pi K^{-1}) \\ \sin(2\pi K^{-1}) \\ \pm r \end{pmatrix}$$

in the horizontal planes at height $\pm r$. We consider a semi-discrete catenoid (i.e. a surface with rotational symmetry by angle $2\pi K^{-1}$ about the x_3-axis) with those two loops as boundary. This catenoid is comprised of K congruent pieces, and each piece is foliated by horizontal line segments. One such piece would have two boundary curves parametrized by

$$c_1(t) = \begin{pmatrix} x(t) \\ 0 \\ t \end{pmatrix} \text{ and } c_2(t) = \begin{pmatrix} x(t)\cos(2\pi K^{-1}) \\ x(t)\sin(2\pi K^{-1}) \\ t \end{pmatrix} \tag{18}$$

in vertical planes, with $t \in [-r, r]$ and with

$$x(r) = x(-r) = 1.$$

The area of this piece is

$$A = \int_{-r}^{r} x\cdot\sqrt{2(1-\cos(2\pi K^{-1})) + (\sin(2\pi K^{-1}))^2(x')^2}dt.$$

Then consider a variation $x(t) \to x(t,\lambda)$ with $x(t,0) = x(t)$ and $x(\pm r,\lambda) = 1$, so λ is the variation parameter. Note that we are only considering rotationally invariant variations here, as was done by Machigashira [**50**]. An interesting question is whether

we are also in effect considering variations that are not rotationally invariant as well, by some semi-discrete version of the symmetric criticality principle, see [**57**]. Set

$$x' := \frac{\partial x}{\partial t},\ x_\lambda := \frac{\partial x}{\partial \lambda},\ (x')_\lambda := \frac{\partial^2 x}{\partial \lambda \partial t}.$$

We wish to have that the following derivative with respect to λ is zero, where $c := \cos(2\pi K^{-1})$ and $s := \sin(2\pi K^{-1})$ and $D := 2(1-c) + s^2(x')^2$:

$$\begin{aligned}\frac{d}{d\lambda}A(\lambda)\Big|_{\lambda=0} &= \int_{-r}^{r} \frac{x_\lambda D + x x'(x')_\lambda s^2}{\sqrt{D}} dt\Big|_{\lambda=0} \\ &= \int_{-r}^{r} \left(\hat{x}\sqrt{D} + s^2 \hat{x}' \frac{1}{2} \frac{((x(t))^2)'}{\sqrt{D}} \right) dt\ ,\end{aligned}$$

when $x(t,\lambda) = x(t) + \lambda \cdot \hat{x}(t) + \mathcal{O}(\lambda^2)$. Then, using integration by parts, we wish to have, with $x = x(t)$,

$$\begin{aligned}0 &= \int_{-r}^{r} \hat{x} \left(\sqrt{D} - s^2 \frac{2(1-c)((x')^2 + xx'') + s^2(x')^4}{\sqrt{D}^3} \right) dt \\ &= 2\int_{-r}^{r} \hat{x} \left((1-c)^2 \frac{2 - (1+c)(xx'' - (x')^2)}{\sqrt{D}^3} \right) dt\end{aligned}$$

for all variations. This implies

$$xx'' - (x')^2 = \frac{2}{1+c},$$

and hence we obtain that

$$x = c_1 e^{-c_3 t} + c_2 e^{c_3 t}\ ,\quad c_1 = \frac{1}{2(1+c)c_2 c_3^2},$$

where c_2, c_3 are free constants. The conditions $x(\pm r) = 1$ imply $c_1 = c_2 = (2\cosh(c_3 r))^{-1}$, so we obtain

$$x(t) = 2c_1 \cosh(c_3 t) = \frac{\cosh(c_3 t)}{\cosh(c_3 r)}. \tag{19}$$

Then automatically $x'(0) = 0$. From the above relations amongst the c_j, we obtain that

$$\cosh^2(c_3 r) = \frac{c_3^2(1+c)}{2}. \tag{20}$$

Thus c_3 is determined by r. These catenoids have been determined by using a variational property, like the $M^{va}_{pd,rs}$-catenoids were, so we call them $M^{va}_{ps,rd}$-catenoids.

For r that allow for solutions c_3 to (20), a profile curve of an $M^{va}_{ps,rd}$-catenoid is $c_1(t)$ as in (18) with $x(t)$ as in (19). Rescaling this c_1 by $\cosh(c_3 r)$ and appropriately rescaling the parameter t, we find that this catenoid's profile curve can be

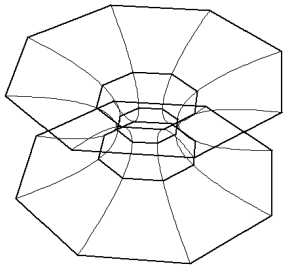

FIGURE 6. a $M^{va}_{ps,rd}$-catenoid

parametrized as

$$\begin{pmatrix} \cosh\left(\frac{\sqrt{2}t}{\sqrt{1+\cos\frac{2\pi}{K}}}\right) \\ 0 \\ t \end{pmatrix}.$$

9. Proof of Theorem 1

We list parametrizations of the profile curves of the various catenoids again here in Table 2.

Comparing all profile curves, we obtain the following proof of Theorem 1:

Proof. The statements in items 1, 2, 4, 5 and 6 of Theorem 1 are obvious, so we prove only item 3 here. By way of contradiction, suppose $BP^{in}_{pd,rd}$-catenoid profile curves and $M^{va}_{pd,rs}$-catenoid profile curve can be the same. From the parametrizations in Table 2,

$$\cosh(\operatorname{arc\,sinh}\ell) = 1 + \frac{1}{2}\ell^2. \tag{21}$$

Since $\cosh(\operatorname{arc\,sinh}\ell) = \sqrt{1+\ell^2}$, (21) implies $\ell = 0$, which does not occur. Similarly, suppose $BP^{in}_{pd,rd}$-catenoid profile curves and $PR^{va}_{pd,rd}$-catenoid profile curve can be the same. Then we have

$$\cosh(\operatorname{arc\,sinh}\ell) = 1 + \frac{1}{1+\cos\frac{2\pi}{K}}\ell^2,$$

namely,

$$\Leftrightarrow \left(\frac{-2}{1+\cos\frac{2\pi}{K}} + 1\right)\ell^2 = \left(\frac{1}{1+\cos\frac{2\pi}{K}}\right)^2 \ell^4. \tag{22}$$

The left-hand-side of (22) is negative and the right-hand-side of (22) is positive, which is impossible. □

	parametrizations of profile curves
smooth catenoid	$\begin{pmatrix}\cosh t\\0\\t\end{pmatrix} \quad (t\in\mathbb{R})$
$PR^{va}_{pd,rd}$-catenoid	$\begin{pmatrix}\cosh(n\cdot\operatorname{arccosh}(1+\frac{\ell^2}{1+\cos\frac{2\pi}{K}}))\\0\\n\cdot\ell\end{pmatrix}$
$M^{va}_{pd,rs}$-catenoid	$\begin{pmatrix}\cosh(n\cdot\operatorname{arccosh}(1+\frac{1}{2}\ell^2))\\0\\n\cdot\ell\end{pmatrix}$
$BP^{in}_{pd,rd}$-catenoid	$\begin{pmatrix}\cosh(n\cdot\operatorname{arcsinh}\ell)\\0\\n\cdot\ell\end{pmatrix}$
$MW^{in}_{pd,rs}$-catenoid	$\begin{pmatrix}\cosh(n\cdot\operatorname{arcsinh}\ell)\\0\\n\cdot\ell\end{pmatrix}$
$MW^{in}_{ps,rd}$-catenoid	$\begin{pmatrix}\cosh t\\0\\t\end{pmatrix}$
$M^{va}_{ps,rd}$-catenoid	$\begin{pmatrix}\cosh\left(\frac{\sqrt{2}t}{\sqrt{1+\cos\frac{2\pi}{K}}}\right)\\0\\t\end{pmatrix}$

TABLE 2. Parametrizations of seven types of catenoids

CHAPTER 2

Discrete maximal surfaces with singularities in Minkowski space

1. Introduction and main results

Bobenko and Pinkall [**13**], [**14**] introduced discrete isothermic surfaces in Euclidean 3-space $\mathbb{R}^3$ based on integrable systems methods, and Kinoshita and Rossman [**46**] introduced discrete spacelike isothermic surfaces in Minkowski 3-space $\mathbb{R}^{2,1}$. Discrete spacelike isothermic surfaces (parametrized by $m,\ n \in \mathbb{Z}$) in $\mathbb{R}^{2,1}$ are those for which every quadrilateral face has vertices lying on the Minkowski space analog of a circle, i.e. the intersection of a translated light cone and a spacelike plane, so that the cross ratio of those vertices is $-\frac{\alpha_m}{\beta_n}$, where $\alpha_m > 0$ and $\beta_n > 0$ depend only on the discrete parameter m and n, respectively.

In this paper, we introduce special classes of discrete isothermic surfaces in $\mathbb{R}^{2,1}$ called discrete maximal surfaces, whose mean curvatures are identically 0 in the sense of [**19**], [**46**]. We have a Weierstrass representation for discrete maximal surfaces, as in our first main result below, which is analogous to the Weierstrass representation for discrete minimal surfaces in $\mathbb{R}^3$ [**13**]. In this theorem, discrete holomorphic functions are defined the same way as discrete spacelike isothermic surfaces are defined above, having cross ratios on the faces being $-\frac{\alpha_m}{\beta_n}$, but now the target of the map is $\mathbb{C}$ rather than $\mathbb{R}^{2,1}$.

THEOREM 3. Discrete maximal surfaces F, maps from a domain $\mathbb{D} \subset \mathbb{Z}^2$ to $\mathbb{R}^{2,1}$, can be constructed using discrete holomorphic functions g from $\mathbb{D}$ to the complex plane $\mathbb{C}$ by solving

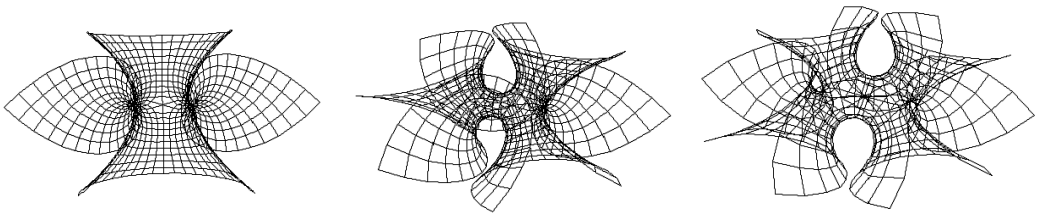

FIGURE 1. Discrete minimal surfaces in $\mathbb{R}^3$ via the Weierstrass representation described in [**13**], coming from the discrete analogs (see [**10**]) of the holomorphic functions z^γ, $\gamma \in (0, 2)$.

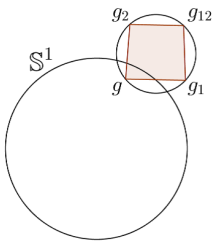

FIGURE 2. $\mathcal{G}$ inscribing a circle that intersects $\mathbb{S}^1$ (the case where a singular face appears)

$$\begin{aligned}\Delta_1 F &= \frac{1}{2}\mathrm{Re}\left(\frac{\alpha_m}{\Delta_1 g}\begin{pmatrix}1+g_{m+1,n}g_{m,n}\\ \mathrm{i}(1-g_{m+1,n}g_{m,n})\\ -(g_{m+1,n}+g_{m,n})\end{pmatrix}\right)\\ \Delta_2 F &= -\frac{1}{2}\mathrm{Re}\left(\frac{\beta_n}{\Delta_2 g}\begin{pmatrix}1+g_{m,n+1}g_{m,n}\\ \mathrm{i}(1-g_{m,n+1}g_{m,n})\\ -(g_{m,n+1}+g_{m,n})\end{pmatrix}\right)\end{aligned} \tag{23}$$

with α_m and β_n cross ratio factorizing functions for g, where

$$\Delta_1 F := F_{m+1,n} - F_{m,n},\ \Delta_2 F := F_{m,n+1} - F_{m,n}.$$

Conversely, any discrete maximal surface satisfies (23) for some discrete holomorphic function g.

Non-spacelike faces do appear on discrete maximal surfaces F, and have vertices lying on a hyperbola or parabola with their cross ratios being $-\frac{\alpha_m}{\beta_n}$ if they do not have any lightlike edge. We refer to such faces as GVP ("G"eneric "V"ertex "P"lacement) singular faces. We also see cases of non-spacelike faces with at least one lightlike edge, and we refer to such faces as NVP ("N"on-generic "V"ertex "P"lacement) singular faces. For the study of NVP singular faces, we introduce the notion of limit cross ratios (see Section 7).

In the smooth case, maximal surfaces generally have certain singularities (for example, see [**69**]). The discrete analogs of maximal surfaces generally have singular faces, and these singular faces are the natural discretization of singularities of smooth spacelike maximal surfaces. Our second main result is the following Theorem 4 (in the statement, we replace $F_{m,n}$, $F_{m+1,n}$, $F_{m+1,n+1}$, $F_{m,n+1}$, with the simpler notations F, F_1, F_{12}, F_2, respectively), see Figure 2.

THEOREM 4. Let $g : \mathbb{D} \to \mathbb{C}$ be a discrete holomorphic function and let F be a discrete maximal surface determined from g. Then the face $\mathcal{F} = (F, F_1, F_{12}, F_2)$ is a singular face if and only if the circle passing through the vertices of the associated face $\mathcal{G} = (g, g_1, g_{12}, g_2)$ intersects the unit circle $\mathbb{S}^1 = \{z \in \mathbb{C} \mid |z| = 1\}$.

Our third theorem, a classification of the possible types of singular faces, is as follows:

THEOREM 5. For the four vertices of a singular face $\mathscr{F}$ of a discrete maximal surface F, which lie in a non-spacelike plane, we have the following:

- When $\mathscr{F}$ is GVP, the four vertices lie in a hyperbola or parabola, that is, they either
  (1) lie in the intersection of a translated light cone and a non-spacelike plane, and the singular face is embedded unless exactly two vertices lie in each component of a hyperbola, in which case the face is non-embedded, or
  (2) the four vertices lie in an exceptional hyperbola (as defined in Section 3).
- When $\mathscr{F}$ is NVP, only the following cases can occur:
  (1) all four image points under g lie in $\mathbb{S}^1$, and then all four vertices of the (degenerate) face are the same single point,
  (2) exactly two image points under g lie in $\mathbb{S}^1$, and then the two corresponding vertices of the face are the same and the remaining two vertices are distinct,
  (3) exactly one image point under g lies in $\mathbb{S}^1$, and then all four of the vertices of the face are distinct, but one vertex lies on a line determined by two other vertices.

Moreover, all cases described in this theorem do actually occur.

The proofs of these theorems and some examples are found in Sections 6, 8, 9, 10.

2. Smooth maximal surfaces

Here we briefly review smooth maximal surfaces. For more theory, see [**47**], [**69**] for example. Let

$$\mathbb{R}^{2,1} := (\{(x_1, x_2, x_0)^t | x_j \in \mathbb{R}\}, \langle \cdot, \cdot \rangle)$$

be 3-dimensional Minkowski space with the Lorentz metric

$$\langle (x_1, x_2, x_0)^t, (y_1, y_2, y_0)^t \rangle = x_1 y_1 + x_2 y_2 - x_0 y_0,$$

and squared norm $\|(x_1, x_2, x_0)^t\|^2 = \langle (x_1, x_2, x_0)^t, (x_1, x_2, x_0)^t \rangle$, which can be negative.

Note that, for fixed $d \in \mathbb{R}$ and vector $n \in \mathbb{R}^{2,1} \setminus \{0\}$, a plane $\mathcal{P} = \{x \in \mathbb{R}^{2,1} \mid \langle x, n \rangle = d\}$ is *spacelike* or *timelike* or *lightlike* when n is timelike or spacelike or lightlike, respectively. Furthermore, a smooth surface in $\mathbb{R}^{2,1}$ is spacelike if its tangent planes are spacelike. Let $F : \Sigma \to \mathbb{R}^{2,1}$ be a conformal immersion, where Σ is a simply-connected domain in $\mathbb{C}$ with complex coordinate $z = u + iv$, $u,\ v \in \mathbb{R}$. F is a maximal surface if it is spacelike (which follows automatically from the conformality condition) with mean curvature identically 0.

Defining

$$\mathbb{H}^2_+ := \{x = (x_1, x_2, x_0)^t \in \mathbb{R}^{2,1} | \|x\|^2 = -1,\ x_0 > 0\},$$

$$\mathbb{H}^2_- := \{x = (x_1, x_2, x_0)^t \in \mathbb{R}^{2,1} | \|x\|^2 = -1,\ x_0 < 0\},$$

we have the following proposition, analogous to the case of smooth minimal surfaces in $\mathbb{R}^3$ (and having a similar proof):

PROPOSITION 3. Away from umbilic points, smooth maximal surfaces lie in the class of isothermic surfaces. In addition, a spacelike immersion $F = F(u, v)$ is a maximal surface if and only if it has a dual surface F^*, which solves

$$F_u^* = \frac{F_u}{\|F_u\|^2}, \quad F_v^* = -\frac{F_v}{\|F_v\|^2},$$

contained in $\mathbb{H}^2_+ \cup \mathbb{H}^2_-$. This dual surface is the Gauss map of the maximal surface.

Locally, we can construct any smooth maximal surface F with isothermic coordinates u, v from a smooth holomorphic function $g : \Sigma \to \mathbb{C}$ by solving

$$F = \mathrm{Re} \int \left(\frac{1+g^2}{g'}, \frac{\mathrm{i}(1-g^2)}{g'}, -\frac{2g}{g'} \right)^t dz. \tag{24}$$

This function g is stereographic projection of the Gauss map F^* (up to scaling and translation). Conversely, any maximal surface F is described in this way by some holomorphic function g. See [**47**].

Differentiating (24) gives the following system of differential equations:

$$F_u = \mathrm{Re} \left(\frac{1+g^2}{g_u}, \frac{\mathrm{i}(1-g^2)}{g_u}, -\frac{2g}{g_u} \right)^t,$$

$$F_v = -\mathrm{Re} \left(\frac{1+g^2}{g_v}, \frac{\mathrm{i}(1-g^2)}{g_v}, -\frac{2g}{g_v} \right)^t.$$

Our Theorem 3 gives a discrete analog of the above system of differential equations.

Remark. Unlike the case of the Weierstrass representation for minimal surfaces in $\mathbb{R}^3$, smooth maximal surfaces in $\mathbb{R}^{2,1}$ have singularities when $|g| = 1$, because the metrics

$$\frac{(1-|g|^2)^2}{|g'|^2} dz d\bar{z} \tag{25}$$

of the smooth maximal surfaces degenerate. Note that we have a minus sign in the numerator in (25), unlike the plus sign we would have had for minimal surfaces in $\mathbb{R}^3$. □

3. The cross ratio in Minkowski 3-space

In order to describe discrete isothermic surfaces in $\mathbb{R}^{2,1}$, we first define the cross ratio of four points in $\mathbb{R}^{2,1}$. Identifying $\mathbb{R}^{2,1}$ with the Lie algebra $\mathrm{su}_{1,1}$ of the Lie group $\mathrm{SU}_{1,1}$, by identifying

$$\mathbb{R}^{2,1} \ni (x_1, x_2, x_0)^t \leftrightarrow \begin{pmatrix} \mathrm{i}x_0 & x_1 - \mathrm{i}x_2 \\ x_1 + \mathrm{i}x_2 & -\mathrm{i}x_0 \end{pmatrix} \in \mathrm{su}_{1,1},$$

we give an analogy of the cross ratio defined by Bobenko and Pinkall [**13**], [**14**].

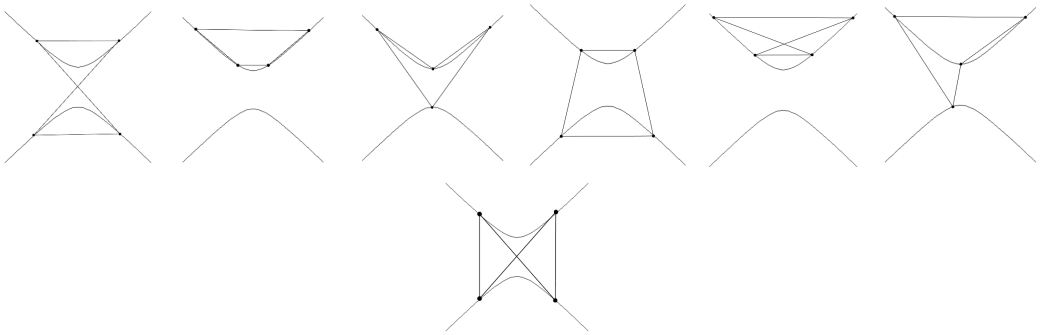

FIGURE 3. Types of faces with vertices lying in the intersection of a timelike plane with a translated light cone

DEFINITION 6. Let X_1, X_2, X_3, X_4 be four distinct points in $\mathbb{R}^{2,1}$. The unordered pair $cr(X_1, X_2, X_3, X_4) := \{q_1, q_2\}$ of eigenvalues of the matrix

$$Q(X_1, X_2, X_3, X_4) = (X_1 - X_2)(X_2 - X_3)^{-1}(X_3 - X_4)(X_4 - X_1)^{-1}$$

is called the *cross ratio* of the quadrilateral (X_1, X_2, X_3, X_4).

Remark. The pair of numbers $\{q_1, q_2\}$ will be either real or complex conjugate. If $q_1 = q_2 \in \mathbb{R}$, then we regard this single real number as the cross ratio. □

LEMMA 3. The unordered pair $\{q_1, q_2\}$ in Definition 6 is invariant under isometries and homotheties of $\mathbb{R}^{2,1}$.

Proof. The pair $\{q_1, q_2\}$ is obviously invariant under translations and homotheties of $\mathbb{R}^{2,1}$. To see that $\{q_1, q_2\}$ is invariant under rotation, consider the action $X \mapsto RXR^{-1}$ representating general rotations of $\mathbb{R}^{2,1}$, where

$$R = \begin{pmatrix} \alpha_1 + \mathrm{i}\alpha_2 & \beta_1 + \mathrm{i}\beta_2 \\ \beta_1 - \mathrm{i}\beta_2 & \alpha_1 - \mathrm{i}\alpha_2 \end{pmatrix} \in \mathrm{SU}_{1,1} \quad (\alpha_1,\ \alpha_2,\ \beta_1,\ \beta_2 \in \mathbb{R},\ \alpha_1^2 + \alpha_2^2 - \beta_1^2 - \beta_2^2 = 1).$$

Clearly,

$$cr(RX_1R^{-1}, RX_2R^{-1}, RX_3R^{-1}, RX_4R^{-1})$$

is invariant of choice of $R \in \mathrm{SU}_{1,1}$. □

In Proposition 4 we treat the case that the four vertices of each quadrilateral lie on a translated light cone $\mathbb{L}_p^2$, where

$$\mathbb{L}_p^2 := \{x \in \mathbb{R}^{2,1} | \|x - p\|^2 = 0\}$$

for each $p \in \mathbb{R}^{2,1}$. The following proposition is easily shown.

PROPOSITION 4. Suppose X_1, X_2, X_3, $X_4 \in \mathbb{L}_p^2$ are co-planar in a plane that is spacelike, and that none of $X_1 - X_2$, $X_2 - X_3$, $X_3 - X_4$, $X_4 - X_1$ are lightlike. Then $cr(X_1, X_2, X_3, X_4) \in \mathbb{R}$ has a single real value, and is the same as the standard cross ratio for conic sections (see [**46**], [**33**]), and then X_1, X_2, X_3, X_4 form an embedded quadrilateral if and only if $cr(X_1, X_2, X_3, X_4) < 0$.

Remark. (about Proposition 4)

- When X_1, X_2, X_3 and X_4 are co-planar in a plane that is timelike, rather, the conic section that X_1, X_2, X_3 and X_4 lie on is a hyperbola, and again $cr(X_1, X_2, X_3, X_4) \in \mathbb{R}$. However, even when $cr(X_1, X_2, X_3, X_4)$ is negative, it is possible that (X_1, X_2, X_3, X_4) forms a non-embedded face. The first three figures in Figure 3 show the possible cases with negative cross ratios.
- When X_1, X_2, X_3 and X_4 are co-planar in a plane that is lightlike, rather, the conic section that X_1, X_2, X_3 and X_4 lie on is a parabola, and here as well $cr(X_1, X_2, X_3, X_4) \in \mathbb{R}$. Then, like in the case that (X_1, X_2, X_3, X_4) lie in a spacelike plane, when $cr(X_1, X_2, X_3, X_4)$ is negative, the face (X_1, X_2, X_3, X_4) is embedded, and if $cr(X_1, X_2, X_3, X_4)$ is positive, then (X_1, X_2, X_3, X_4) is non-embedded.
- Thus the case of a hyperbolic conic section is more complicated than the cases of parabolic and elliptic conic sections, because the hyperbolic conic sections have two connected components, not just one. We list all the cases of faces and the signature of their cross ratios in Table 1.
- When X_1, X_2, X_3, X_4 are not contained in any translated light cone, then $\{q_1, q_2\}$ will be complex conjugate if X_1, X_2, X_3, X_4 lie in a spacelike plane, and will be real if X_1, X_2, X_3, X_4 lie in a timelike plane, and will be real and equal if X_1, X_2, X_3, X_4 lie in a lightlike plane.

□

Also, the following Proposition 5 holds. In this proposition, any curve in $\mathbb{R}^{2,1}$ which is isometric to

$$\mathbb{H}(\rho) := \{x = (x_1, 0, x_0)^t \in \mathbb{R}^{2,1} \mid \|x\|^2 = \rho^{-2}\} \quad (\rho \in \mathbb{R} \setminus \{0\})$$

will be called an *exceptional hyperbola*. We use the word "exceptional" because this curve does not lie in any translated light cone $\mathbb{L}^2_p$.

Proposition 5. If X_1, X_2, X_3, $X_4 \in \mathbb{L}^2_p$ for some p, then $cr(X_1, X_2, X_3, X_4)$ is a single real value and $Q(X_1, X_2, X_3, X_4)$ is scalar multiple of $cr(X_1, X_2, X_3, X_4)$ and identity matrix.

Conversely, suppose that the four non-collinear but co-planar points X_1, X_2, X_3, $X_4 \in \mathbb{R}^{2,1}$ satisfy that none of $X_1 - X_2$, $X_2 - X_3$, $X_3 - X_4$, $X_4 - X_1$ is lightlike and that $cr(X_1, X_2, X_3, X_4)$ is a single real value, and that $Q(X_1, X_2, X_3, X_4)$ equals the scalar $cr(X_1, X_2, X_3, X_4)$ times the identity matrix. Then the four vertices X_1, X_2, X_3, X_4 lie in the intersection of a translated light cone and a plane, or in an exceptional hyperbola.

Remark. (about Proposition 5)

- When four points lie in a straight line, their cross ratio is real. However, we do not consider such a case.
- The case that some of $X_1 - X_2$, $X_2 - X_3$, $X_3 - X_4$, $X_4 - X_1$ are lightlike will be considered in Section 7.
- When the plane containing X_1, X_2, X_3, $X_4 \in \mathbb{L}^2_p$ is timelike, it is possible that this plane passes through the cone point p, and then if the quadrilateral

shape of quadrilateral	signature of plane	signature of cross ratio
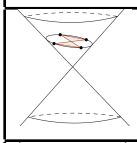	spacelike	positive
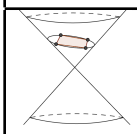	spacelike	negative
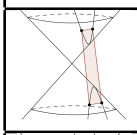	timelike	positive
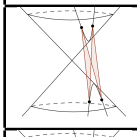	timelike	positive
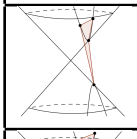	timelike	positive
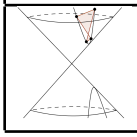	timelike	positive

shape of quadrilateral	signature of plane	signature of cross ratio
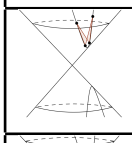	timelike	positive
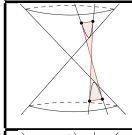	timelike	negative
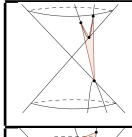	timelike	negative
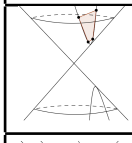	timelike	negative
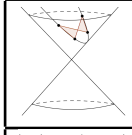	lightlike	positive
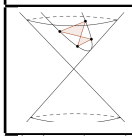	lightlike	positive
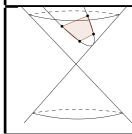	lightlike	negative

TABLE 1. A list of the types of faces with vertices lying on a conic section and the signature of their cross ratios

(X_1, X_2, X_3, X_4) does not have any lightlike edge, its cross ratio will be positive.

□

Let X_1, X_2, X_3, X_4 be points in $\mathbb{L}_p^2$ with $p = 0$. From direct computation (which is considerably simplified by the fact that $p = 0$), we have

$$cr(X_1, X_2, X_3, X_4) = \frac{\langle X_1, X_2\rangle\langle X_3, X_4\rangle - \langle X_1, X_3\rangle\langle X_2, X_4\rangle + \langle X_1, X_4\rangle\langle X_2, X_3\rangle}{2\langle X_1, X_4\rangle\langle X_2, X_3\rangle}.$$

When X_1, X_2, X_3, X_4 are points in $\mathbb{L}_p^2$ for general choice of p,

$$cr(X_1, X_2, X_3, X_4) = cr(X_1 - p, X_2 - p, X_3 - p, X_4 - p), \tag{26}$$

and inserting $\|X_i - X_j\|^2 = \|(X_i - p) - (X_j - p)\|^2 = -2\langle X_i - p, X_j - p\rangle$ (i, j=1, 2, 3, 4) into Equation (26), we have:

LEMMA 4.

$$cr(X_1, X_2, X_3, X_4) =$$

$$\frac{\|X_1 - X_2\|^2\|X_3 - X_4\|^2 - \|X_1 - X_3\|^2\|X_2 - X_4\|^2 + \|X_1 - X_4\|^2\|X_2 - X_3\|^2}{2\|X_1 - X_4\|^2\|X_2 - X_3\|^2}. \tag{27}$$

4. Discrete isothermic surfaces in Minkowski 3-space

In Definition 7 we define discrete isothermic surfaces in $\mathbb{R}^{2,1}$, analogous to the definition of discrete isothermic surfaces in $\mathbb{R}^3$ [**13**].

DEFINITION 7. Let $F : \mathbb{D} \to \mathbb{R}^{2,1}$ be a discrete surface parametrized by two discrete parameters m, n. Then F is a *discrete spacelike isothermic surface* if the faces (F,F_1,F_{12},F_2) of F satisfy

(1) F, F_1, F_{12}, $F_2 \in \mathbb{L}^2_p \cap \mathcal{P}$ for some $p \in \mathbb{R}^{2,1}$ and some spacelike plane $\mathcal{P} \subset \mathbb{R}^{2,1}$ (p and $\mathcal{P}$ can be different for different faces of F), and
(2) $cr(F, F_1, F_{12}, F_2) = -\frac{\alpha_m}{\beta_n}$, where α_m, resp. β_n, is a positive scalar function depending only on m, resp. n.

Analogous to discrete isothermic surfaces in $\mathbb{R}^3$ [**13**], we now define the dual surface of an isothermic surface. The F^* defined just below exists, just like in the case of $\mathbb{R}^3$ [**13**].

DEFINITION 8. [and Lemma] Let $F : \mathbb{D} \to \mathbb{R}^{2,1}$ be a discrete isothermic surface with cross ratios on the faces given by $-\frac{\alpha_m}{\beta_n}$. A surface F^* given by the equations

$$\begin{aligned} F^*_{m+1,n} - F^*_{m,n} &= \alpha_m \frac{F_{m+1,n} - F_{m,n}}{\|F_{m+1,n} - F_{m,n}\|^2}, \\ F^*_{m,n+1} - F^*_{m,n} &= -\beta_n \frac{F_{m,n+1} - F_{m,n}}{\|F_{m,n+1} - F_{m,n}\|^2} \end{aligned} \tag{28}$$

exists, and is also a discrete isothermic surface with the same cross ratios as F. We call F^* the *discrete dual surface* of F.

PROPOSITION 6. Let $F : \mathbb{D} \to \mathbb{R}^{2,1}$ be an isothermic surface with dual surface F^*. Then

$$F_{12} - F \parallel F^*_1 - F^*_2, \quad F_1 - F_2 \parallel F^*_{12} - F^*.$$

The proof of this opposite diagonal parallelity for discrete isothermic surfaces in $\mathbb{R}^3$ can be found in [**18**]. In this paper, in preparation for showing that the mean curvature of discrete maximal surfaces is identically 0 (Lemma 6), we prove Proposition 6 here as well.

Proof. The condition $cr(F, F_1, F_{12}, F_2) = -\frac{\alpha}{\beta}$ gives

$$\begin{aligned} &\alpha(F_{12} - F_1)(F_1 - F)^{-1} = -\beta(F_{12} - F_2)(F_2 - F)^{-1} \\ \Leftrightarrow\ &\alpha(F_{12} - F)(F_1 - F)^{-1} - \alpha I = -\beta(F_{12} - F)(F_2 - F)^{-1} + \beta I. \end{aligned} \tag{29}$$

Multiplying Equation (29) on the left by $(F_{12} - F)^{-1}$ and using the definition of dual surfaces of discrete isothermic surfaces, one can check that the first equation in (31) holds.

Similarly, using the condition $cr(F^*, F_1^*, F_{12}^*, F_2^*) = -\frac{\alpha}{\beta}$, one can check that

$$F_1 - F_2 = (\alpha + \beta)(F_{12}^* - F^*)^{-1}. \tag{30}$$

Multiplying Equation (30) on the left by $(F_{12}^* - F^*)$ and on the right by $(F_1 - F_2)^{-1}$, we get the second equation below:

$$\begin{aligned} F_1^* - F_2^* &= (\alpha + \beta)\frac{F_{12} - F}{\|F_{12} - F\|^2}, \\ F_{12}^* - F^* &= (\alpha + \beta)\frac{F_1 - F_2}{\|F_1 - F_2\|^2}. \end{aligned} \tag{31}$$

In particular, $F_{12} - F \parallel F_1^* - F_2^*$ and $F_1 - F_2 \parallel F_{12}^* - F$, proving the proposition. □

5. Mean curvature of discrete isothermic surfaces

Mean curvatures of discrete isothermic surfaces in $\mathbb{R}^3$ were defined in [**15**], [**17**], [**46**], with geometric definitions of discrete minimal surfaces and discrete constant mean curvature (CMC) surfaces given in [**13**], [**14**]. Initially, a definition of discrete spacelike CMC surfaces in $\mathbb{R}^{2,1}$ was given in [**46**]. We will define the mean curvature of discrete surfaces in $\mathbb{R}^{2,1}$ in the same way as in [**15**], and then, like in [**13**] and [**14**], we give geometric descriptions of discrete maximal surfaces and discrete CMC surfaces. We will see that the mean curvatures in these two senses are equivalent when they are constant. Furthermore, in the case of discrete maximal surfaces, we will see that these definitions are also compatible with the definition using conserved quantities in [**19**].

First, we introduce the definition of CMC surfaces given in [**46**]. For $x = (x_1, x_2, x_0)^t$, $y = (y_1, y_2, y_0)^t \in \mathbb{R}^{2,1}$ and $\mathbf{e}_1 = (1, 0, 0)^t$, $\mathbf{e}_2 = (0, 1, 0)^t$, $\mathbf{e}_0 = (0, 0, 1)^t$,

$$x \wedge y := \begin{vmatrix} \mathbf{e}_1 & \mathbf{e}_2 & -\mathbf{e}_0 \\ x_1 & x_2 & x_0 \\ y_1 & y_2 & y_0 \end{vmatrix}$$

denotes the wedge product of x and y in $\mathbb{R}^{2,1}$, and $x \wedge y \perp x$ and $x \wedge y \perp y$.

In [**46**], CMC surfaces were defined as follows in the case that F has spacelike faces, and we extend this definition here to allow for non-spacelike faces:

Definition 9. Let $F = F_{m,n}$ be a discrete isothermic surface in $\mathbb{R}^{2,1}$ as in Definition 7. F is a discrete CMC surface if there exist constant values $h \in \mathbb{R} \setminus \{0\}$, $H \in \mathbb{R}$ and vectors $N = N_{m,n}$ such that (using $N_1 = N_{m+1,n}$, $N_2 = N_{m,n+1}$)

- $\langle N, N \rangle = -1$,
- $\Delta_i F \wedge N_i + N \wedge \Delta_i F = 0$,
- $\langle \Delta_i F, N + N_i \rangle = 0$,
- $\Delta_i N + H \Delta_i F = h \Delta_i F^*$.

The constant H is called the *mean curvature* of F.

Remark. In [**46**], discrete CMC surfaces with quadrilaterals (F, F_1, F_{12}, F_2) lying in spacelike planes were considered. However, more generally, discrete spacelike CMC surfaces can be considered which have some quadrilaterals (F, F_1, F_{12}, F_2) with vertices lying in the intersection of a plane (perhaps not spacelike) and some $\mathbb{L}^2_p$. Furthermore, the vertices F, F_1, F_{12}, F_2 could lie on an exceptional hyperbola. We will see here that discrete maximal surfaces, in particular, can and do have faces in non-spacelike planes, i.e. singular faces. □

Like in [**13**], we give a geometric definition of discrete maximal surfaces in $\mathbb{R}^{2,1}$, motivated by Proposition 3.

Definition 10. Let $F : \mathbb{D} \to \mathbb{R}^{2,1}$ be a discrete isothermic surface. F is a *discrete maximal surface* if its dual F^* can be chosen to lie in $\mathbb{H}^2_+ \cup \mathbb{H}^2_-$.

We will give a definition for mean curvature of discrete isothermic surfaces in $\mathbb{R}^{2,1}$, as in Definition 13. We first make some preparations in Definitions 11 and 12, and Lemma 5. For the case of $\mathbb{R}^3$, see [**15**], [**17**].

Definition 11. Let $F : \mathbb{D} \to \mathbb{R}^{2,1}$ be a discrete isothermic surface, and let $l : \mathbb{D} \to \{\text{straight lines in } \mathbb{R}^{2,1}\}$ with $F_{m,m} \in l_{m,m}$. (F, l) is called a *line congruence net* if every pair of neighbouring lines, either $l_{m,n}$ and $l_{m+1,n}$, and also $l_{m,n}$ and $l_{m,n+1}$, intersect, for any edge $(m, n)(m+1, n)$ or $(m, n)(m, n+1)$, respectively, with endpoints in $\mathbb{D}$.

A line congruence has a 1-parameter family of parallel line congruences $\{F_t \mid t \in \mathbb{R}\}$ that have parallel faces and share the same lines, i.e. $F^t_{m,n} \in l_{m,n}$, and this leads to a definition of Gauss and mean curvatures for discrete surfaces (Definition 13), as we will now explain. The oriented area of an n-gon P with vertices $(p_0, p_1, \cdots, p_{n-1})$ and lying in a spacelike plane with timelike unit normal N is

$$A(P) = \frac{1}{2} \sum_{i=0}^{n-1} \det(p_i, p_{i+1}, N) \tag{32}$$

with $p_0 = p_n$. For any given planar polygon P, the set of all polygons with parallel corresponding edges to those of P forms a vector space.

Definition 12. Let $P = (p_0, p_1, \cdots, p_{n-1})$ and $Q = (q_0, q_1, \cdots, q_{n-1})$ be polygons (in planes with unit normal N) with parallel corresponding edges. Then

$$A(P, Q) := \frac{1}{4} \sum_{i=0}^{n-1} (\det(p_i, q_{i+1}, N) + \det(q_i, p_{i+1}, N)) \tag{33}$$

is called the mixed area of P and Q.

We say that quadrilaterals P and Q (so $n = 4$) with parallel corresponding edges are *dual* if $A(P, Q) = 0$.

Lemma 5. The mixed area has the following properties:

(1) $A(P, Q)$ is a symmetric bilinear form on the vector space of polygons with parallel corresponding edges.

(2) $A(P) = A(P, P)$.
(3) $A(P + tQ) = A(P) + 2t(P, Q) + t^2 A(Q)$.
(4) Quadrilaterals $P = (p_0, p_1, p_2, p_3)$ and $Q = (q_0, q_1, q_2, q_3)$ with parallel corresponding edges are dual to each other if and only if their opposite diagonals are parallel, like the property in Proposition 6.

For a given line congruence net (F, l), we define a normal map N by choosing a normal $N_{m,n}$ at one vertex (m, n) such that $F_{m,n} + N_{m,n} \in l_{m,n}$ and determine the length of the normals at all other vertices so that $F + N \in l$ is a mesh with edges parallel to the corresponding edges of F. Then $F + N$ has quadrilateral faces parallel to the corresponding faces of F, and N does as well, so we have

$$A(F + tN) = A(F) + 2tA(F, N) + t^2 A(N).$$

Note that the choice of N is not unique.

Like in [**15**], [**17**], [**37**], where the Steiner formula for smooth surfaces was used to motivate the definitions, we define the mean and Gauss curvatures of discrete surfaces as in Definition 13 below. We now include the additional assumption that $\langle N, N\rangle$ is constantly -1, like in the first item of Definition 9.

Definition 13. Let (F, l) be a line congruence net with normal map N such that $\langle N, N\rangle \equiv -1$. Then the mean curvature $\hat{H}$ and the Gauss curvature K are defined as

$$\hat{H} = -\frac{A(F, N)}{A(F)},\ K = \frac{A(N)}{A(F)}$$

on each quadrilateral (F, F_1, F_{12}, F_2).

The following proposition tells us that the mean curvatures in the two senses above are equal when those mean curvatures are constant.

Proposition 7. When $\hat{H}$ in Definition 13 is constant, there exist h, H satisfying the conditions in Definition 9, and $H = \hat{H}$. Conversely, when there exist h, H satisfying the conditions in Definition 9, then $\hat{H} = H$. Furthermore, $H = \hat{H} = 0$ if and only if Definition 10 is satisfied and we can take $N = F^*$.

Proof. For $\hat{H} \neq 0$ in Definition 13, we have

$$A(F, N) = -\hat{H}A(F) \Leftrightarrow A(F, F + \hat{H}^{-1}N) = 0 \Leftrightarrow F^* = \alpha(F + \hat{H}^{-1}N) \tag{34}$$

for some constant $\alpha \in \mathbb{R} \setminus \{0\}$, by Proposition 6 and Lemma 5. On the other hand, when there exist constants $H \neq 0$ and $h \neq 0$ as in Definition 9, we have $\Delta_i F^* = h^{-1}H(\Delta_i F + H^{-1}\Delta_i N)$. Setting $\alpha = h^{-1}H$, we have

$$\Delta_i F^* = \alpha(\Delta_i F + H^{-1}\Delta_i N). \tag{35}$$

One solution of (35) is F^* as on the right-hand side of (34), and the second sentence of the proposition follows when $H \neq 0$.

To see that the first sentence holds as well when $\hat{H} \neq 0$ is constant, we take α as in (34), and Definition 9 holds with $H = \hat{H}$ and $h = \alpha^{-1}H$.

When $\hat{H} \equiv 0$ in Definition 13, we have $A(F, N) = 0$. So we can take $N = F^*$ and Definition 10 holds. Furthermore, Definition 9 holds with $H = 0$ and $h = 1$.

When Definition 9 holds with $H = 0$, we have $\Delta_i N = h\Delta_i F^*$, so we can again take $F^* = N$, and again Definition 10 holds. Furthermore, $A(F, N) = 0$, so $\hat{H} = 0$ in Definition 13. □

In addition, discrete maximal surfaces as defined here also satisfy a separate characterization found in [**19**]. This is the content of Lemma 6. The papers [**23**], [**22**], [**21**] unify discrete surfaces in Riemannian and Lorentzian spaceforms by using a Lie sphere geometric description. In particular, discrete CMC surfaces are described via constant and linear conserved quantities.

LEMMA 6. Discrete maximal surfaces as defined in Definition 10 satisfy that the mean curvature in the sense of [**19**] is also zero.

Proof. (The Lie sphere geometry employed here does not appear elsewhere in this paper.) Taking a Lie sphere geometric approach to discrete surfaces [**19**], we denote the 6-dimensional Lorentz space with Lorentz metric by

$$\mathbb{R}^{4,2} := \{x = (x_1, x_2, x_3, x_4, x_5, x_6)^t \mid x_i \in \mathbb{R}\ (i = 1, 2, 3, 4, 5, 6)\},$$

$$(x, y) = -x_1y_1 + x_2y_2 + x_3y_3 + x_4y_4 + x_5y_5 - x_6y_6.$$

Taking

$$\mathfrak{p} = (0, 0, 1, 0, 0, 0)^t,\ \mathfrak{q} = (1, -1, 0, 0, 0, 0)^t,$$

we can identify 3-dimensional Minkowski space $R^{2,1}$ with

$$\mathfrak{B} := \{\mathfrak{y} \in \mathbb{R}^{4,2} \mid (\mathfrak{y}, \mathfrak{y}) = 0, (\mathfrak{y}, \mathfrak{q}) = 0, (\mathfrak{y}, \mathfrak{p}) = -1\}.$$

Let F be a discrete maximal surface with dual surface F^* as in Definition 8. Taking lifts

$$F \mapsto \mathfrak{f} := \left(\tfrac{1}{2}(1 + \|F\|^2), \tfrac{1}{2}(1 - \|F\|^2), 0, F^t\right)^t,\ F^* \mapsto \mathfrak{f}^* := \left((F, F^*), -(F, F^*), -1, (F^*)^t\right)^t,$$

we have

$$\mathfrak{f}_1 - \mathfrak{f} = \left(\tfrac{1}{2}(\|F_1\|^2 - \|F\|^2), -\tfrac{1}{2}(\|F_1\|^2 - \|F\|^2), 0, F_1^t - F^t\right)^t. \tag{36}$$

F is also a dual surface of F^*, so, for some cross ratio factorizing function $\alpha > 0$,

$$F_1 - F = \alpha\frac{F_1^* - F^*}{d},\ d := \|F_1^* - F^*\|^2, \text{ and}$$

$$\left\|F_1 - \alpha\frac{F_1^*}{d}\right\|^2 = \left\|F - \alpha\frac{F^*}{d}\right\|^2 \Rightarrow \|F_1\|^2 - \|F\|^2 = \frac{2\alpha}{d}(\langle F_1, F_1^*\rangle - \langle F, F^*\rangle), \tag{37}$$

because $\|F^*\|^2 = -1$. Inserting (37) into (36), we have

$$\mathfrak{f}_1 - \mathfrak{f} = \frac{\alpha}{\|F_1^* - F^*\|^2}(\mathfrak{f}_1^* - \mathfrak{f}^*).$$

Similarly, for the cross ratio factorizing function $\beta > 0$,

$$\mathfrak{f}_2 - \mathfrak{f} = \frac{-\beta}{\|F_2^* - F^*\|^2}(\mathfrak{f}_2^* - \mathfrak{f}^*).$$

In particular, $\mathfrak{f}_1 - \mathfrak{f} \parallel \mathfrak{f}_1^* - \mathfrak{f}^*$ and $\mathfrak{f}_2 - \mathfrak{f} \parallel \mathfrak{f}_2^* - \mathfrak{f}^*$. On the other hand, by (31) with F and F^* reversed, $F_{12} - (\alpha+\beta)\|F_1^* - F_2^*\|^{-2}F_1^* = F - (\alpha+\beta)\|F_1^* - F_2^*\|^{-2}F_2^*$, implying

$$\|F_{12}\|^2 - \|F\|^2 = \frac{2(\alpha+\beta)}{\|F_1^* - F_2^*\|^2}(\langle F_{12}, F_1^*\rangle - \langle F, F_2^*\rangle). \tag{38}$$

Similarly,

$$\|F_{12}\|^2 - \|F\|^2 = \frac{2(\alpha+\beta)}{\|F_1^* - F_2^*\|^2}(\langle F, F_1^*\rangle - \langle F_{12}, F_2^*\rangle), \text{ implying}$$

$$\langle F_{12}, F_1^*\rangle - \langle F, F_2^*\rangle = \langle F, F_1^*\rangle - \langle F_{12}, F_2^*\rangle. \tag{39}$$

Using Equation (38), one can check that $\mathfrak{f}_{12} - \mathfrak{f}$ equals

$$\frac{\alpha+\beta}{\|F_1^* - F_2^*\|^2}\left(\langle F_{12}, F_1^*\rangle - \langle F, F_2^*\rangle, -(\langle F_{12}, F_1^*\rangle - \langle F, F_2^*\rangle), 0, (F_1^*)^t - (F_2^*)^t\right)^t. \tag{40}$$

Note that

$$\alpha = \langle F_{12} - F_2, F_{12}^* - F_2^*\rangle = \langle F_1 - F, F_1^* - F^*\rangle, \tag{41}$$

$$-\beta = \langle F_{12} - F_1, F_{12}^* - F_1^*\rangle = \langle F_2 - F, F_2^* - F^*\rangle. \tag{42}$$

Subtracting (42) from (41) and inserting (39) into the resulting equation, we have

$$-2(\langle F_{12}, F_1^*\rangle + \langle F_2, F_2^*\rangle - \langle F_1, F_1^*\rangle - \langle F, F_2^*\rangle) - \langle F_1 - F_2, F_{12}^* + F^*\rangle = 0.$$

Again by Equation (31) with F and F^* reversed,

$$\langle F_1 - F_2, F_{12}^* + F^*\rangle = \frac{\alpha+\beta}{\|F_{12}^* - F^*\|^2}\langle F_{12}^* - F^*, F_{12}^* + F^*\rangle = 0,$$

because $\|F^*\|^2 = -1$. Thus we have

$$\langle F_{12}, F_1^*\rangle - \langle F, F_2^*\rangle = \langle F_1, F_1^*\rangle - \langle F_2, F_2^*\rangle. \tag{43}$$

Inserting (43) into (40), we have $\mathfrak{f}_{12} - \mathfrak{f} = (\alpha+\beta)\|F_1^* - F_2^*\|^{-2}(\mathfrak{f}_1^* - \mathfrak{f}_2^*)$. Similarly, $\mathfrak{f}_1 - \mathfrak{f}_2 = (\alpha+\beta)\|F_{12}^* - F^*\|^{-2}(\mathfrak{f}_{12}^* - \mathfrak{f}^*)$. In particular, we have

$$\mathfrak{f}_{12} - \mathfrak{f} \parallel \mathfrak{f}_1^* - \mathfrak{f}_2^*,\ \mathfrak{f}_1 - \mathfrak{f}_2 \parallel \mathfrak{f}_{12}^* - \mathfrak{f}^*.$$

In conclusion, the space form projection $(\mathfrak{f}, \mathfrak{f}^*)$ is maximal, that is, $H \equiv 0$ in the sense of [**19**], because $\mathfrak{f}$ and $\mathfrak{f}^*$ are Koenigs dual lifts in $\mathbb{R}^{4,2}$. (See Thm 2.6 in [**19**].) □

Quadrilaterals of a discrete maximal surface do not always lie in a spacelike plane, and we define those that do not to be the "singularities" (singular faces) of the surface, as in Definition 14 below. By Theorem 4, they appear precisely when the corresponding discrete holomorphic function g lies near $\mathbb{S}^1$ (in the sense given in that theorem). This is natural, because in the smooth case, a maximal surface has singularities when its corresponding holomorphic function g (stereographic projection of the Gauss map) satisfies $|g| = 1$.

DEFINITION 14. Let F be a discrete maximal surface. The face $\mathcal{F} = (F, F_1, F_{12}, F_2)$ is a *singular face* if $\mathcal{F}$ lies on a non-spacelike plane. In particular, $\mathcal{F}$ is a *GVP singular face* if $\mathcal{F}$ has no lightlike edges and is a *NVP singular face* if otherwise.

Remark. For a GVP singular face $\mathcal{F}$, we can compute the cross ratio via Definition 6. However, if $\mathcal{F}$ is NVP, this will not work. In Section 7, we will use a different method to define the cross ratio of an NVP singular face. □

6. Proof of Theorem 3

We first prove one direction of Theorem 3.

Let g be a discrete holomorphic function with cross ratio factorizing functions α_m, β_n. Consider

$$g \mapsto F^* := \begin{pmatrix} \frac{-2\mathrm{Re}(g)}{|g|^2-1} \\ \frac{-2\mathrm{Im}(g)}{|g|^2-1} \\ \frac{|g|^2+1}{|g|^2-1} \end{pmatrix} \in \mathbb{H}^2_+ \cup \mathbb{H}^2_- \subset \mathbb{R}^{2,1}.$$

This discrete surface F^* is the image of g under the inverse of a stereographic projection. Using Equation (27), one can check that generically

$$cr(g, g_1, g_{12}, g_2) = cr(F^*, F_1^*, F_{12}^*, F_2^*). \tag{44}$$

We can still establish Equation (44) in non-generic cases, and we will deal with that at the end of this proof.

Still assuming genericity, we define the surface F by (23). This F exists if and only if the compatibility condition $\Delta_1(\Delta_2 F) = \Delta_2(\Delta_1 F)$ holds. Note that, by the second equation in (23),

$$\Delta_1(\Delta_2 F) = -\frac{\beta_n}{4} \begin{pmatrix} \frac{1+g_1g_{12}}{\Delta_2 g_1} + \frac{1+\bar{g_1}\bar{g_{12}}}{\overline{\Delta_2 g_1}} - \frac{1+gg_2}{\Delta_2 g} - \frac{1+\bar{g}\bar{g_2}}{\overline{\Delta_2 g}} \\ \frac{\mathrm{i}(1-g_1g_{12})}{\Delta_2 g_1} - \frac{\mathrm{i}(1-\bar{g_1}\bar{g_{12}})}{\overline{\Delta_2 g_1}} - \frac{\mathrm{i}(1-gg_2)}{\Delta_2 g} + \frac{\mathrm{i}(1-\bar{g}\bar{g_2})}{\overline{\Delta_2 g}} \\ -\frac{g_1+g_{12}}{\Delta_2 g_1} - \frac{\bar{g_1}+\bar{g_{12}}}{\overline{\Delta_2 g_1}} + \frac{g+g_2}{\Delta_2 g} + \frac{\bar{g}+\bar{g_2}}{\overline{\Delta_2 g}} \end{pmatrix}. \tag{45}$$

Using

$$\beta_n = -\alpha_m \frac{\Delta_2 g}{\Delta_1 g} \frac{\Delta_2 g_1}{\Delta_1 g_2} = -\alpha_m \frac{\overline{\Delta_2 g}}{\overline{\Delta_1 g}} \frac{\overline{\Delta_2 g_1}}{\overline{\Delta_1 g_2}}$$

in Equation (45), we have

$$\begin{aligned} \Delta_1(\Delta_2 F) &= \frac{\alpha_m}{4} \begin{pmatrix} \frac{\Delta_2 g(1+g_1g_{12})}{\Delta_1 g \Delta_1 g_2} + \frac{\overline{\Delta_2 g}(1+\bar{g_1}\bar{g_{12}})}{\overline{\Delta_1 g}\,\overline{\Delta_1 g_2}} - \frac{\Delta_2 g_1(1+gg_2)}{\Delta_1 g \Delta_1 g_2} - \frac{\overline{\Delta_2 g_1}(1+\bar{g}\bar{g_2})}{\overline{\Delta_1 g}\,\overline{\Delta_1 g_2}} \\ \frac{\mathrm{i}\Delta_2 g(1-g_1g_{12})}{\Delta_1 g \Delta_1 g_2} - \frac{\mathrm{i}\overline{\Delta_2 g}(1-\bar{g_1}\bar{g_{12}})}{\overline{\Delta_1 g}\,\overline{\Delta_1 g_2}} - \frac{\mathrm{i}\Delta_2 g_1(1-gg_2)}{\Delta_1 g \Delta_1 g_2} + \frac{\mathrm{i}\overline{\Delta_2 g_1}(1-\bar{g}\bar{g_2})}{\overline{\Delta_1 g}\,\overline{\Delta_1 g_2}} \\ -\frac{\Delta_2 g(g_1+g_{12})}{\Delta_1 g \Delta_1 g_2} - \frac{\overline{\Delta_2 g}(\bar{g_1}+\bar{g_{12}})}{\overline{\Delta_1 g}\,\overline{\Delta_1 g_2}} + \frac{\Delta_2 g_1(g+g_2)}{\Delta_1 g \Delta_1 g_2} + \frac{\overline{\Delta_2 g_1}(\bar{g}+\bar{g_2})}{\overline{\Delta_1 g}\,\overline{\Delta_1 g_2}} \end{pmatrix} \\ &= \Delta_2 \left(\frac{\alpha_m}{2} \mathrm{Re} \begin{pmatrix} \frac{1+gg_1}{\Delta_1 g} \\ \frac{\mathrm{i}(1-gg_1)}{\Delta_1 g} \\ -\frac{g+g_1}{\Delta_1 g} \end{pmatrix} \right) = \Delta_2(\Delta_1 F). \end{aligned} \tag{46}$$

Thus the compatibility condition for existence of F is satisfied.

Next, we wish to establish that F and F^* are dual. Still assuming genericity, consider the equation

$$\begin{aligned}\frac{\alpha_m}{\|\Delta_1 F^*\|^2}\Delta_1 F^* &\cong \frac{\alpha_m(|g_1|^2-1)(|g|^2-1)}{4|g_1-g|^2}\begin{pmatrix}\frac{-(|g|^2-1)(g_1+\bar{g_1})+(|g_1|^2-1)(g+\bar{g})}{(|g_1|^2-1)(|g|^2-1)}\\ \frac{-2(|g_1|^2-|g|^2)}{(|g_1|^2-1)(|g|^2-1)}\end{pmatrix}\\ &\cong \frac{1}{2}\mathrm{Re}\left(\frac{\alpha_m}{\Delta_1 g}\begin{pmatrix}1+g_{m+1,n}g_{m,n}\\ \mathrm{i}-\mathrm{i}g_{m+1,n}g_{m,n}\\ -(g_{m+1,n}+g_{m,n})\end{pmatrix}\right), \qquad (47)\end{aligned}$$

and similarly, the equation

$$\frac{-\beta_m}{\|\Delta_2 F^*\|^2}\Delta_2 F^* = -\frac{1}{2}\mathrm{Re}\left(\frac{\beta_n}{\Delta_2 g}\begin{pmatrix}1+g_{m,n+1}g_{m,n}\\ \mathrm{i}-\mathrm{i}g_{m,n+1}g_{m,n}\\ -(g_{m,n+1}+g_{m,n})\end{pmatrix}\right). \qquad (48)$$

Thus

$$\Delta_1 F = \alpha_m \frac{\Delta_1 F^*}{\|\Delta_1 F^*\|^2}, \quad \Delta_2 F = -\beta_n \frac{\Delta_2 F^*}{\|\Delta_2 F^*\|^2}.$$

A computation shows

$$cr(F^*, F_1^*, F_{12}^*, F_2^*) = cr(F, F_1, F_{12}, F_2), \qquad (49)$$

and so α_m and β_n are cross ratio factorizing functions for F as well.

Thus, by Proposition 7, F and F^* are dual, and then, by Definition 10, F is discrete maximal.

Finally, we show the converse direction in Theorem 3. Let F be a discrete maximal surface. Then by definition, there exists a dual F^* that is discrete isothermic and inscribed in $\mathbb{H}^2_+ \cup \mathbb{H}^2_-$. Take

$$g := \psi \circ F^*,$$

where ψ is a stereographic projection $\psi : \mathbb{H}^2_+ \cup \mathbb{H}^2_- \to \mathbb{C}$. Then g is a discrete holomorphic function. One can check that this g produces F via Equation (23), completing the proof in the generic case.

In the case that F has an NVP singular face, at least one of the edge vectors $F - F_1$, $F - F_2$, $F_2 - F_{12}$ and $F_1 - F_{12}$ is lightlike or zero, because at least one of F^*, F_1^*, F_{12}^* and F_2^* blows up. So, $cr(F, F_1, F_{12}, F_2)$ and $cr(F^*, F_1^*, F_{12}^*, F_2^*)$ blow up when (F, F_1, F_{12}, F_2) is an NVP singular face. However, we can treat the cross ratio of NVP singular faces by a limiting process instead, as we do in Section 7. With that treatment, we can establish Equations (44) and (49) in non-generic cases as well, and thus will have also covered the non-generic cases in this proof of Theorem 3.

7. Cross ratios of NVP singular faces

In this section the cross ratio of NVP singular faces is discussed. NVP singular faces occur when at least one of the four vertices of the corresponding discrete holomorphic function lie in $\mathbb{S}^1$. This results in lightlike edges on the singular faces, so we cannot compute the cross ratio of NVP singular faces in the usual ways

as in Section 3. However, by applying some infinitesimal variations using Möbius transformations, we can treat the cross ratio of NVP singular faces in the limit, as in Lemma 7 below.

DEFINITION 15. We call a family of Möbius transformations $\mathcal{M}_\epsilon : \mathbb{C} \cup \{\infty\} \to \mathbb{C} \cup \{\infty\}$, $\epsilon \in (-\epsilon_0, \epsilon_0) \subset \mathbb{R}$, a *Möbius transform variation* of $\mathbb{C} \cup \{\infty\}$ if $\mathcal{M}_0$ is the identity map and the $\mathcal{M}_\epsilon$ change continuously with respect to ϵ.

LEMMA 7 (and Definition). Let $\mathscr{G} = (g, g_1, g_{12}, g_2)$ be a quadrilateral of some discrete holomorphic function and let $\mathscr{F} = (F, F_1, F_{12}, F_2)$ be a NVP singular face determined from $\mathscr{G}$. Let $\mathcal{M}_\epsilon$ be a Möbius transform variation such that

$$g_\epsilon = \mathcal{M}_\epsilon g,\ g_{1,\epsilon} = \mathcal{M}_\epsilon g_1,\ g_{12,\epsilon} = \mathcal{M}_\epsilon g_{12},\ g_{2,\epsilon} = \mathcal{M}_\epsilon g_2 \notin \mathbb{S}^1 \ \text{ for } \epsilon \neq 0,$$

This variation preserves the cross ratio of (g, g_1, g_{12}, g_2). Let $\mathscr{G}^\epsilon := (g_\epsilon, g_{1,\epsilon}, g_{12,\epsilon}, g_{2,\epsilon})$ be the resulting quadrilateral in $\mathbb{C}$ and let $\mathscr{F}^\epsilon$ be the well-defined quadrilateral given by $\mathscr{G}^\epsilon$ via Equation (23). Defining the *limit-cross-ratio* of the NVP singular face as

$$lcr(\mathscr{F}) := \lim_{\epsilon \to 0} cr(\mathscr{F}^\epsilon)\ (= cr(\mathscr{F}^\epsilon) \text{ for all } \epsilon \in (-\epsilon_0, \epsilon_0) \setminus \{0\}),$$

we find that $lcr(\mathscr{F})$ exists and is independent of choice of $\mathcal{M}_\epsilon$, and furthermore

$$lcr(\mathscr{F}) = cr(g, g_1, g_{12}.g_2) \in \mathbb{R}.$$

Proof. $\mathcal{M}_\epsilon$ is a family of Möbius transformations, so $cr(g, g_1, g_{12}, g_2) = cr(g_\epsilon, g_{1,\epsilon}, g_{12,\epsilon}, g_{2,\epsilon})$ for all $\epsilon \in (-\epsilon, \epsilon_0)$. Let F_ϵ be a discrete surface given by $\mathcal{M}_\epsilon g$ via Equation (23). By Equation (46), $\Delta_1\Delta_2 F_\epsilon = \Delta_2\Delta_1 F_\epsilon$, so $\mathscr{F}^\epsilon$ is well-defined, and by Equations (44) and (49) we have

$$cr(F_\epsilon, F_{1,\epsilon}, F_{12,\epsilon}, F_{2,\epsilon}) = cr(g_\epsilon, g_{1,\epsilon}, g_{12,\epsilon}, g_{2,\epsilon}) = cr(g, g_1, g_{12}, g_2),$$

and $\mathscr{F}_\epsilon$ has no lightlike edges, because we chose $g_\epsilon,\ g_{1,\epsilon},\ g_{12,\epsilon},\ g_{2,\epsilon}$ so that none of $g_\epsilon,\ g_{1,\epsilon},\ g_{12,\epsilon},\ g_{2,\epsilon} \notin \mathbb{S}^1$ for $\epsilon \neq 0$. Because $\mathscr{F}^\epsilon$ is a part of a discrete maximal surface, which is in particular a discrete isothermic surface with singular faces, $\mathscr{F}_\epsilon$ is co-planar. This means that the cross ratio of $\mathscr{F}_\epsilon$ does not depend on the choice of $\epsilon \neq 0$. Thus we have

$$\lim_{\epsilon \to 0} \mathscr{F}_\epsilon = \mathscr{F}, \quad \lim_{\epsilon \to 0} cr(\mathscr{F}_\epsilon) = cr(g, g_1, g_{12}, g_2),$$

proving the lemma. □

8. Proof of Theorem 4

Let g be a discrete holomorphic function, and let F be the maximal surface given by g as in Theorem 1. Let $\mathcal{F}$ be a face, for which the four values of g (at the vertices) lie in a circle which may or may not intersect $\mathbb{S}^1$. Since the edges of F^* are parallel to the corresponding edges of F, to consider whether $\mathcal{F}$ is singular, it suffices to consider whether the corresponding face $(F^*, F_1^*, F_{12}^*, F_2^*)$ on F^* is in a non-spacelike plane.

Let $\mathcal{C} \subset \mathbb{C}$ be a circle passing through the vertices of (g, g_1, g_{12}, g_2) with center $a + \mathrm{i}b$ and radius r. The face $(F^*, F_1^*, F_{12}^*, F_2^*)$ is given by the image of the inverse

of stereographic projection of (g, g_1, g_{12}, g_2). Taking $p \in \mathcal{C} \setminus \mathbb{S}^1$, the image of the inverse stereographic projection map

$$\mathbb{C} \ni p := x + \mathrm{i}y \mapsto \left(-\frac{2x}{|p|^2-1}, -\frac{2y}{|p|^2-1}, \frac{|p|^2+1}{|p|^2-1} \right)^t \in \mathbb{H}^2_+ \cup \mathbb{H}^2_-$$

lies in the plane

$$\mathcal{P} := \{(x_1, x_2, x_0)^t \in \mathbb{R}^{2,1} | \langle (x_1, x_2, x_0)^t, n \rangle = -(a^2 + b^2 - r^2 - 1)\}$$

with normal $n = (-2a, -2b, a^2 + b^2 - r^2 + 1)^t$. Thus $F^*, F_1^*, F_{12}^*, F_2^* \in \mathcal{P}$ and n is normal to the face $(F^*, F_1^*, F_{12}^*, F_2^*)$. The plane $\mathcal{P}$ is not spacelike exactly when n is not timelike. Because $\|n\|^2 = -\{(a^2+b^2) - (r-1)^2\}\{(a^2+b^2) - (r+1)^2\}$, n not being timelike is equivalent to

$$|r-1| \leq \sqrt{a^2+b^2} \leq r+1. \tag{50}$$

On the other hand, also $\mathcal{C}$ intersects $\mathbb{S}^1$ if and only if (50) holds, proving the theorem.

9. Proof of Theorem 5

Now we give a classification of GVP and NVP singular faces by considering separate cases that cover all possibilities. Throughout this section, by isometries and scalings of $\mathbb{R}^{2,1}$, $(F^*, F_1^*, F_{12}^*, F_2^*)$ will be transformed to corresponding points that we denote by (X_1, X_2, X_3, X_4).

Case 1: GVP singular faces for which the four vertices F^*, F_1^*, F_{12}^*, F_2^* lie in one connected component of a hyperbola. In this case, the plane passing through $(F^*, F_1^*, F_{12}^*, F_2^*)$ is timelike. By an isometry and appropriate scaling, without loss of generality, we can transform the vertices $(F^*, F_1^*, F_{12}^*, F_2^*)$ to four points (X_1, X_2, X_3, X_4) lying in

$$\{(x_1, x_2, x_0)^t \in \mathbb{L}^2 |\ x_2 = 1\}. \tag{51}$$

For example, like in Figure 4, setting

$$\begin{aligned} X_1 = (\sinh(\alpha_1), 1, \cosh(\alpha_1))^t,\ X_2 = (\sinh(\alpha_2), 1, \cosh(\alpha_2))^t, \\ X_3 = (\sinh(\alpha_3), 1, \epsilon_1 \cosh(\alpha_3))^t,\ X_4 = (\sinh(\alpha_4), 1, \epsilon_2 \cosh(\alpha_4))^t \end{aligned} \tag{52}$$

for some $\alpha_j \in \mathbb{R}$, and with $\epsilon_1 = \epsilon_2 = 1$, one can check that

$$cr(X_1, X_2, X_3, X_4) = cr(F^*, F_1^*, F_{12}^*, F_2^*) = cr(F, F_1, F_{12}, F_2) = -\frac{\sinh\frac{\alpha_1-\alpha_2}{2}\sinh\frac{\alpha_3-\alpha_4}{2}}{\sinh\frac{\alpha_2-\alpha_3}{2}\sinh\frac{\alpha_1-\alpha_4}{2}}.$$

Since $cr(F, F_1, F_{12}, F_2) < 0$, (F, F_1, F_{12}, F_2) is embedded and the vertices F, F_1, F_{12}, F_2 lies in one component of the intersection of a translated light cone and a timelike plane.

Such GVP singular faces appear in Examples 3 and 5 in Section 10.

Case 2: GVP singular faces for which two vertices amongst F^*, F_1^*, F_{12}^*, F_2^* lie in one connected component of a hyperbola and other two points lie in the other component. Here, like in Case 1, we can assume the vertices X_1,

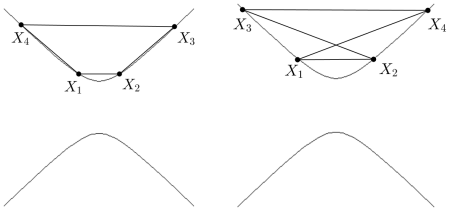

FIGURE 4. the Gauss map of Case 1

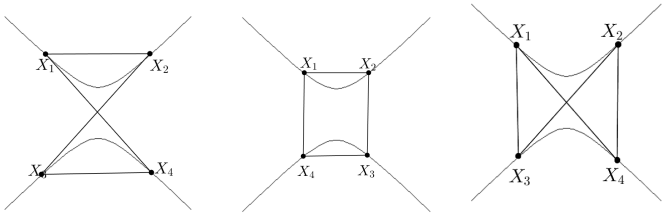

FIGURE 5. the Gauss map of Case 2

X_2, X_3, X_4 lie in the set (51). For example, like in Figure 5, having X_1, X_2, X_3, X_4 as in (52) for some $\alpha_j \in \mathbb{R}$, but now with $\epsilon_1 = \epsilon_2 = -1$, one can check that

$$cr(F, F_1, F_{12}, F_2) = -\frac{\sinh\frac{\alpha_1-\alpha_2}{2}\sinh\frac{\alpha_3-\alpha_4}{2}}{\cosh\frac{\alpha_2+\alpha_3}{2}\cosh\frac{\alpha_1+\alpha_4}{2}}.$$

Since again $cr(F, F_1, F_{12}, F_2) < 0$, (F, F_1, F_{12}, F_2) is non-embedded like in the left-hand picture in Figure 5 and (F, F_1, F_{12}, F_2) lies on the intersection of a translated light cone and a timelike plane.

Such GVP singular faces appear in Examples 3 and 5 in Section 10.

Case 3: GVP singular faces for which three vertices amongst F^*, F_1^*, F_{12}^*, F_2^* lie in one connected component of a hyperbola and the other lies in the other component. Here again, like in Case 1, we can assume X_1, X_2, X_3, X_4 lie in (51). Then, like in the left-hand picture in Figure 6, having X_1, X_2, X_3, X_4 as in (52) for some $\alpha_j \in \mathbb{R}$, but now with $-\epsilon_1 = \epsilon_2 = 1$, one can check that

$$cr(F, F_1, F_{12}, F_2) = \frac{\sinh\frac{\alpha_1-\alpha_2}{2}\cosh\frac{\alpha_3+\alpha_4}{2}}{\cosh\frac{\alpha_2+\alpha_3}{2}\sinh\frac{\alpha_1-\alpha_4}{2}}.$$

Alternately, like in the right-hand picture in Figure 6, if $\epsilon_1 = -\epsilon_2 = 1$, one can check that

$$cr(F, F_1, F_{12}, F_2) = -\frac{\sinh\frac{\alpha_1-\alpha_2}{2}\cosh\frac{\alpha_3+\alpha_4}{2}}{\sinh\frac{\alpha_2-\alpha_3}{2}\cosh\frac{\alpha_1+\alpha_4}{2}}.$$

As $cr(F, F_1, F_{12}, F_2) < 0$, (F, F_1, F_{12}, F_2) is a face like in the left-hand picture of Figure 6. Furthermore, we have the following proposition, which is the unique case where the vertices of a singular face of F lie in an exceptional hyperbola:

PROPOSITION 8. When F^*, F_1^*, F_{12}^*, F_2^* are placed as in the left-hand picture in Figure 7, the quadrilateral (F, F_1, F_{12}, F_2) lies in an exceptional hyperbola.

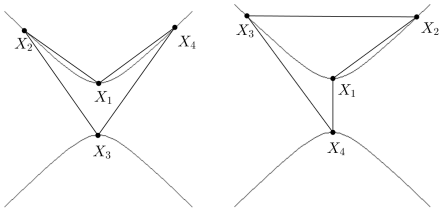

FIGURE 6. the Gauss map of Case 3

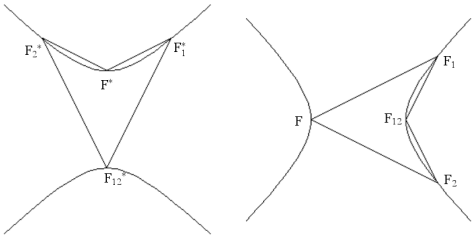

FIGURE 7. a quadrilateral of a Gauss map on the left-hand side, and its dual quadrilateral (a GVP singular face) on the right-hand side

Proof. By way of contradiction, assume that $F^* = X_1$, $F_1^* = X_2$, $F_{12}^* = X_3$ and $F_2^* = X_4$ with $-\epsilon_1 = \epsilon_2 = 1$ and $\alpha_4 < \alpha_1 < \alpha_2$ (or $\alpha_4 < \alpha_1 < \alpha_2$) in (52) (other cases can be handled similarly), and that (F, F_1, F_{12}, F_2) lies on the intersection $\mathcal{H}$ of a translated light cone and a timelike plane. By Proposition 6, $F_1^* - F_2^* \parallel F_{12} - F$. In particular, $F_{12} - F$ is spacelike. So F_{12}, F lie in one component of the hyperbola $\mathcal{H}$. Similarly, $F_{12}^* - F^* \parallel F_1 - F_2$, and $F_1 - F_2$ is timelike. So F_1 lies in one component of $\mathcal{H}$ and F_2 lies in the other one. So exactly one of F_1 and F_2 lies in the same component of $\mathcal{H}$ that F and F_{12} lie in. However, both $F_{12} - F_1$ and $F_{12} - F_2$ are timelike. So both F_1 and F_2 do not lie in the component of $\mathcal{H}$ containing F and F_{12}. This contradiction proves the proposition. □

Such GVP singular faces appear in Examples 3 and 5 in Section 10.

Case 4: GVP singular faces for which three vertices amongst F^*, F_1^*, F_{12}^*, F_2^* lie in the intersection of a translated light cone and a lightlike plane. Here, we can assume X_1, X_2, X_3, X_4 lie in the set

$$\{(2t, t^2 - 1, t^2 + 1)^t \in \mathbb{L}^2 | t \in \mathbb{R}\}.$$

Transforming F^*, F_1^*, F_{12}^*, F_2^* to

$$X_1 = (2t_1, t_1^2 - 1, t_1^2 + 1)^t,\ X_2 = (2t_2, t_2^2 - 1, t_2^2 + 1)^t,$$

$$X_3 = (2t_3, t_3^2 - 1, t_3^2 + 1)^t,\ X_4 = (2t_4, t_4^2 - 1, t_4^2 + 1)^t$$

for some $t_j \in \mathbb{R}$, one can check that

$$cr(F, F_1, F_{12}, F_2) = -\frac{(t_1 - t_2)(t_3 - t_4)}{(t_2 - t_3)(t_4 - t_1)}.$$

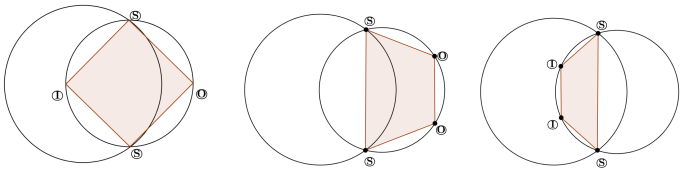

FIGURE 8. two points lying in $\mathbb{S}^1$

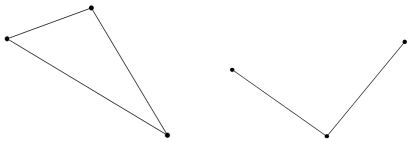

FIGURE 9. NVP singular faces in F, as in Case 6

Using $cr(F, F_1, F_{12}, F_2) < 0$, (F, F_1, F_{12}, F_2) is embedded and (F, F_1, F_{12}, F_2) lies on the intersection of a translated light cone and a lightlike plane. For example, such a GVP singular face appears when we choose the discrete holomorphic function $g = (-1 + \frac{6}{5}m) + \mathrm{i}(-\frac{4}{5} + \frac{8}{5}n)$. Then the face $(F_{1,0}, F_{2,0}, F_{2,1}, F_{1,1})$ is such a GVP singular face.

In conclusion, the possible cases of GVP singular faces that appear in discrete maximal surfaces are exhibited in the left-hand pictures in Figures 4 and 5, and in the right-hand picture in Figure 7.

Next, we give a classification of NVP singular faces. For this, first we consider where the vertices of $\mathcal{G} = (g, g_1, g_{12}, g_2)$ lie. In Figures 8 and 10, we use the label Ⓢ, ①, Ⓞ when a vertex lies on $\mathbb{S}^1$, in the region inside $\mathbb{S}^1$, in the region outside $\mathbb{S}^1$, respectively.

Case 5: NVP singular faces when all vertices $g,\ g_1\ , g_{12}\ , g_2$ lie on $\mathbb{S}^1$. Note that all edge vectors given by $g,\ g_1\ , g_{12}\ , g_2$ become zero, by (23). Thus the corresponding face in F becomes just one point.

For example, such an NVP singular face $(F_{0,0}, F_{1,0}, F_{1,1}, F_{0,1})$ appears when we choose the discrete holomorphic function $g = \sqrt{2}\{(m - \frac{1}{2}) + \mathrm{i}(n - \frac{1}{2})\}$.

Case 6: NVP singular faces when two of $g,\ g_1\ , g_{12}\ , g_2$ lie on $\mathbb{S}^1$. The vertices of $\mathcal{G}$ lie like in Figure 8. Then the faces in F corresponding to the first two left-hand pictures in Figure 8 become triangles, and the one corresponding to the right-hand picture in Figure 8 becomes a 1-dimensional V-shape. The resulting NVP singular faces are pictured in Figure 9, and appear in Examples 3 and 4 in Section 10.

Case 7: NVP singular faces when one of $g,\ g_1\ , g_{12}\ , g_2$ lies on $\mathbb{S}^1$. The vertices of $\mathcal{G}$ are like in Figure 10. The corresponding faces in F become like in Figure 11. Such NVP singular faces appear in Example 3 in Section 10.

This completes the proof of Theorem 5.

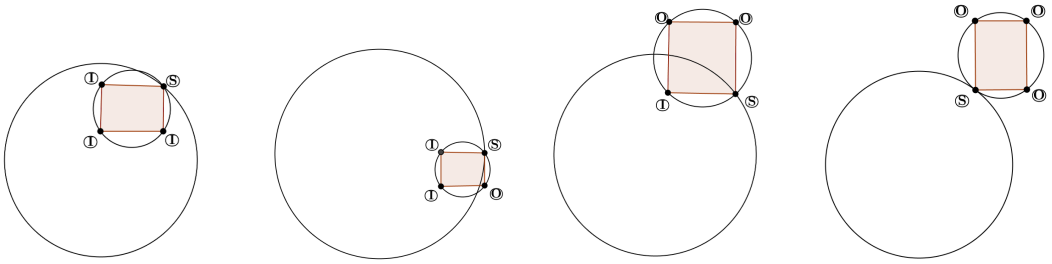

FIGURE 10. one point lying in $\mathbb{S}^1$

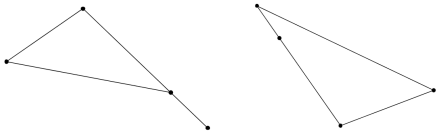

FIGURE 11. NVP singular faces as in Case 7

10. Examples

EXAMPLE 3. The discrete maximal Enneper surfaces can be constructed via Theorem 3 with

$$g(m,n) = c(m + \mathrm{i}n),$$

for any choice of $c \in \mathbb{R} \setminus \{0\}$. The picture in Figure 12 is such a maximal Enneper surface, and some singular faces appear. For example, the face $(F_{1,5}, F_{2,5}, F_{2,6}, F_{1,6})$ is a GVP singular face as in Case 1 in Section 9, the face $(F_{1,4}, F_{2,4}, F_{2.5}, F_{1,5})$ is a GVP singular face as in Case 2, the face $(F_{3,3}, F_{4,3}, F_{4,4}, F_{3,4})$ is a NVP singular face like in the right-hand picture of Figure 9, as in Case 6, and $(F_{4,2}, F_{5,2}, F_{5,3}, F_{4,3})$ and $(F_{4,3}, F_{5,3}, F_{5,4}, F_{4,4})$ are NVP singular faces as in Case 7.

If we choose $g = \frac{1}{6}(m + \mathrm{i}n)$, the face $(F_{4,4}, F_{5,4}, F_{5.5}, F_{4,5})$ is a GVP singular face as in Case 3.

EXAMPLE 4. The discrete maximal catenoids can be constructed via Theorem 3 with

$$g(m,n) = \exp(\alpha m + \mathrm{i}\beta n),$$

for any choices of $\alpha,\ \beta \in \mathbb{R} \setminus \{0\}$. The picture in Figure 13 is such a catenoid, and some singular faces appear. For example, the face $(F_{0,0}, F_{1,0}, F_{1,1}, F_{0,1})$ is a NVP singular face like in the left-hand picture in Figure 9 (Case 6).

EXAMPLE 5. A third example can be constructed via Theorem 3 with the discrete holomorphic function $g_{m,n}$ called z^γ. (See [**10**].) The pictures in Figures 14, 15, 16 are such maximal surfaces, coming from cz^γ for $c \in \mathbb{R} \setminus \{0\}$. If $\gamma = \frac{2n-2}{n}$ for $n \geq 2$ $(n \in \mathbb{N})$, we have higher order maximal Enneper surfaces.

EXAMPLE 6. A fourth example can be constructed via Theorem 3 with

$$g(m,n) = \tanh(\alpha m + \mathrm{i}\beta n),$$

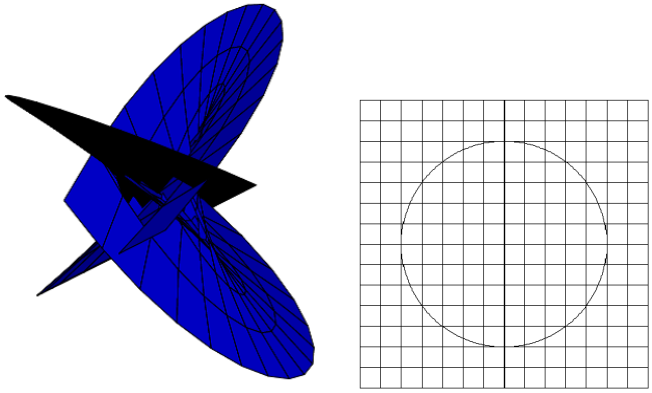

FIGURE 12. a discrete maximal Enneper surface with $c = \frac{1}{5}$ and its discrete holomorphic function

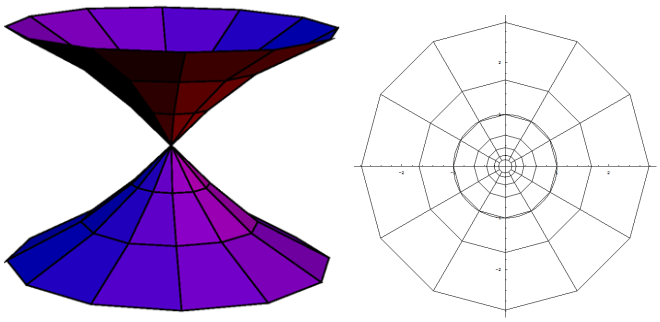

FIGURE 13. a discrete maximal catenoid and its discrete holomorphic function

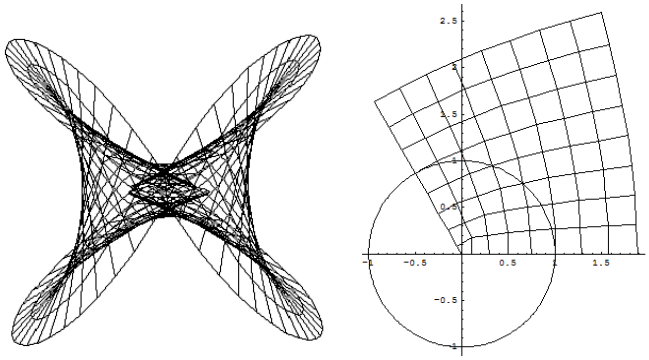

FIGURE 14. a maximal surface made using $\frac{1}{10}z^{\frac{4}{3}}$ and its discrete holomorphic function

for any choices of $\alpha,\ \beta \in \mathbb{R} \setminus \{0\}$.

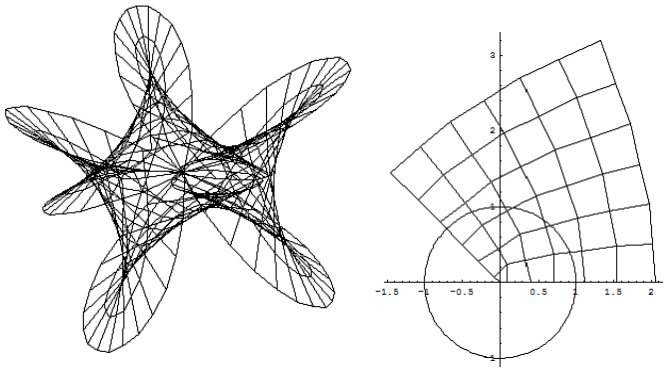

FIGURE 15. a maximal surface made using $\frac{1}{10}z^{\frac{3}{2}}$ and its discrete holomorphic function

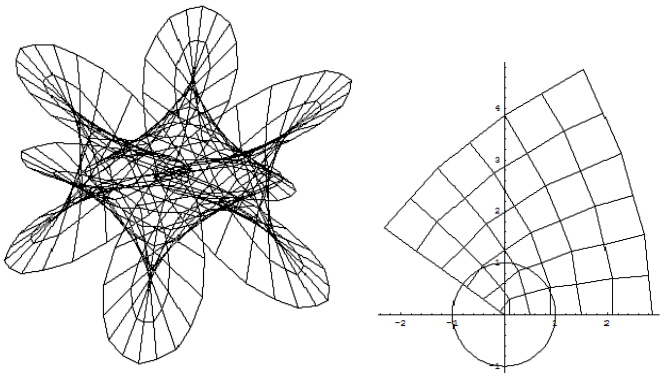

FIGURE 16. a maximal surface made using $\frac{1}{20}z^{\frac{8}{5}}$ and its discrete holomorphic function

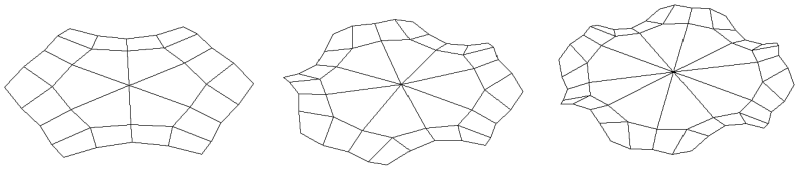

FIGURE 17. neighborhoods of central vertices of higher order Enneper surfaces, that would be umbilic points for the corresponding smooth surfaces.

CHAPTER 3

Semi-discrete maximal surfaces with singularities in Minkowski space

1. Introduction

Bobenko and Pinkall [**13**], [**14**] introduced discrete isothermic surfaces based on integrable systems methods in Euclidean 3-space $\mathbb{R}^3$, and they described the discrete minimal surfaces and a Weierstrass representation for them. Mueller and Wallner [**53**] introduced semi-discrete isothermic surfaces and semi-discrete minimal surfaces based on integrable systems methods in $\mathbb{R}^3$, and Rossman and the author [**64**] gave a Weierstrass representation for semi-discrete minimal surfaces in $\mathbb{R}^3$.

In this paper, we introduce a particular special class of semi-discrete isothermic surfaces in Minkowski 3-space $\mathbb{R}^{2,1}$ called semi-discrete maximal surfaces. In the smooth case, an isothermic surface is maximal if and only if its dual surface can be inscribed in the two sheeted hyperbolic 2-plane $\mathbb{H}^2_+ \cup \mathbb{H}^2_-$ (defined in Section 2 here) and becomes its own Lorentz Gauss map, as mentioned in [**70**]. Using this property, we will define semi-discrete maximal surfaces in $\mathbb{R}^{2,1}$. Furthermore, in Proposition 11, we will show that semi-discrete maximal surfaces in this sense satisfy that the mean curvature is identically 0.

On the other hand, in the smooth case, maximal surfaces generally have singularities (for example, see [**69**]). And also in the discrete case, the author [**70**] described discrete maximal surfaces with singularities in $\mathbb{R}^{2,1}$. (In [**70**], singularities of discrete maximal surfaces are called *singular faces*, as also defined in Subsection 2.2 here.) Therefore, unlike the case of semi-discrete minimal surfaces in $\mathbb{R}^3$, we can expect that semi-discrete maximal surfaces in $\mathbb{R}^{2,1}$ also have singularities. In fact, we define singularities of semi-discrete maximal surfaces called *singular edges*, which we will see are a natural description of singularities on semi-discrete maximal surfaces (see Definition 23).

Let $x : \mathbb{Z}\times\mathbb{R}$ (or some subdomain) $\to \mathbb{R}^{2,1}$ be a semi-discrete surface parametrized by $k \in \mathbb{Z}$, $t \in \mathbb{R}$. In this paper we abbreviate

$$x = x(k,t),\ x_1 := x(k+1,t),\ \partial x = x' := \frac{dx}{dt},\ \Delta x := x_1 - x,$$

and $[x, x_1]$ denotes the edge with the two endpoints x and x_1.

In order to introduce our theorems, here we define singularities of semi-discrete maximal surfaces (these terminologies are explained in Section 3). Let x be a semi-discrete maximal surface. Then we call $[x, x_1]$ a *singular edge* if the plane spanned by $\{\partial x, \Delta x_1, \partial\Delta x\}$ is non-spacelike. We will see that a natural way to separate singular edges into two kinds as follows: We call $[x, x_1]$ a GVP ("G"eneric "V"ertex

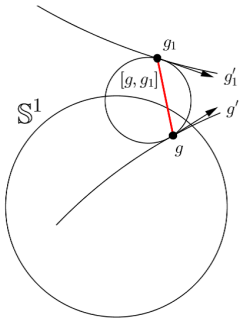

FIGURE 1. An example for which the tangent circle $\mathscr{C}$ at g, g_1 intersects $\mathbb{S}^1$, and thus for which the singular edge $[x, x_1]$ appears.

"P"lacement) *singular edge* if the plane spanned by $\{\partial x, \Delta x_1, \partial\Delta x\}$ is not spacelike but both ∂x and Δx are not lightlike. On the other hand, we call an edge $[x, x_1]$ an *NVP* ("N"on-generic "V"ertex "P"lacement) *singular edge* if either ∂x or ∂x_1 is lightlike.

Admitting singular edges, we have a Weierstrass-type representation for semi-discrete maximal surfaces. Our first main result is as follows:

THEOREM 6. Semi-discrete maximal surfaces x can be constructed using semi-discrete holomorphic functions g (defined in Section 3 here, along with the associated functions τ, σ) from $\mathbb{Z} \times \mathbb{R}$ (on the same domain as x) to the complex plane $\mathbb{C}$ by solving

$$\partial x = -\frac{\tau}{2}\mathrm{Re}\begin{pmatrix} \frac{1+g^2}{g'} \\ \frac{i(1-g^2)}{g'} \\ \frac{-2g}{g'} \end{pmatrix}, \quad \Delta x = \frac{\sigma}{2}\mathrm{Re}\begin{pmatrix} \frac{1+gg_1}{\Delta g} \\ \frac{i(1-gg_1)}{\Delta g} \\ \frac{-(g+g_1)}{\Delta g} \end{pmatrix} \tag{53}$$

with τ and σ determined from g. Conversely, any semi-discrete maximal surface satisfies (53) for some semi-discrete holomorphic function g

Our second main result is the following. In Theorem 7, $\mathscr{C}$ denotes the tangent circle at g, g_1, which is the circle that passes through g and g_1 and is tangent to g', g_1' there, as in Figure 1.

THEOREM 7. Let $g : \mathbb{Z} \times \mathbb{R} \to \mathbb{C}$ be a semi-discrete holomorphic function and let x be a semi-discrete maximal surface determined from g. Then the edge $[x, x_1]$ is a singular edge if and only if the tangent circle $\mathscr{C}$ at g, g_1 intersects $\mathbb{S}^1 = \{z \in \mathbb{C} \mid |z| = 1\}$.

Our third theorem is as follows: In the next theorem, the phrase "tangent conic section" refers to the 1-dimensional conic section (or simply a circle with respect to the Minkowski metric) that lies in the plane $\mathcal{P}(x, x_1)$ containing x, x_1, ∂x and ∂x_1 and is tangent to ∂x (resp. ∂x_1) at x (resp. x_1).

THEOREM 8. The tangent conic section of a GVP singular edge $[x, x_1]$ is a hyperbolic or parabolic conic section, and either case can occur for edges of either GVP or NVP type. In particular, we have the following cases:

- **GVP case:** In the GVP case, only the following cases can occur:
  (1) If the tangent conic section is hyperbolic and Δx is spacelike, ∂x, ∂x_1 lie to the same side of the straight line within $\mathcal{P}(x, x_1)$ spanned by Δx.
  (2) If the tangent conic section is parabolic and Δx is spacelike, ∂x, ∂x_1 lie to the same side of the straight line within $\mathcal{P}(x, x_1)$ spanned by Δx.
  (3) If one image point under g lies inside $\mathbb{S}^1$, and the other one lies outside $\mathbb{S}^1$, then the tangent conic section is a hyperbolic conic section, Δx is timelike, and ∂x, ∂x_1 lie to the opposite sides of the straight line within $\mathcal{P}(x, x_1)$ spanned by Δx.
- **NVP case:** In the NVP case, only the following cases can occur:
  (1) Exactly one of the two image points under g lies in $\mathbb{S}^1$, and then that corresponding vertex itself is a singular point of the curve it lies in, but two endpoints of the edge are not the same,
  (2) the two image points under g both lie in $\mathbb{S}^1$, and then the corresponding edge in x collapses to a single point.

Moreover, all cases described here do occur.

Furthermore, as the simplest examples of smooth, discrete and semi-discrete maximal surfaces, we will compare the profile curve of smooth, discrete and semi-discrete maximal surfaces of revolution. In all three cases, by an isometry in $\mathbb{R}^{2,1}$, there are three kinds of axes of revolution. The first kind is that the axis is timelike axis, the second one is spacelike, and the third is that the axis is lightlike. Then we have our final fourth theorem. In Theorem 9, we abbreviate smooth, discrete and semi-discrete elliptic (resp. hyperbolic, parabolic) catenoids as "EC" (resp. "HC", "PC"), that is, "EC" (resp. "HC", "PC") denotes a smooth, discrete or semi-discrete maximal surface with timelike (spacelike, lightlike) axis. Furthermore, the superscript pd (resp. ps) means that the profile curve is discrete (resp. smooth), and rd (resp. rs) means that the rotational direction is discrete (resp. smooth):

THEOREM 9. After appropriate normalizations, we have the following:

- EC^{pd}_{rd}-catenoids (resp. HC^{pd}_{rd}-catenoids, PC^{pd}_{rd}-catenoids) and EC^{pd}_{rs}-catenoids (resp. HC^{pd}_{rs}-catenoids, PC^{pd}_{rs}-catenoids) have the same profile curves.
- Smooth elliptic (resp. hyperbolic, parabolic) catenoids and EC^{ps}_{rd}-catenoids (resp. HC^{ps}_{rd}-catenoids, PC^{ps}_{rd}-catenoids) have the same profile curves.
- Smooth elliptic (resp. hyperbolic, parabolic) catenoid profile curves and EC^{pd}_{rd}-catenoid (resp. HC^{pd}_{rd}-catenoids, PC^{pd}_{rd}-catenoids) profile curves are never the same.

2. Preliminaries

Unless otherwise noted, throughout this paper f (resp. F, x) denotes a smooth (resp. discrete, semi-discrete) surface.

2.1. Smooth maximal surfaces in $\mathbb{R}^{2,1}$. Here we briefly review smooth maximal surfaces. For more theory, see [**47**], [**69**] for example. Let

$$\mathbb{R}^{2,1} := (\{(x_1, x_2, x_0)^t | x_j \in \mathbb{R}\}, \langle \cdot, \cdot \rangle)$$

be 3-dimensional Minkowski space with the Lorentz metric

$$\langle (x_1, x_2, x_0)^t, (y_1, y_2, y_0)^t \rangle = x_1 y_1 + x_2 y_2 - x_0 y_0,$$

and squared norm $\|(x_1, x_2, x_0)^t\|^2 = \langle (x_1, x_2, x_0)^t, (x_1, x_2, x_0)^t \rangle$, which can be negative or zero.

Note that, for fixed $d \in \mathbb{R}$ and vector $n \in \mathbb{R}^{2,1} \setminus \{0\}$, a plane $\mathcal{P} = \{x \in \mathbb{R}^{2,1} \mid \langle x, n \rangle = d\}$ is *spacelike* or *timelike* or *lightlike* when n is timelike or spacelike or lightlike, respectively. Furthermore, a smooth surface in $\mathbb{R}^{2,1}$ is spacelike if its tangent planes are spacelike. Let $f : \Sigma \to \mathbb{R}^{2,1}$ be a conformal immersion, where Σ is a simply-connected domain in $\mathbb{C}$ with complex coordinate $z = u+iv$, $u,\ v \in \mathbb{R}$. f is a maximal surface if it is spacelike (which follows automatically from the conformality condition) with mean curvature identically 0.

Defining

$$\mathbb{H}^2_+ := \{x = (x_1, x_2, x_0)^t \in \mathbb{R}^{2,1} | \|x\|^2 = -1,\ x_0 > 0\},$$

$$\mathbb{H}^2_- := \{x = (x_1, x_2, x_0)^t \in \mathbb{R}^{2,1} | \|x\|^2 = -1,\ x_0 < 0\},$$

we have the following proposition, analogous to the case of smooth minimal surfaces in $\mathbb{R}^3$ (and having a similar proof):

Proposition 9. Away from umbilic points, smooth maximal surfaces lie in the class of isothermic surfaces. In addition, a spacelike immersion $f = f(u, v)$ is a maximal surface if and only if it has a dual surface f^*, which solves

$$f^*_u = \frac{f_u}{\|f_u\|^2}, \quad f^*_v = -\frac{f_v}{\|f_v\|^2},$$

contained in $\mathbb{H}^2_+ \cup \mathbb{H}^2_-$. This dual surface is the Gauss map of the maximal surface.

Locally, we can construct any smooth maximal surface f with isothermic coordinates u, v from a smooth holomorphic function $g : \Sigma \to \mathbb{C}$ by solving

$$f = \mathrm{Re} \int \left(\frac{1+g^2}{g'}, \frac{i(1-g^2)}{g'}, -\frac{2g}{g'} \right)^t dz. \tag{54}$$

This function g is stereographic projection of the Gauss map f^* (up to scaling and translation of f^*). Conversely, any maximal surface f is described in this way by some holomorphic function g. See [**47**].

Differentiating Equation (54) gives the following system of differential equations:

$$f_u = \mathrm{Re} \left(\frac{1+g^2}{g_u}, \frac{i(1-g^2)}{g_u}, -\frac{2g}{g_u} \right)^t,$$

$$f_v = -\mathrm{Re} \left(\frac{1+g^2}{g_v}, \frac{i(1-g^2)}{g_v}, -\frac{2g}{g_v} \right)^t.$$

Our Theorem 6 gives a semi-discrete analog of the above system of differential equations.

Remark. Unlike the case of the Weierstrass representation for minimal surfaces in $\mathbb{R}^3$, smooth maximal surfaces in $\mathbb{R}^{2,1}$ have singularities when $|g| = 1$, because the metrics

$$\frac{(1-|g|^2)^2}{|g'|^2}dzd\bar{z} \tag{55}$$

of the smooth maximal surfaces degenerate. Note that we have a minus sign in the numerator in Equation (55), unlike the plus sign we would have had for minimal surfaces in $\mathbb{R}^3$. □

2.2. Fully-discrete maximal surfaces in $\mathbb{R}^{2,1}$. In order to compare smooth, discrete and semi-discrete maximal surfaces of revolution, here we introduce discrete maximal surfaces in $\mathbb{R}^{2,1}$ and their singularities, as described in [**70**].

Definition 16. For the second item below, the definition of $cr(F_{m,n}, F_{m+1,n}, F_{m+1,n+1}, F_{m,n+1})$ can be found in [**70**].

- Let g be a map from $\mathbb{D} \subset \mathbb{Z}^2$ to $\mathbb{C}$ parametrized by two discrete parameters m, n. This map g is a *discrete holomorphic function* if it satisfies
$$\frac{(g_{m,n}-g_{m+1,n})(g_{m+1,n+1}-g_{m,n+1})}{(g_{m+1,n}-g_{m+1,n+1})(g_{m,n+1}-g_{m,n})} = -\frac{\alpha_m}{\beta_n},$$
where α_m (resp. β_n) is a positive scalar function depending only on m (resp. n).
- $F : \mathbb{D} \to \mathbb{R}^{2,1}$ is a *discrete isothermic surface* if F satisfies
$$cr(F_{m,n}, F_{m+1,n}, F_{m+1,n+1}, F_{m,n+1}) = -\frac{\alpha_m}{\beta_n}.$$
- Let F be a discrete isothermic surface in $\mathbb{R}^{2,1}$ with cross ratios on the faces given by $-\frac{\alpha_m}{\beta_n}$. Then F is a *discrete maximal surface* if the dual surface F^* of F satisfying
$$F^*_{m+1,n} - F^*_{m,n} = \alpha_m \frac{F_{m+1,n}-F_{m,n}}{\|F_{m+1,n}-F_{m,n}\|^2},$$
$$F^*_{m,n+1} - F^*_{m,n} = -\beta_n \frac{F_{m,n+1}-F_{m,n}}{\|F_{m,n+1}-F_{m,n}\|^2}$$
can be inscribed in $\mathbb{H}^2_+ \cup \mathbb{H}^2_-$.
- Let $F : \mathbb{Z}^2 \to \mathbb{R}^{2,1}$ be a discrete maximal surface. Then the face $\mathcal{F} = (F_{m,n}, F_{m+1,n},$
$F_{m+1,n+1}, F_{m,n+1})$ (for some m, n) is a *singular face* if $\mathcal{F}$ lies on a non-spacelike plane.

Any discrete maximal surface can be described via the Weierstrass-type representation using discrete holomorphic functions (see [**70**]). Furthermore, we have criteria for singular faces of discrete maximal surfaces:

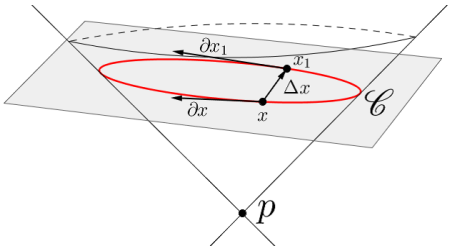

FIGURE 2. Part of a semi-discrete circular surface in $\mathbb{R}^{2,1}$

PROPOSITION 10. Let $g : \mathbb{Z}^2 \to \mathbb{C}$ be a discrete holomorphic function and let F be a discrete maximal surface determined from g. Then the face $\mathcal{F} = (F, F_1, F_{12}, F_2)$ is a singular face if and only if the circle passing through the vertices of the face $\mathcal{G} = (g, g_1, g_{12}, g_2)$ intersects the unit circle $\mathbb{S}^1 = \{z \in \mathbb{C} \mid |z| = 1\}$.

Our second main result describes the similar criteria for singularities of semi-discrete maximal surfaces, analogous to Proposition 10.

3. Semi-discrete isothermic surfaces in $\mathbb{R}^{2,1}$

Here we define semi-discrete conjugate and circular nets in $\mathbb{R}^{2,1}$. The notion of semi-discrete surfaces here is almost the same as in $\mathbb{R}^3$ (see [**53**]). In Definition 17, "circle" denotes the intersection of a translated light cone $\mathbb{L}^2_p$ and a plane, where $\mathbb{L}^2_p := \{x \in \mathbb{R}^{2,1} | \|x - p\|^2 = 0\}$ for fixed $p \in \mathbb{R}^{2,1}$. The main goal of this paper is to discretize spacelike isothermic immersions, so we will assume that the planes are spacelike.

DEFINITION 17. Let $x : \mathbb{Z} \times \mathbb{R} \to \mathbb{R}^{2,1}$ be a semi-discrete surface.

- x is a semi-discrete conjugate net if ∂x, Δx and $\partial \Delta x$ are linearly dependent.
- x is a semi-discrete circular net if there exists a circle $\mathscr{C}$ passing through x and x_1 that is tangent to ∂x, ∂x_1 there (for all k, t).

In the smooth case, smooth isothermic surfaces contains many important classes of surfaces. In particular, minimal surfaces and constant mean curvature (for short, CMC) surfaces in $\mathbb{R}^3$ and maximal surfaces and CMC surfaces in $\mathbb{R}^{2,1}$ lie in the class of isothermic surfaces. Furthermore, Christoffel duals of smooth isothermic surfaces play important roles. As mentioned in Subsection 2.1, a dual surface of a smooth isothermic maximal surface is characterized as a surface inscribed in $\mathbb{H}^2_+ \cup \mathbb{H}^2_-$, and the dual surface of a smooth isothermic CMC surface in $\mathbb{R}^{2,1}$ is characterized as the parallel surface at distance $1/H$. And also in the discrete case, discrete maximal and CMC surfaces in $\mathbb{R}^{2,1}$ have the same properties (see [**70**]).

Mueller, Wallner [**53**] described semi-discrete dualizable surfaces in $\mathbb{R}^3$. For semi-discrete circular surfaces, isothermity is equivalent to the existence of Christoffel duals. In particular, Rossman and the author [**64**] applied their theory to semi-discrete minimal surfaces in $\mathbb{R}^3$ and Mueller [**52**] applied it to semi-discrete CMC surfaces in $\mathbb{R}^3$. So it is natural to consider semi-discrete circular surfaces possessing Christoffel duals in $\mathbb{R}^{2,1}$.

DEFINITION 18. Suppose x, x^* are semi-discrete conjugate surfaces. Then x and x^* are *dual* to each other if there exists a function $\nu : \mathbb{Z} \times \mathbb{R} \to \mathbb{R}^+$ so that

$$\partial x^* = -\frac{1}{\nu^2}\partial x,\ \Delta x^* = \frac{1}{\nu\nu_1}\Delta x.$$

Like in $\mathbb{R}^3$, we have the following proposition. The proof of Lemma 8 is the same as in [**53**], so here we state only the result.

LEMMA 8. We have the following two facts:

- Let x be a conjugate semi-discrete surface. Then x has a dual surface x^* if and only if there exists a positive scalar function $\nu : \mathbb{Z} \times \mathbb{R} \to \mathbb{R}^+$ such that

$$\Delta\partial x = \frac{\nu_1}{\nu}\partial x - \frac{\nu}{\nu_1}\partial x_1 + \frac{\partial\nu \cdot \nu_1 + \partial\nu_1 \cdot \nu}{\nu\nu_1}\Delta x. \tag{56}$$

- If x has a dual surface x^*, the vectors ∂x, ∂x_1 lie to the same side of the straight line spanned by Δx within the plane through x and x_1, and tangent to ∂x, ∂x_1.

The definition of semi-discrete isothermic surfaces in $\mathbb{R}^{2,1}$ is almost the same as in $\mathbb{R}^3$, as defined in [**53**], but for the case in $\mathbb{R}^{2,1}$, we assume that the circles lie on spacelike planes.

DEFINITION 19. A semi-discrete circular surface x is *semi-discrete isothermic* if there exist positive functions $\nu,\ \sigma,\ \tau$ such that

$$\|\Delta x\|^2 = \sigma\nu\nu_1,\ \|\partial x\|^2 = \tau\nu^2,\ \text{with } \partial\sigma = \Delta\tau = 0.$$

As already mentioned in Section 1, motivated by Proposition 9, we define semi-discrete maximal surfaces as follows:

DEFINITION 20. A semi-discrete isothermic surface x is *semi-discrete maximal* if its dual x^* can be inscribed in $\mathbb{H}^2_+ \cup \mathbb{H}^2_-$.

Here we define Gaussian and mean curvatures for semi-discrete circular surfaces. In $\mathbb{R}^3$, they have already been defined in [**42**], [**52**]. In Definition 21, n plays the role of the Lorentz Gauss map of the original semi-discrete circular surface x.

DEFINITION 21. Let $x : \mathbb{Z} \times \mathbb{R} \to \mathbb{R}^{2,1}$ be a semi-discrete circular surface, and let $n : \mathbb{Z} \times \mathbb{R} \to \mathbb{H}^2_+ \cup \mathbb{H}^2_-$ be a semi-discrete circular surface with $\partial x \parallel \partial n$ and $\Delta x \parallel \Delta n$. Then K and H defined by

$$K = \frac{\det(\partial n + \partial n_1, \Delta n, N)}{\det(\partial x + \partial x_1, \Delta x, N)},$$
$$H = -\frac{\det(\partial x + \partial x_1, \Delta n, N) + \det(\partial n + \partial n_1, \Delta x, N)}{2\det(\partial x + \partial x_1, \Delta x, N)}$$

are called the *Gaussian* and *mean curvatures* of x, where N is a timelike unit vector perpendicular to the plane spanned by $\{\partial x, \Delta x, \partial\Delta x\}$ (see Figure 3).

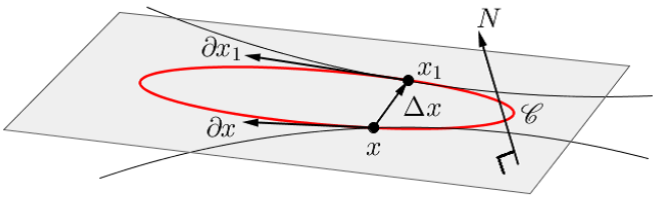

FIGURE 3. Part of a semi-discrete circular surface with timelike unit normal vector N. N is perpendicular to the plane spanned by ∂x, ∂x_1, Δx if $\langle X, N\rangle = 0$, where X is any vector in the plane (in the sense of $\mathbb{R}^{2,1}$).

Note that Gaussian and mean curvatures K^d and H^d of the parallel surface $x^d := x + d \cdot n$ of x with distance d are

$$K^d = \frac{K}{1 - 2d \cdot H + d^2 \cdot K}, \quad H^d = \frac{H - d \cdot K}{1 - 2d \cdot H + d^2 \cdot K}, \tag{57}$$

which are the same conditions as in both the smooth and discrete cases in $\mathbb{R}^3$ (see [**15**]).

Furthermore, for a semi-discrete circular surface x and its dual x^*, dualizability is equivalent to the condition

$$\det(\partial x + \partial x_1, \Delta x^*, N) + \det(\partial x^* + \partial x_1^*, \Delta x, N) = 0,$$

which follows from Equation (56). In the case of $\mathbb{R}^3$, this fact had been mentioned in [**52**].

This gives the following proposition:

PROPOSITION 11. Let x be a semi-discrete isothermic surface, and let x^* be its dual surface. Then

- $H \equiv 0 \Leftrightarrow$ we can choose x^* (up to translation and scaling) so that $n = x^*$,
- $H = \text{const.} \Leftrightarrow$ we can choose x^* (up to translation and scaling) so that $x^* = x + \frac{1}{H} n$.

Proof. The condition $H \equiv 0$ is equivalent to

$$H \equiv 0 \Leftrightarrow \det(\partial x + \partial x_1, \Delta n, N) + \det(\partial n + \partial n_1, \Delta x, N) = 0 \Leftrightarrow n = x^*.$$

And the condition $H \equiv \text{const.}$ is equivalent to

$$\begin{aligned}
&\det(\partial x + \partial x_1, \Delta n, N) + \det(\partial n + \partial n_1, \Delta x, N) \\
&= -2H \det(\partial x + \partial x_1, \Delta x, N) \\
&\Leftrightarrow \det\left(\partial x + \partial x_1, \Delta\left(x + \frac{1}{H} n\right), N\right) \\
&+ \det\left(\partial\left(x + \frac{1}{H} n\right) + \partial\left(x_1 + \frac{1}{H} n_1\right), \Delta x, N\right) = 0 \\
&\Leftrightarrow x^* = x + \frac{1}{H} n,
\end{aligned}$$

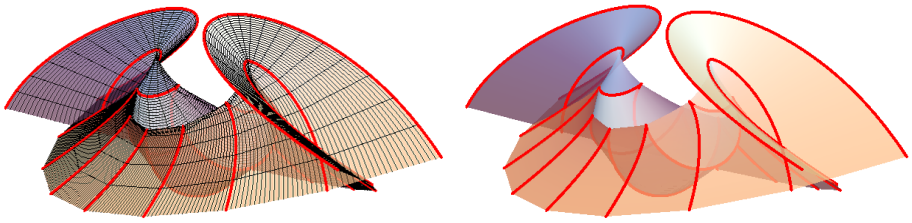

FIGURE 4. Parallel surfaces of a semi-discrete minimal Enneper surface in $\mathbb{R}^3$, with mesh shown and without mesh shown. This surface appears to have singularities.

proving the proposition. □

Remark. For a semi-discrete maximal surface x, by Equation (57), parallel surfaces x^d of x are new semi-discrete surfaces satisfying the condition

$$d \cdot K^d + H^d = 0.$$

This also holds for the fully-discrete case in $\mathbb{R}^{2,1}$, and also for both the discrete and semi-discrete cases in $\mathbb{R}^3$. □

Semi-discrete holomorphic functions were first defined in [**64**]. The following definition is the semi-discrete analogue of discrete holomorphic functions in [**13**], and as in Theorem 6, semi-discrete holomorphic functions are used to describe the Weierstrass representation for semi-discrete maximal surfaces.

DEFINITION 22. A semi-discrete isothermic surface g is a *semi-discrete holomorphic function* if the image of g lies in $\mathbb{R}^2 \cong \mathbb{C}$.

Note that, as in Figure 4, even when we consider semi-discrete circular surfaces in $\mathbb{R}^3$, they may have configurations that appear to have "singularities". Unlike the case of discrete surfaces, semi-discrete surfaces can be considered as a discrete one-parameter family of smooth curves, so each curve may have singularities. We can also consider semi-discrete surfaces as a discrete one-parameter family of the strips $\{(1-s)x_k + s \cdot x_{k+1} | s \in [0,1]\}$, and we can imagine finding singularities of each strip in terms of the two smooth parameters t, s. In this sense, Mueller, Wallner [**53**] showed that each strip of a semi-discrete isothermic surface does not have singularities.

However, semi-discrete surfaces actually depend on only a discrete parameter k and a smooth parameter t, so we wish to define "singularities" of semi-discrete surfaces in a way that depends on only k and t. From this viewpoint, it is suitable to define singularities of semi-discrete surfaces as we do in Definition 23 below. At present, we do not have a general definition of singularities on semi-discrete surfaces, but in the case of semi-discrete maximal surfaces, we can define their singular edges as below. In the smooth case, except at singularities, the tangent planes at all points are spacelike, which leads to this natural description of singularities of semi-discrete maximal surfaces:

DEFINITION 23. Let x be a semi-discrete maximal surface. Then the edge $[x, x_1]$ for some k, t is a *singular edge* if the plane spanned by $\{\partial x, \Delta x, \partial\Delta x\}$ is not spacelike. In particular, $[x, x_1]$ is a *GVP singular edge* if neither of ∂x, ∂x_1 is lightlike, and $[x, x_1]$ is an *NVP singular edge* if at least one of ∂x, ∂x_1 is lightlike.

4. Semi-discrete maximal surfaces of revolution

In this section we discuss semi-discrete maximal surfaces of revolution in $\mathbb{R}^{2,1}$. Unlike the case in $\mathbb{R}^3$, there are three kinds of axes of revolution. Using isometries of $\mathbb{R}^{2,1}$, we can think without loss of generality that the three types of axes are $\mathrm{span}\{(0,0,1)^t\}$, $\mathrm{span}\{(0,1,0)^t\}$, $\mathrm{span}\{(1,0,1)^t\}$. In the smooth case, there are three kinds of maximal surfaces of revolution called elliptic, hyperbolic, parabolic catenoids, where an elliptic (resp. hyperbolic, parabolic) catenoid is a surface of revolution with axis in the direction $(0,0,1)^t$ (resp. $(0,1,0)^t$, $(1,0,1)^t$). We will use EC-catenoid (resp. HC-catenoid, PC-catenoid) to denote an elliptic (resp. hyperbolic, parabolic) catenoid. Then we can give explicit parametrizations of six types of semi-discrete EC^{pd}_{rs}, EC^{ps}_{rd}, HC^{pd}_{rs}, HC^{ps}_{rd}, PC^{pd}_{rs}, PC^{ps}_{rd}-catenoids, where pd (resp. ps) means that the profile curve is discrete (resp. smooth), and rd (resp. rs) means that the rotational direction is discrete (resp. smooth).

4.1. Semi-discrete elliptic catenoids with discrete profile curve. Take the parametrization for EC^{pd}_{rs}-catenoids:

$$x(k,t) = \begin{pmatrix} f(k)\cos t \\ f(k)\sin t \\ h\cdot k \end{pmatrix}$$

where h is positive, and $f(k)$ is a function of k. Then, with $f_1 = f(k+1)$,

$$\|\Delta x\|^2 = (f_1 - f)^2 - h^2,\ \|\partial x\|^2 = f^2.$$

One can check that x is isothermic by taking

$$\nu = f,\ \ \tau = 1 \ \text{ and } \ \sigma = \frac{(\Delta f)^2 - h^2}{f\cdot f_1}.$$

We compute x^* by solving

$$x^* = -\frac{1}{\nu^2}\int \partial x dt = -\frac{1}{f}\begin{pmatrix}\cos t \\ \sin t \\ 0\end{pmatrix} + \overrightarrow{c_k},$$

where $\overrightarrow{c_k}$ depends on k but not t. We now have

$$\Delta x^* = \frac{1}{f\cdot f_1}\begin{pmatrix}\Delta f\cdot\cos t \\ \Delta f\cdot\sin t \\ 0\end{pmatrix} + \overrightarrow{c_{k+1}} - \overrightarrow{c_k}.$$

Therefore, x^* is dual to x if

$$\overrightarrow{c_{k+1}} - \overrightarrow{c_k} = \frac{h}{f\cdot f_1}\begin{pmatrix}0\\0\\1\end{pmatrix}.$$

Without loss of generality, we can take $\overrightarrow{c_k}$ as $(0,0,c(k))^t$ with

$$c(k+1) = c(k) + \frac{h}{f(k)f(k+1)}. \tag{58}$$

For x to be semi-discrete maximal, we wish to have $\|x^*\|^2 \equiv$ constant for some choice of $c(0)$. Then the condition $\|x_1^*\|^2 = \|x^*\|^2$ gives

$$\frac{1}{f_1^2} - c_1^2 = \frac{1}{f^2} - c^2. \tag{59}$$

Inserting (58) into (59), we have

$$c(k) = -\frac{f(k+1)^2 - f(k)^2 - h^2}{2hf(k)f(k+1)}. \tag{60}$$

Again inserting (60) into (58), we have

$$\begin{aligned} &(f(k+2)+f(k))(f(k+2)f(k) - f(k+1)^2 + h^2) = 0 \\ &\Rightarrow f(k+2) = \frac{f(k+1)^2 - h^2}{f(k)}. \end{aligned} \tag{61}$$

Now we assume that $f(1) = -f(-1)$. By Equation (61), we have

$$f(1)f(-1) = f(0)^2 - h^2 \Rightarrow f(1)^2 = -f(0)^2 + h^2.$$

Taking $f(0) = 0$, the solution to Equation (61) is

$$f(k) = \sinh(\operatorname{arcsinh}(h) \cdot k).$$

The left-hand picture in Figure 5 is such a semi-discrete elliptic catenoid.

4.2. Semi-discrete elliptic catenoids with smooth profile curve. Take the following parametrization for EC_{rd}^{ps}-catenoids:

$$x(k,t) = \begin{pmatrix} f(t)\cos(h\cdot k) \\ f(t)\sin(h\cdot k) \\ t \end{pmatrix},$$

where the function $f(t)$ and constant α are positive. We assume $f(0) = 0$ and $f'(0) = 1$. Then

$$\|\Delta x\|^2 = 4f(t)^2 \sin^2\frac{h}{2},\ \|\partial x\|^2 = (f'(t))^2 - 1.$$

One can confirm that x is isothermic by taking

$$\nu = f(t),\quad \tau = \frac{(f'(t))^2 - 1}{(f(t))^2} \quad \text{and} \quad \sigma = 4\sin^2\frac{h}{2}.$$

Now,

$$x^* = \begin{pmatrix} -\cos(h\cdot k)\int \frac{f'}{f^2}dt \\ -\sin(h\cdot k)\int \frac{f'}{f^2}dt \\ -\int \frac{1}{f^2}dt \end{pmatrix} = \begin{pmatrix} \frac{\cos(h\cdot k)}{f} \\ \frac{\sin(h\cdot k)}{f} \\ \ell(t) \end{pmatrix} + \overrightarrow{c_k},$$

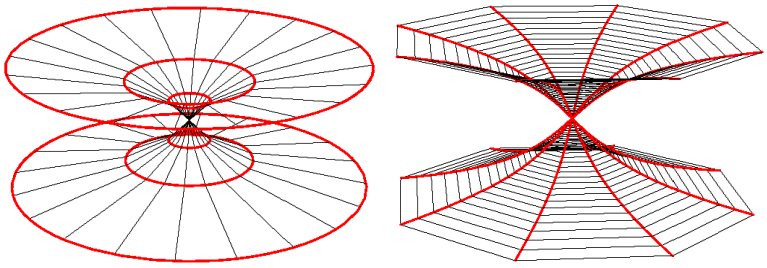

FIGURE 5. Two semi-discrete elliptic catenoids

where $\ell(t) = -\int_0^t f(t)^{-2}dt$ depends on t but not k. We compute that

$$\Delta x^* = \frac{1}{f}\begin{pmatrix}\Delta(\cos(h\cdot k))\\ \Delta(\sin(h\cdot k))\\ 0\end{pmatrix} + \overrightarrow{c_{k+1}} - \overrightarrow{c_k}.$$

Therefore, x^* is dual to x if $\overrightarrow{c_k}$ is a constant vector. For x to be semi-discrete maximal, x^* must be inscribed in a hyperbolic plane and therefore we can choose $\overrightarrow{c_0} = (0,0,c_0)^t$ so that $\|x^*\|^2$ is constant. From this condition, we have

$$\frac{1}{f^2} - \left(\int_0^t \frac{1}{(f(t))^2}dt - c_0\right)^2 = \text{constant}.$$

Differentiation gives that

$$\int_0^t \frac{1}{(f(t))^2}dt = -\frac{f'}{f} + c_0 \Rightarrow f''f - (f')^2 = -1.$$

We find from the initial conditions of f and f' that $f(t) = \sinh t$.

Thus semi-discrete elliptic catenoids with smooth profile curves and fixed h are unique up to homotheties. Furthermore, the shape of the smooth profile curve is independent of h. The right-hand picture in Figure 5 is such a semi-discrete elliptic catenoid.

4.3. Semi-discrete hyperbolic catenoids with discrete profile curve. Take the following parametrization for HC^{pd}_{rs}-catenoids:

$$x(k,t) = \begin{pmatrix} f(k)\sinh t\\ h\cdot k\\ f(k)\cosh t\end{pmatrix},$$

where the function $f = f(k)$ and constant h are positive. Then, with $f_1 = f(k+1)$,

$$\|\Delta x\|^2 = (f_1 - f)^2 - h^2,\ \|\partial x\|^2 = f^2.$$

One can check that x is isothermic by taking

$$\nu = f,\quad \tau = 1 \quad\text{and}\quad \sigma = \frac{-(\Delta f)^2 + h^2}{f\cdot f_1}.$$

We compute x^* by solving

$$x^* = -\frac{1}{\nu^2}\int \partial x dt = -\frac{1}{f}\begin{pmatrix}\sinh t\\ 0\\ \cosh t\end{pmatrix} + \overrightarrow{c_k}.$$

We now have

$$\Delta x^* = \frac{1}{f\cdot f_1}\begin{pmatrix}\Delta f\cdot\sinh t\\ 0\\ \Delta f\cdot\cosh t\end{pmatrix} + \overrightarrow{c_{k+1}} - \overrightarrow{c_k}.$$

Therefore, x^* is dual to x if

$$\overrightarrow{c_{k+1}} - \overrightarrow{c_k} = \frac{h}{f\cdot f_1}\begin{pmatrix}0\\1\\0\end{pmatrix}.$$

Without loss of generality, we can take $\overrightarrow{c_k}$ as $(0, b(k), 0)^t$ with

$$b(k+1) = b(k) + \frac{h}{f(k)f(k+1)}. \tag{62}$$

For x to be semi-discrete maximal, we wish to have $\|x^*\|^2 \equiv$ constant for some choice of $b(0)$. The condition $\|x_1^*\|^2 = \|x^*\|^2$ gives

$$-\frac{1}{f_1^2} + b_1^2 = -\frac{1}{f^2} + b^2. \tag{63}$$

Inserting (62) into (63), we have

$$b(k) = -\frac{f(k+1)^2 - f(k)^2 - h^2}{2hf(k)f(k+1)}. \tag{64}$$

Again inserting Equation (64) into (62), we have

$$\begin{aligned}&(f(k+2)+f(k))(f(k+2)f(k) - f(k+1)^2 + h^2) = 0\\ &\Rightarrow f(k+2) = \frac{f(k+1)^2 - h^2}{f(k)}.\end{aligned} \tag{65}$$

We now assume that $f(1) = f(-1)$. By Equation (65), we have

$$f(1)f(-1) = f(0)^2 - h^2 \Rightarrow f(1)^2 = -f(0)^2 + h^2.$$

Taking $f(0) = 1$, the solution to Equation (65) is

$$f(k) = \cos(\arcsin(h)\cdot k).$$

The left-hand picture in Figure 6 is such a HC_{rs}^{pd}-catenoid.

4.4. Semi-discrete hyperbolic catenoids with smooth profile curve. Take the following parametrization for HC^{ps}_{rd}-catenoids:

$$x(k,t) = \begin{pmatrix} f(t)\sinh(h\cdot k) \\ t \\ f(t)\cosh(h\cdot k) \end{pmatrix}.$$

We assume $f(0)=1$ and $f'(0)=0$. Then

$$\|\Delta x\|^2 = 4f(t)^2\sinh^2\frac{h}{2},\ \|\partial x\|^2 = -(f'(t))^2+1.$$

One can confirm that x is isothermic by taking

$$\nu = f(t),\quad \tau = \frac{-(f'(t))^2+1}{(f(t))^2}\quad\text{and}\quad \sigma = 4\sin^2\frac{h}{2}.$$

Now,

$$x^* = \begin{pmatrix} -\sinh(hk)\int\frac{f'}{f^2}dt \\ -\int\frac{1}{f^2}dt \\ -\cosh(hk)\int\frac{f'}{f^2}dt \end{pmatrix} = \begin{pmatrix} \frac{\sinh(hk)}{f} \\ \ell(t) \\ \frac{\cosh(hk)}{f} \end{pmatrix} + \overrightarrow{c_k},$$

where $\ell(t) = -\int_0^t f(t)^{-2}dt$. We compute that

$$\Delta x^* = \frac{1}{f}\begin{pmatrix} \Delta\sinh(hk) \\ 0 \\ \Delta\cosh(hk) \end{pmatrix} + \overrightarrow{c_{k+1}} - \overrightarrow{c_k}.$$

Therefore, x^* is dual to x if $\overrightarrow{c_k}$ is a constant vector. For x to be semi-discrete maximal, x^* must be inscribed in a hyperbolic plane and therefore we can choose $\overrightarrow{c_0} = (0,b_0,0)^t$ so that $\|x^*\|^2$ is constant. This condition gives

$$-\frac{1}{f^2} + \left(\int_0^t \frac{1}{(f(t))^2}dt - b_0\right)^2 = \text{constant}.$$

Differentiation gives that

$$\int_0^t \frac{1}{(f(t))^2}dt = -\frac{f'}{f} + b_0 \Rightarrow f''f - (f')^2 = -1.$$

We find from the initial conditions of f and f' that $f(t) = \cos t$.

Thus semi-discrete hyperbolic catenoids with smooth profile curves and fixed h are unique up to homotheties. Furthermore, the shape of the smooth profile curve is independent of h. The right-hand picture in Figure 6 is such a semi-discrete hyperbolic catenoid.

4.5. Semi-discrete parabolic catenoids with discrete profile curve. Take the following parametrization for PC^{pd}_{rs}-catenoids:

$$x(k,t) = \begin{pmatrix} f(k)+(1-t^2)(h\cdot k) \\ -2t(h\cdot k) \\ f(k)-(1+t^2)(h\cdot k) \end{pmatrix}.$$

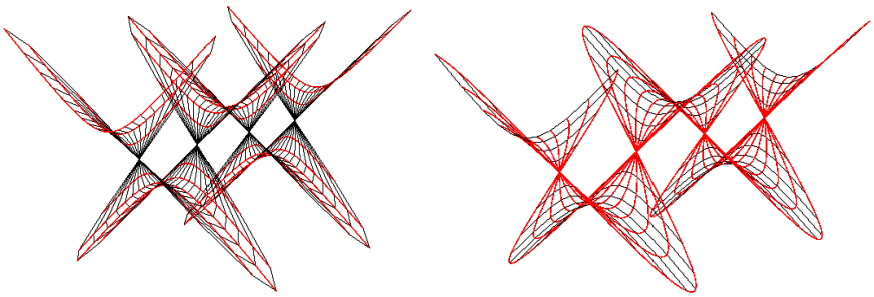

FIGURE 6. Two semi-discrete hyperbolic catenoids

Then

$$\|\Delta x\|^2 = 4h^2 \cdot k^2,\ \|\partial x\|^2 = 4\Delta f \cdot h = \frac{4\Delta f \cdot h}{k(k+1)} k(k+1).$$

Then one can check that x is isothermic by taking

$$\nu = k, \quad \tau = 4h^2 \ \text{ and } \ \sigma = \frac{4h \cdot \Delta f}{k(k+1)}.$$

We compute x^* by solving

$$x^* = -\frac{1}{\nu^2} \int \partial x dt = h \begin{pmatrix} \frac{t^2}{k} \\ \frac{2t}{k} \\ \frac{t^2}{k} \end{pmatrix} + \overrightarrow{c_k}.$$

We now have

$$\Delta x^* = -\frac{h}{k(k+1)} \begin{pmatrix} t^2 \\ 2t \\ t^2 \end{pmatrix} + \overrightarrow{c_{k+1}} - \overrightarrow{c_k}.$$

Therefore, x^* is dual to x if

$$\overrightarrow{c_{k+1}} - \overrightarrow{c_k} = \frac{1}{k(k+1)} \begin{pmatrix} \Delta f + h \\ 0 \\ \Delta f - h \end{pmatrix}.$$

Setting $\overrightarrow{c_k} = (a(k), b(k), c(k))^t$, then

$$\Delta a = \frac{1}{k(k+1)}(\Delta f + h),\ \Delta b = 0,\ \Delta c = \frac{1}{k(k+1)}(\Delta f - h). \tag{66}$$

Without loss of generality, we can take $b(k) = 0$. Set $x^* = \left(\frac{h \cdot t^2}{k} + a, \frac{2h \cdot t}{k}, \frac{h \cdot t^2}{k} + c\right)^t$, then

$$\|x^*\|^2 = \frac{2h \cdot t^2}{k^2}(k(a-c) + 2h) + (a+c)(a-c).$$

If $\|x^*\|^2 \equiv$ constant, that is, $\|x^*\|^2$ is independent of t and k,

$$k(a-c) + 2h = 0,\ (a+c)(a-c) \equiv -\beta\ (\beta: \text{ constant},\ \beta > 0).$$

Then we have

$$a - c = -\frac{2h}{k},\ a + c = \frac{\beta k}{2h}. \tag{67}$$

On the other hand, by Equation (66) and (67), we have

$$\Delta(a + c) = \frac{2\Delta f}{k(k+1)}. \tag{68}$$

Inserting the right-hand equation in Equation (67) into Equation (66), we have

$$f = \frac{\beta}{12h}(k-1)k(k+1).$$

The left-hand picture in Figure 7 is such a semi-discrete parabolic catenoid.

4.6. Semi-discrete parabolic catenoids with smooth profile curve. Take the following parametrization for PC^{ps}_{rd}-catenoids:

$$x(k,t) = \begin{pmatrix} f(t) + (1 - (h\cdot k)^2)t \\ -2(h\cdot k)t \\ y(t) - (1 + (h\cdot k)^2)t \end{pmatrix}.$$

We assume $f(0) = 0$ and $f'(0) = 1$. Then

$$\|\Delta x\|^2 = 4h^2 \cdot t^2,\ \|\partial x\|^2 = 4y' = \frac{4y'}{t^2}t^2.$$

One can confirm that x is isothermic by taking

$$\nu = t,\ \ \tau = \frac{4y'}{t^2}\ \text{ and }\ \sigma = 4h^2.$$

Now,

$$x^* = \begin{pmatrix} -\ell(t) + \frac{1-(h\cdot k)^2}{t} \\ -\frac{2h\cdot k}{t} \\ -\ell(t) - \frac{1+(h\cdot k)^2}{t} \end{pmatrix} + \overrightarrow{c_k},$$

where $\ell(t) = -\int_0^t t^{-2}y'dt$. We compute that

$$\Delta x^* = -\frac{1}{t}\begin{pmatrix} h^2(2k+1) \\ 2h \\ h^2(2k+1) \end{pmatrix} + \overrightarrow{c_{k+1}} - \overrightarrow{c_k}.$$

Therefore, x^* is dual to x if $\overrightarrow{c_k}$ is a constant vector. For x to be semi-discrete maximal, x^* must be inscribed in a hyperbolic plane and therefore we can choose $\overrightarrow{c_0} = (0,0,0)^t$ so that $\|x^*\|^2$ is constant. From this condition, we have

$$-\frac{4}{t}\ell(t) = \text{constant}.$$

Differentiation gives that

$$\int_0^t \frac{t'}{t^2}dt = \frac{y'}{t} \Rightarrow t\cdot f'' - 2f' = 0.$$

We find from the initial conditions of f and f' that $(t) = t^3$.

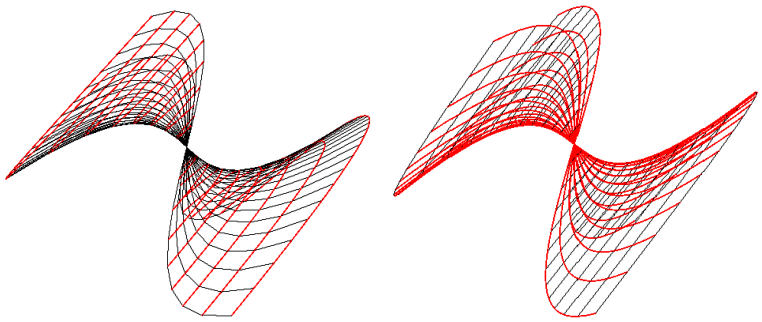

FIGURE 7. Two semi-discrete parabolic catenoids

Thus semi-discrete parabolic catenoids with smooth profile curves and fixed h are unique up to homotheties. Furthermore, the shape of the smooth profile curve is independent of h. The right-hand picture in Figure 7 is such a semi-discrete parabolic catenoid.

5. Fully-discrete maximal surfaces of revolution

In this section we discuss fully discrete maximal surfaces of revolution in the sense of [**70**]. Definitions of discrete holomorphic functions and discrete maximal surfaces are as in Subsection 2.2.

In order to compare profile curves of smooth, discrete and semi-discrete maximal surfaces of revolution, we give explicit parametrizations of discrete maximal surfaces of revolution.

In Figure 8 we show graphics of a HC^{pd}_{rd}-catenoid and PC^{pd}_{rd}-catenoid and visually note where the singular faces appear in these surfaces.

In $\mathbb{R}^3$, Bobenko, Suris [**18**] characterized discrete isothermic surfaces as circular Koenigs nets. In particular, if $F : \mathbb{Z}^2 \to \mathbb{R}^i$ $(i = 2, 3)$ is a discrete isothermic surface parametrized by two discrete parameters m and n, there exists a scalar function $s : \mathbb{Z}^2 \to \mathbb{R}^+$ such that

$$\begin{aligned} \|F_{m+1,n} - F_{m,n}\|^2 &= \alpha_m \cdot s_{m,n} \cdot s_{m+1,n}, \\ \|F_{m,n+1} - F_{m,n}\|^2 &= \beta_n \cdot s_{m,n} \cdot s_{m,n+1} \end{aligned} \tag{69}$$

hold, where $\alpha_m > 0$, $\beta_n > 0$ are given by

$$cr(F_{m,n}, F_{m+1,n}, F_{m+1,n+1}, F_{m,n+1}) = -\frac{\alpha_m}{\beta_n},$$

with $cr(F_{m,n}, F_{m+1,n}, F_{m+1,n+1}, F_{m,n+1})$ as defined in [**13**] (see Theorem 4.8 in [**18**]). Furthermore, a dual surface F^* of a discrete isothermic surface F is given by

$$\begin{aligned} F^*_{m+1,n} - F^*_{m,n} &= \frac{1}{s_{m,n} \cdot s_{m+1,n}} \left(F_{m+1,n} - F_{m,n}\right), \\ F^*_{m,n+1} - F^*_{m,n} &= -\frac{1}{s_{m,n} \cdot s_{m,n+1}} \left(F_{m,n+1} - F_{m,n}\right). \end{aligned} \tag{70}$$

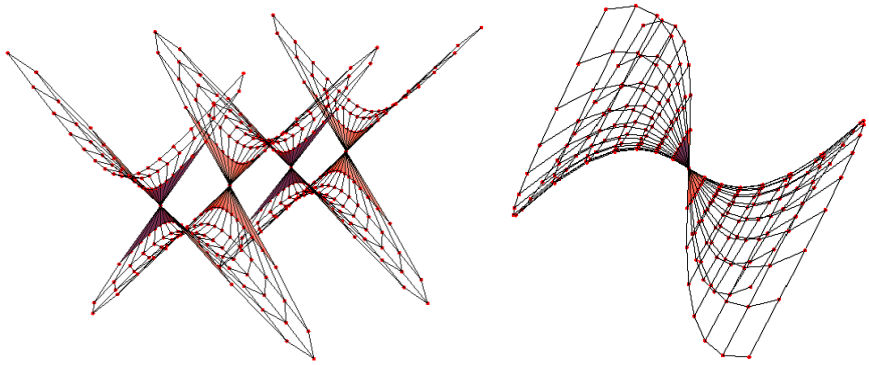

FIGURE 8. Discrete hyperbolic and parabolic catenoids, and their singular faces (the singular faces have been darkened)

Away from singular faces of discrete maximal surfaces, one can check that Equations (69) and (70) still hold. In fact, for discrete maximal surfaces, setting

$$\|g_{m+1,n} - g_{m,n}\|^2 = \alpha_m \cdot \hat{s}_{m,n} \cdot \hat{s}_{m+1,n},$$
$$\|g_{m,n+1} - g_{m,n}\|^2 = \beta_n \cdot \hat{s}_{m,n} \cdot \hat{s}_{m,n+1},$$

we can take $s_{m,n} := (\|g_{m,n}\|^2 - 1)\hat{s}^{-1}_{m,n}$.

In order to give explicit parametrizations of discrete maximal surfaces of revolution, like in Subsections 4.1, 4.3, 4.5, we set parametrizations for three kinds of discrete maximal surfaces of revolution as follows:

$$F_{m,n} = \begin{pmatrix} f(m)\cos(c\cdot n) \\ f(m)\sin(c\cdot n) \\ h\cdot m \end{pmatrix}, \begin{pmatrix} f(m)\sinh(c\cdot n) \\ h\cdot m \\ f(m)\cosh(c\cdot n) \end{pmatrix}, \begin{pmatrix} f(m) + (1-(c\cdot n)^2)(h\cdot m) \\ -2(c\cdot n)\cdot(h\cdot m) \\ f(m) - (1+(c\cdot n)^2)(h\cdot m) \end{pmatrix}.$$

Using Equation (70), by similar computations as in Subsections 4.1, 4.3, 4.5 we can explicitly compute the parametrizations of EC^{pd}_{rd}, HC^{pd}_{rd}, PC^{pd}_{rd} and derive

$$EC^{rd}_{pd}(m,n) = \begin{pmatrix} \sinh(\operatorname{arcsinh}(h)\cdot m)\cos(c\cdot n) \\ \sinh(\operatorname{arcsinh}(h)\cdot m)\sin(c\cdot n) \\ h\cdot m \end{pmatrix},$$
$$HC^{rd}_{pd}(m,n) = \begin{pmatrix} \cos(\arcsin(h)\cdot m)\sinh(c\cdot n) \\ h\cdot m \\ \cos(\arcsin(h)\cdot m)\cosh(c\cdot n) \end{pmatrix},$$
$$PC^{rd}_{pd}(m,n) = \begin{pmatrix} \frac{\beta}{12h}(m-1)m(m+1) + (1-(c\cdot n)^2)h\cdot m \\ -2(c\cdot n)\cdot(h\cdot m) \\ \frac{\beta}{12h}(m-1)m(m+1) - (1+(c\cdot n)^2)h\cdot m \end{pmatrix}.$$

6. Proof of Theorem 6

We start by proving the first half of Theorem 6. Let g be a semi-discrete holomorphic function such that $|\Delta g|^2 = \sigma\nu\nu_1$, $|g'| = \tau\nu^2$ for some positive functions ν,

σ, τ. First we temporarily assume that $|g| \neq 1$, and then

$$x^* := \frac{1}{|g|^2-1}\begin{pmatrix} -2\mathrm{Re}(g) \\ -2\mathrm{Im}(g) \\ |g|^2+1 \end{pmatrix} \in \mathbb{H}^2_+ \cup \mathbb{H}^2_- \subset \mathbb{R}^{2,1} \cong \mathbb{C}\times\mathbb{R}$$

is semi-discrete isothermic, because x^* is the image of g under the inverse of stereographic projection. (Here, the symbol "$\cong$" is used simply because we are identifying $\mathbb{R}^{2,1}$ and $\mathbb{C}\times\mathbb{R}$.) Then

$$\partial x^* \cong \frac{2}{(|g|^2-1)^2}\begin{pmatrix} g' + \overline{g'}g^2 \\ -(g'\bar{g} + \overline{g'}g) \end{pmatrix},$$
$$\Delta x^* \cong \frac{2}{(|g|^2-1)(|g_1|^2-1)}\begin{pmatrix} \Delta g + \overline{\Delta g}gg_1 \\ -(\Delta g\bar{g}_1 + \overline{\Delta g}g) \end{pmatrix}.$$

It follows that

$$\|\partial x^*\|^2 = \frac{4|g'|^2}{(|g|^2-1)^2} = \frac{4\tau\nu^2}{(|g|^2-1)^2},$$
$$\|\Delta x^*\|^2 = \frac{4|\Delta g|^2}{(|g|^2-1)(|g_1|^2-1)} = \frac{4\sigma\nu\nu_1}{(|g|^2-1)(|g_1|^2-1)},$$

so we can take the data τ^*, σ^*, ν^* for the isothermic surface x^* to be

$$\tau^* = \tau,\ \sigma^* = \sigma,\ \nu^* = \frac{2\nu}{|g|^2-1}.$$

Here, σ^* depends only on k, and τ^* depends only on t. Identifying $\mathbb{C}\times\mathbb{R}$ and $\mathbb{R}^3$, we have

$$\frac{-1}{(\nu^*)^2}\partial x^* \cong \frac{-1}{2\nu^2}\begin{pmatrix} g' + \bar{g}'g^2 \\ g'\bar{g} + \bar{g}'g \end{pmatrix} = \frac{-\tau}{2|g'|^2}\begin{pmatrix} g' - \bar{g}'g^2 \\ g'\bar{g} + \bar{g}'g \end{pmatrix}$$
$$= -\frac{\tau}{2}\begin{pmatrix} \mathrm{Re}\left(\frac{1+g^2}{g'}\right) + i\mathrm{Re}\left(\frac{i(1-g^2)}{g'}\right) \\ -\mathrm{Re}\left(\frac{2g}{g'}\right) \end{pmatrix} \cong -\frac{\tau}{2}\mathrm{Re}\begin{pmatrix} \frac{1+g^2}{g'} \\ \frac{i(1-g^2)}{g'} \\ -\frac{2g}{g'} \end{pmatrix} = \partial x.$$

Similarly,

$$\frac{1}{\nu^*\nu_1^*}\Delta x^* \cong \frac{\sigma}{2|\Delta g|^2}\begin{pmatrix} \Delta g + gg_1\overline{\Delta g} \\ -(\overline{g_1}\Delta g + g\overline{\Delta g}) \end{pmatrix}$$
$$= \frac{\sigma}{2}\begin{pmatrix} \mathrm{Re}\left(\frac{1+gg_1}{\Delta g}\right) + i\mathrm{Re}\left(\frac{i(1-gg_1)}{\Delta g}\right) \\ -\mathrm{Re}\left(\frac{g+g_1}{\Delta g}\right) \end{pmatrix} \cong \frac{\sigma}{2}\mathrm{Re}\begin{pmatrix} \frac{1+gg_1}{\Delta g} \\ \frac{i(1-gg_1)}{\Delta g} \\ -\frac{g+g_1}{\Delta g} \end{pmatrix} = \Delta x.$$

Thus if x solving (53) exists, x and x^* are dual to each other. A direct computation shows

$$\|\Delta x\|^2 = \sigma\left(\frac{|g|^2-1}{2\nu}\right)\left(\frac{|g_1|^2-1}{2\nu_1}\right),\ \|\partial x\|^2 = \tau\left(\frac{|g|^2-1}{2\nu}\right)^2,$$

so x will be semi-discrete isothermic. Since x^* is inscribed in $\mathbb{H}^2_+ \cup \mathbb{H}^2_-$, x must then be a semi-discrete maximal surface. Thus it remains to check existence of x.

To show existence of x, we need to show compatibility of the two equations in (53), and this amounts to showing that the two operators Δ and ∂ in (53) commute, that is,

$$\partial\left(\frac{\sigma}{2}\mathrm{Re}\begin{pmatrix}\frac{1+gg_1}{\Delta g}\\ \frac{i(1-gg_1)}{\Delta g}\\ -\frac{g+g_1}{\Delta g}\end{pmatrix}\right) = \Delta\left(-\frac{\tau}{2}\mathrm{Re}\begin{pmatrix}\frac{1+g^2}{g'}\\ \frac{i(1-g^2)}{g'}\\ -\frac{2g}{g'}\end{pmatrix}\right). \tag{71}$$

Remark. In the case of semi-discrete minimal surfaces in $\mathbb{R}^3$, any semi-discrete minimal surface can be obtained by dualizing isothermic surfaces inscribed in $\mathbb{S}^2$ (see [**64**]). It is already known from [**53**] that we can dualize any semi-discrete isothermic surface in $\mathbb{R}^3$, and this implies the same statement for the special case of semi-discrete minimal surfaces. (In spite of this, in [**64**], we did in fact computationally show the compatibility condition for semi-discrete minimal surfaces.) Similarly, semi-discrete maximal surfaces can be generally obtained by dualizing isothermic surfaces inscribed in $\mathbb{H}^2_+ \cup \mathbb{H}^2_-$. However, we cannot take a dual when the dual surface would blow up, which can happen in this case because $\mathbb{H}^2_+ \cup \mathbb{H}^2_-$ is not compact (unlike $\mathbb{S}^2$). In fact, when $|g| = 1$, x^* as defined in this section does indeed blow up. In this case, x^* might not be semi-discrete isothermic. So unlike the case of $\mathbb{R}^3$, we do have to show the compatibility condition for x to exist even when x^* might have vertices in the ideal boundaries $\partial\mathbb{H}^2_+$, $\partial\mathbb{H}^2_-$. □

One can compute

$$\begin{aligned}
&\text{Left-hand side of (71)}\\
=\ & \frac{\sigma}{2}\mathrm{Re}\left(\frac{1}{(\Delta g)^2}\begin{pmatrix}-g_1'+g'+g'g_1^2-g^2g_1'\\ i(-g_1'+g'-g'g_1^2+g^2g_1')\\ -2g'g_1+2gg_1'\end{pmatrix}\right)\\
=\ & \frac{\tau|\Delta g|^2}{2|g'||g_1'|}\mathrm{Re}\left(\frac{1}{(\Delta g)^2}\begin{pmatrix}-g_1'+g'+g'g_1^2-g^2g_1'\\ i(-g_1'+g'-g'g_1^2+g^2g_1')\\ -2g'g_1+2gg_1'\end{pmatrix}\right)\\
=\ & \frac{\tau}{2}\mathrm{Re}\left(\frac{\overline{\Delta g}}{|g'||g_1'|\Delta g}\begin{pmatrix}-g_1'+g'+g'g_1^2-g^2g_1'\\ i(-g_1'+g'-g'g_1^2+g^2g_1')\\ -2g'g_1+2gg_1'\end{pmatrix}\right)\\
=\ & -\frac{\tau}{2}\mathrm{Re}\left(\frac{1}{g'g_1'}\begin{pmatrix}g'(1+g_1^2)-g_1'(1+g^2)\\ ig'(1-g_1^2)-ig_1'(1-g^2)\\ -2g'g_1+2gg_1'\end{pmatrix}\right).\\
=\ & \text{right-hand side of (71).}
\end{aligned}$$

Now we prove the final sentence of Theorem 6. Let x be a semi-discrete maximal surface, and ψ be stereographic projection $\psi : \mathbb{H}^2_+ \cup \mathbb{H}^2_- \to \mathbb{C}$. Then by definition, there exists a dual x^* that is semi-discrete isothermic and inscribed in $\mathbb{H}^2_+ \cup \mathbb{H}^2_-$.

Taking

$$g := \psi \circ x^*,$$

g is a semi-discrete holomorphic function. Then g produces x via Equation (53), which completes the proof.

7. Proof of Theorem 7

Let g be a semi-discrete holomorphic function, and let x be the maximal surface given by g. Let $[x, x_1]$ be an edge for which the two values of g lie in a corresponding circle $\mathscr{C}$ which may or may not intersect $\mathbb{S}^1$. The dual surface x^* has tangent planes along edges that are parallel to those of x, so it suffices to consider whether the conic section passing through x^* and x_1^* lies in a non-spacelike plane.

Let $\mathscr{C} \subset \mathbb{C}$ be a circle tangent to g', g_1' at g, g_1 with center $a + ib$ and radius r, and let $[x^*, x_1^*]$ be the edge given by the image of the inverse of the stereographic projection. Taking $p \in \mathscr{C}$, the image of the map

$$\mathbb{C} \ni p := x + iy \mapsto \left(-\frac{2x}{|p|^2 - 1}, -\frac{2y}{|p|^2 - 1}, \frac{|p|^2 + 1}{|p|^2 - 1} \right) \in \mathbb{H}^2_+ \cup \mathbb{H}^2_-$$

lies in a plane

$$\mathcal{P} := \{(x_1, x_2, x_0)^t \in \mathbb{R}^{2,1} | \langle (x_1, x_2, x_0)^t, N \rangle = -(a^2 + b^2 - r^2 - 1)\},$$

where $N = (-2a, -2b, a^2 + b^2 - r^2 + 1)^t$. $\mathcal{P}$ is not spacelike if and only if n is not timelike. By using the circularity condition of g, one can check that x^* and x_1^* lies in a plane

$$\mathcal{P} := \{(x_1, x_2, x_0)^t \in \mathbb{R}^{2,1} | \langle (x_1, x_2, x_0)^t, N \rangle = 0\}$$

One can compute that

$$\|N\|^2 = -\{(a^2 + b^2) - (r - 1)^2\}\{(a^2 + b^2) - (r + 1)^2\}.$$

So the condition that n is not timelike gives $|r-1| \leq \sqrt{a^2 + b^2} \leq r+1$. On the other hand, considering the distance between the origin and $a + ib$, and the radii of $\mathbb{S}^1$ and $\mathscr{C}$, one can check that $\mathscr{C}$ intersects $\mathbb{S}^1$ if and only if $|r - 1| \leq \sqrt{a^2 + b^2} \leq r + 1$, proving the theorem.

8. Proof of Theorem 8

8.1. Case 1 of GVP singular edges. Let x be a semi-discrete maximal surface and let g be a semi-discrete holomorphic function. We need to consider the case that the tangent circle $\mathscr{C}$ has two intersection points with $\mathbb{S}^1$ but $[g, g_1]$ does not intersects $\mathbb{S}^1$. In this case one can check that the functions ν, ν_1 determined by x are not zero and ν and ν_1 have the same sign, that is, Δx is spacelike. Furthermore, the plane spanned by $\partial x, \Delta x, \partial \Delta x$ is a timelike plane. So $\mathscr{C}$ is a hyperbolic conic section, and from Lemma 8, ∂x and ∂x_1 lie to the same side of the straight line (within that plane) spanned by Δx. Such singular edges appear in Examples 7, 8.

8.2. Case 2 of GVP singular edges. We need to consider the case that the tangent circle $\mathscr{C}$ has one intersection point with $\mathbb{S}^1$ but $[g, g_1]$ does not intersect $\mathbb{S}^1$. In this case one can check that the functions ν, ν_1 determined by x are not zero and ν and ν_1 have the same sign, that is, Δx is spacelike. And the plane spanned by $\partial x, \Delta x, \partial\Delta x$ is a lightlike plane. So $\mathscr{C}$ is a parabolic conic section, and from Lemma 8, ∂x and ∂x_1 lie to the same side of the straight line spanned (within that plane) by Δx. Such singular edges appear in Examples 7, 8.

8.3. Case 3 of GVP singular edges. We need to consider the case that the tangent circle $\mathscr{C}$ has two intersection points with $\mathbb{S}^1$ and $[g, g_1]$ intersects $\mathbb{S}^1$. In this case one can check that the functions ν, ν_1 determined by x are not zero and ν and ν_1 have the opposite sign, that is, Δx is timelike. And the plane spanned by $\partial x, \Delta x, \partial\Delta x$ is a timelike plane. So $\mathscr{C}$ is a hyperbolic conic section, and from Lemma 8, ∂x and ∂x_1 lie to the opposite side of the straight line (within that plane) spanned by Δx. Such singular edges appear in Examples 7, 8.

8.4. Case 1 of NVP singular edges. We need to consider the case that g or g_1 lies in $\mathbb{S}^1$. In this case one can check that the function ν (resp. ν_1) determined by x is zero when g (resp. g_1) lies in $\mathbb{S}^1$. Moreover, x (resp. x_1) is a singularity of the smooth curve it lies in. One can check that Δx is lightlike but is not zero. Such singular edges appear in Example 7, but not in Example 8.

8.5. Case 2 of NVP singular edges. We need to consider the case that g or g_1 lies in $\mathbb{S}^1$. In this case one can check that the function ν (resp. ν_1) determined by x is zero when g (resp. g_1) lies in $\mathbb{S}^1$. One can check that Δx is zero, that is, x and x_1 are the same point. Such singular edges appear in Example 8, but not in Example 7.

9. Examples

Example 7. We can construct a semi-discrete maximal Enneper surface by taking

$$g(k,t) = c(k+it) \text{ (resp. } g(k,t) = c(k+it)) \ (c \in \mathbb{R} \setminus \{0\})$$

in Theorem 6.

Example 8. In Section 4, we gave the full class of all semi-discrete maximal surfaces of revolution. Choosing suitable semi-discrete holomorphic functions, we can construct all of those semi-discrete maximal surfaces of revolution.

	parametrizations of profile curves
smooth elliptic catenoid	$\begin{pmatrix}\sinh t\\0\\t\end{pmatrix}$ $(t\in\mathbb{R})$
smooth hyperbolic catenoid	$\begin{pmatrix}0\\t\\\cos t\end{pmatrix}$
smooth parabolic catenoid	$\begin{pmatrix}t^3+t\\0\\t^3-t\end{pmatrix}$
EC^{pd}_{rd}-catenoid	$\begin{pmatrix}\sinh(\ell\cdot n)\\0\\\sinh\ell\cdot n\end{pmatrix}$ $(n\in\mathbb{Z},\ \ell\in\mathbb{R}\setminus\{0\})$
EC^{pd}_{rs}-catenoid	$\begin{pmatrix}\sinh(\ell\cdot n)\\0\\\sinh\ell\cdot n\end{pmatrix}$
EC^{ps}_{rd}-catenoid	$\begin{pmatrix}\sinh t\\0\\t\end{pmatrix}$
HC^{pd}_{rd}-catenoid	$\begin{pmatrix}0\\\sin\ell\cdot n\\\cos(\ell\cdot n)\end{pmatrix}$ $(\ell\in(-1,1)\setminus\{0\})$
HC^{pd}_{rs}-catenoid	$\begin{pmatrix}0\\\sin\ell\cdot n\\\cos(\ell\cdot n)\end{pmatrix}$
HC^{ps}_{rd}-catenoid	$\begin{pmatrix}0\\t\\\cos t\end{pmatrix}$
PC^{pd}_{rd}-catenoid	$\begin{pmatrix}\ell^3\cdot n(n-1)(n+1)+\ell\cdot n\\0\\\ell^3\cdot n(n-1)(n+1)-\ell\cdot n\end{pmatrix}$ $(\ell\in\mathbb{R}\setminus\{0\})$
PC^{pd}_{rs}-catenoid	$\begin{pmatrix}\ell^3\cdot n(n-1)(n+1)+\ell\cdot n\\0\\\ell^3\cdot n(n-1)(n+1)-\ell\cdot n\end{pmatrix}$
PC^{ps}_{rd}-catenoid	$\begin{pmatrix}t^3+t\\0\\t^3-t\end{pmatrix}$

TABLE 1. Parametrizations of seven types of catenoids

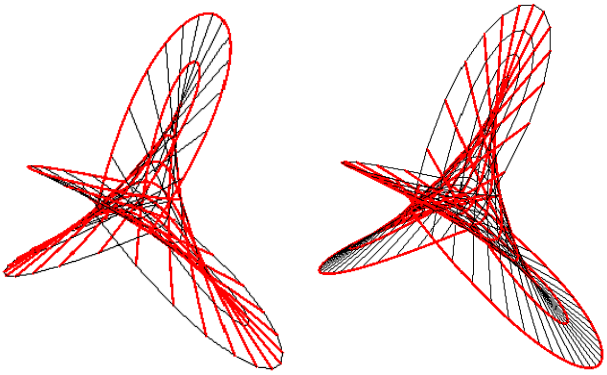

FIGURE 9. Two semi-discrete maximal Enneper surfaces

CHAPTER 4

Bour surface companions in non-Euclidean space forms

1. Introduction

Minimal surfaces in 3-dimensional Euclidean space $\mathbb{R}^3$ isometric to rotational surfaces were first introduced by Bour [**8**] in 1862. All such minimal surfaces are given via the well-known Weierstrass representation for minimal surfaces by choosing suitable data depending on a parameter m, as shown by Schwarz [**65**]. They are called Bour's minimal surfaces $\mathfrak{B}_m$ of value m. Furthermore, when m is an integer greater than 1, $\mathfrak{B}_m$ become algebraic, that is, there is an implicit polynomial equation satisfied by the three coordinates of $\mathfrak{B}_m$, see also [**30, 55, 73**].

Kobayashi [**47**] gave an analogous Weierstrass-type representation for conformal spacelike surfaces with mean curvature identically 0, called maximal surfaces, in 3-dimensional Minkowski space $\mathbb{R}^{2,1}$. However, unlike the case of minimal surfaces in $\mathbb{R}^3$, maximal surfaces generally have singularities. Details about singularities of maximal surfaces can be found in [**27, 69**]. We remark that Magid [**51**] gave a Weierstrass-type representation for timelike surfaces with mean curvature identically 0, called timelike minimal surfaces, in $\mathbb{R}^{2,1}$, see also [**40**].

On the other hand, Lawson [**48**] showed that there is an isometric correspondence between constant mean curvature (CMC for short) surfaces in Riemannian space forms, and Palmer [**58**] showed that there is an analogous correspondence between spacelike CMC surfaces in Lorentzian space forms. In particular, minimal surfaces in $\mathbb{R}^3$ correspond to CMC 1 surfaces in 3-dimensional hyperbolic space $\mathbb{H}^3$, and maximal surfaces in $\mathbb{R}^{2,1}$ correspond to CMC 1 surfaces in 3-dimensional de Sitter space $\mathbb{S}^{2,1}$. Thus it is natural to expect existence of corresponding Weierstrass-type representations in these cases. Bryant [**16**] gave such a representation formula for CMC 1 surfaces in $\mathbb{H}^3$, and Umehara, Yamada [**67**] applied it. Similarly, Aiyama, Akutagawa [**1**] gave a representation formula for CMC 1 surfaces in $\mathbb{S}^{2,1}$. However,

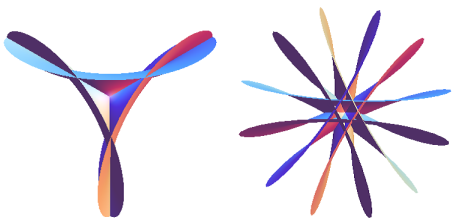

FIGURE 1. Bour's minimal surfaces of value 3 and 6 in $\mathbb{R}^3$. These surfaces are isometric to rotational surfaces in $\mathbb{R}^3$.

analogues of Bour's surfaces in other 3-dimensional space forms had not yet been studied.

In Sections 2 and 3 of this paper, in order to show that several maximal and timelike minimal Bour's surfaces of value m are algebraic, we review Weierstrass-type representations for maximal surfaces and timelike minimal surfaces in $\mathbb{R}^{2,1}$, and give explicit parametrizations for spacelike and timelike minimal Bour's surfaces of value m. In Section 4, we introduce Bour type CMC 1 surfaces in $\mathbb{H}^3$ and $\mathbb{S}^{2,1}$, and show several properties of those surfaces. Finally, in Section, 5 we calculate the degrees, classes and implicit equations of the maximal and timelike minimal Bour's surfaces of values 2, 3, 4 in $\mathbb{R}^{2,1}$ in terms of their coordinates. We remark that in the cases of $\mathbb{H}^3$ and $\mathbb{S}^{2,1}$, all surfaces are algebraic in some sense, because the Lorentz ($\mathbb{R}^{3,1}$) norm of all elements in $\mathbb{H}^3 \subset \mathbb{R}^{3,1}$ or $\mathbb{S}^{2,1} \subset \mathbb{R}^{3,1}$ is constant. However, we have the following two remaining problems:

PROBLEM 1.
- What is the class of maximal and timelike minimal Bour's surfaces of general value m in $\mathbb{R}^{2,1}$?
- Are there any other implicit equations for CMC 1 Bour type surfaces? If there exist implicit equations, what are the corresponding degrees and classes?

2. Spacelike maximal Bour type surfaces in $\mathbb{R}^{2,1}$

Let

$$\mathbb{R}^{n,1} := \left(\{x = (x_1, \cdots, x_n, x_0)^t | x_i \in \mathbb{R}\}, \langle \cdot, \cdot \rangle\right)$$

be the $(n+1)$-dimensional Lorentz-Minkowski (for short, Minkowski) space with Lorentz metric $\langle x, y\rangle = x_1 y_1 + \cdots + x_n y_n - x_0 y_0$. Then the 3-dimensional hyperbolic space $\mathbb{H}^3$ and 3-dimensional de Sitter space $\mathbb{S}^{2,1}$ are defined as follows:

$$\mathbb{H}^3 := \{x \in \mathbb{R}^{3,1} | \langle x, x\rangle = -1,\ x_0 > 0\} \cong \left\{F\bar{F}^t | F \in \mathrm{SL}_2\mathbb{C}\right\},$$
$$\mathbb{S}^{2,1} := \{x \in \mathbb{R}^{3,1} | \langle x, x\rangle = 1\} \cong \left\{F \begin{pmatrix} 1 & 0 \\ 0 & -1 \end{pmatrix} \bar{F}^t | F \in \mathrm{SL}_2\mathbb{C}\right\}.$$

A vector $x \in \mathbb{R}^{n,1}$ is called spacelike if $\langle x, x\rangle > 0$, timelike if $\langle x, x\rangle < 0$, and lightlike if $x \neq 0$ and $\langle x, x\rangle = 0$. A surface in $\mathbb{R}^{n,1}$ is called spacelike (resp. timelike, lightlike) if the induced metric on the tangent planes is a positive definite Riemannian (resp. Lorentzian, degenerate) metric.

Kobayashi [**47**] found a Weierstrass-type representation for spacelike conformal maximal surfaces in $\mathbb{R}^{2,1}$.

THEOREM 10. Let g be a meromorphic function and let ω be a holomorphic function defined on a simply connected open subset $\mathcal{U} \subset \mathbb{C}$ such that ω does not vanish on $\mathcal{U}$. Then

$$f(z) = \mathrm{Re} \int \begin{pmatrix} (1+g^2)\,\omega \\ i\,(1-g^2)\,\omega \\ 2g\omega \end{pmatrix} dz$$

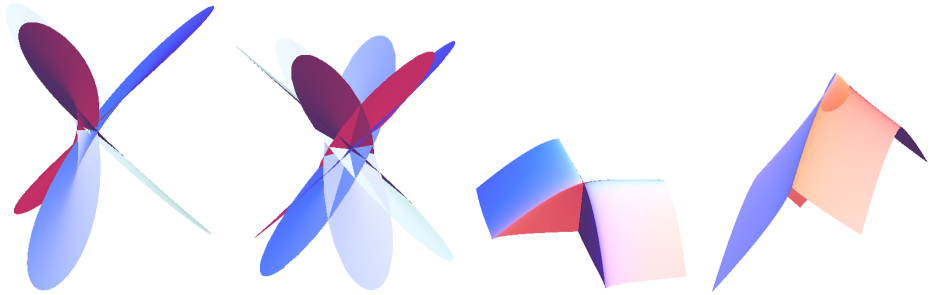

FIGURE 2. Left two pictures: spacelike $\mathfrak{B}_3$ and $\mathfrak{B}_6$ in $\mathbb{R}^{2,1}$, right two pictures: timelike $\mathfrak{B}_3$ and $\mathfrak{B}_6$ in $\mathbb{R}^{2,1}$

is a spacelike conformal immersion with mean curvature identically 0 (i.e. spacelike conformal maximal surface). Conversely, any spacelike conformal maximal surface can be described in this manner.

Remark. A pair of a holomorphic function g and a holomorphic function ω (g, ω) is called Weierstrass data for a maximal surface. In Section 4 we also call (g, ω) the Weierstrass data for CMC 1 surfaces in $\mathbb{H}^3$ and $\mathbb{S}^{2,1}$. □

We call maximal surfaces $\mathfrak{B}_m$ $(m \in \mathbb{Z}_{\geq 2} := \{n \in \mathbb{Z} | n \geq 2\})$ given by $(g, \omega) = (z, z^{m-2})$ the spacelike Bour's maximal surfaces $\mathfrak{B}_m$ of value m (spacelike $\mathfrak{B}_m$, for short). Several properties of spacelike $\mathfrak{B}_m$ can be found in the first author's paper [**32**]. The parametrization of spacelike $\mathfrak{B}_m$ is

$$\mathfrak{B}_m(u,v) = \operatorname{Re}\left(\sum_{k=0}^{m-1}\begin{pmatrix} \frac{1}{m-1}\binom{m-1}{k}u^{m-1-k}(iv)^k + \frac{1}{m+1}\binom{m+1}{k}u^{m+1-k}(iv)^k \\ \frac{i}{m-1}\binom{m-1}{k}u^{m-1-k}(iv)^k - \frac{i}{m+1}\binom{m+1}{k}u^{m+1-k}(iv)^k \\ \frac{2}{m}\binom{m}{k}u^{m-k}(iv)^k \end{pmatrix}\right) \tag{72}$$

with Gauss map

$$n = \left(\frac{2u}{u^2+v^2-1}, \frac{2v}{u^2+v^2-1}, \frac{u^2+v^2+1}{u^2+v^2-1}\right),$$

where $z = u + iv$. The left two pictures in Figure 2 are two examples of spacelike $\mathfrak{B}_m$.

3. Timelike minimal Bour type surfaces in $\mathbb{R}^{2,1}$

Next, we give the Weierstrass-type representation for timelike minimal surfaces in $\mathbb{R}^{2,1}$, which was obtained by M. Magid [**51**] (see also [**40**]).

THEOREM 11. Let $g_1(u)$, $\omega_1(u)$ (resp. $g_2(v)$, $\omega_2(v)$) be smooth functions depending on only u (resp. v) on a connected orientable 2-manifold with local coordinates

u, v. Then

$$\hat{f}(u,v) = \int \begin{pmatrix} 2g_1\omega_1 \\ (1-g_1^2)\,\omega_1 \\ -(1+g_1^2)\,\omega_1 \end{pmatrix} du + \int \begin{pmatrix} 2g_2\omega_2 \\ (1-g_2^2)\,\omega_2 \\ (1+g_2^2)\,\omega_2 \end{pmatrix} dv$$

is a timelike surface with mean curvature identically 0 (i.e. timelike minimal surface). Conversely, any timelike minimal surface can be described in this manner.

The timelike minimal surfaces given by $(g_1(u), \omega_1(u)) = (u, u^{m-2})$, $(g_2(v), \omega_2(v)) = (v, v^{m-2})$ are called timelike Bour surfaces $\mathfrak{B}_m$ of value m (timelike $\mathfrak{B}_m$, for short) in $\mathbb{R}^{2,1}$, where $m \in \mathbb{Z}_{\geq 2}$. The parametrization of timelike $\mathfrak{B}_m$ is

$$\mathfrak{B}_m(u,v) = \begin{pmatrix} \frac{2}{m}\,(u^m + v^m) \\ \frac{1}{m-1}\,(u^{m-1} + v^{m-1}) - \frac{1}{m+1}\,(u^{m+1} + v^{m+1}) \\ -\frac{1}{m-1}\,(u^{m-1} - v^{m-1}) - \frac{1}{m+1}\,(u^{m+1} - v^{m+1}) \end{pmatrix}, \tag{73}$$

with Gauss map

$$n = \left(\frac{uv-1}{1+uv}, \frac{u+v}{1+uv}, \frac{u-v}{1+uv} \right).$$

The right two pictures in Figure 2 are two examples of timelike $\mathfrak{B}_m$.

4. CMC 1 Bour type surfaces in $\mathbb{H}^3$ and $\mathbb{S}^{2,1}$

In this section we consider CMC 1 surfaces in $\mathbb{H}^3$ and $\mathbb{S}^{2,1}$. Here we identify elements in $\mathbb{H}^3$ and $\mathbb{S}^{2,1}$ with $\mathrm{SL}_2\mathbb{C}$ matrix forms as in Section 2. In this setting Bryant [**16**] showed the following representation formula for CMC 1 surfaces in $\mathbb{H}^3$:

THEOREM 12. Let $F \in \mathrm{SL}_2\mathbb{C}$ be a solution of the equation

$$dF = F \begin{pmatrix} g & -g^2 \\ 1 & -g \end{pmatrix} \omega, \;\; F|_{z=z_0} \in \mathrm{SL}_2\mathbb{C} \tag{74}$$

for some z_0 in a given domain, where (g, ω) is Weierstrass data. Then the surface $f = F\bar{F}^t$ is a conformal CMC 1 immersion into $\mathbb{H}^3$. Conversely, any conformal CMC 1 immersion in $\mathbb{H}^3$ can be described in this way. The metric of f is $(1+|g|^2)^2|\omega|^2$.

Similarly, Aiyama and Akutagawa [**1**] showed the following Bryant-type representation formula for CMC 1 surfaces in $\mathbb{S}^{2,1}$:

THEOREM 13. Let $\hat{F} \in \mathrm{SL}_2\mathbb{C}$ be a solution of Equation (74), where (g, ω) is Weierstrass data. Then the surface $f = F \begin{pmatrix} 1 & 0 \\ 0 & -1 \end{pmatrix} \bar{F}^t$ is a spacelike conformal CMC 1 immersion into $\mathbb{S}^{2,1}$. Conversely, any spacelike conformal CMC 1 immersion in $\mathbb{S}^{2,1}$ is described in this way. The metric of f is $(1-|g|^2)^2|\omega|^2$.

Note that, unlike in $\mathbb{H}^3$, CMC 1 surfaces in $\mathbb{S}^{2,1}$ generally have singularities. Their singularities have been investigated in [**27, 69**].

We call CMC 1 surfaces in $\mathbb{H}^3$ and $\mathbb{S}^{2,1}$ given by the Weierstrass data $(g, \omega) = (z, z^{m-2})$ the Bour type CMC 1 cousins $\mathfrak{B}_m$ of value m ($\mathfrak{B}_m$ cousin, for short). We now describe F explicitly:

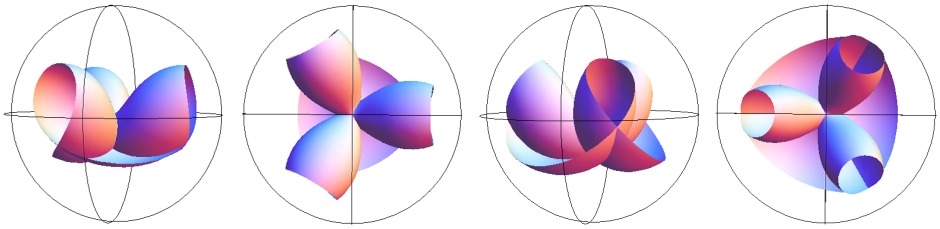

FIGURE 3. Left two pictures: $\mathfrak{B}_3$ cousin in $\mathbb{H}^3$, right two picures: its dual cousin in $\mathbb{H}^3$ (in the Poincaré ball model for $\mathbb{H}^3$)

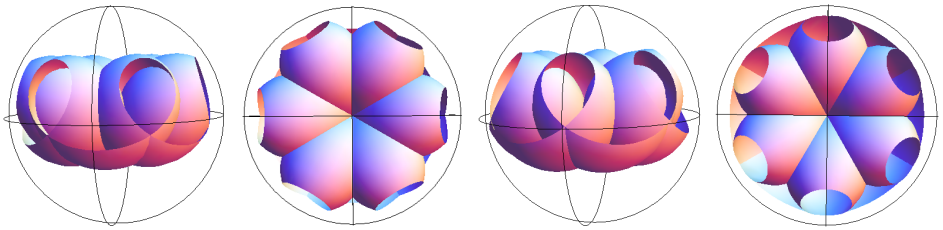

FIGURE 4. Left two pictures: $\mathfrak{B}_6$ cousin in $\mathbb{H}^3$, right two pictures: its dual cousin in $\mathbb{H}^3$

THEOREM 14. Let $F(z) = \begin{pmatrix} a(z) & b(z) \\ c(z) & d(z) \end{pmatrix} \in \mathrm{SL}_2\mathbb{C}$ be a solution of Equation (74) with $(g, \omega) = (z, z^{m-2}dz)$ and with initial condition $F(0) = \begin{pmatrix} 1 & 0 \\ 0 & 1 \end{pmatrix}$. Then

$$
\begin{aligned}
a(z) &= m^{\frac{1}{m}}\Gamma\left(\frac{m+1}{m}\right) z^{\frac{m-1}{2}}\,\mathrm{Bessel\,I}\left(-\frac{m-1}{m}, \frac{2}{m}z^{\frac{m}{2}}\right), \\
b(z) &= -m^{\frac{1}{m}}\Gamma\left(\frac{m+1}{m}\right) z^{\frac{m+1}{2}}\,\mathrm{Bessel\,I}\left(\frac{m+1}{m}, \frac{2}{m}z^{\frac{m}{2}}\right), \\
c(z) &= m^{\frac{-1}{m}}\Gamma\left(\frac{m-1}{m}\right) z^{\frac{m-1}{2}}\,\mathrm{Bessel\,I}\left(\frac{m-1}{m}, \frac{2}{m}z^{\frac{m}{2}}\right), \\
d(z) &= -m^{\frac{-1}{m}}\Gamma\left(\frac{m-1}{m}\right) z^{\frac{m+1}{2}}\,\mathrm{Bessel\,I}\left(-\frac{m+1}{m}, \frac{2}{m}z^{\frac{m}{2}}\right),
\end{aligned}
\tag{75}
$$

where Γ denotes the Gamma function and Bessel I represents the modified Bessel function. The definition of Bessel I can be found in standard textbooks, for example, see [**39**].

Proof. Equation (74) gives

$$
X'' - \frac{\omega'}{\omega}X' - g'\omega X = 0, \quad (X = a(z),\ c(z)), \tag{76}
$$

$$
Y'' - \frac{(g^2\omega)'}{g^2\omega}Y' - g'\omega Y = 0 \quad (Y = b(z),\ d(z)), \tag{77}
$$

which are given in [**67**]. Here we solve Equation (76). Inserting $(g, \omega) = (z, z^{m-2})$ into Equation (76), we have

$$X'' - \frac{m-2}{z}X' - z^{m-2}X = 0. \quad (m \in \mathbb{Z}_{\geq 2}) \tag{78}$$

We give two independent power series solutions of the differential equation (78) by the Frobenius method. The indicial equation at $z = 0$ is $\rho(\rho - 1) - (m - 2)\rho = 0$. So we see that the characteristic exponents of the equation (78) are 0 and $m - 1$. Then we have a solution of the form

$$z^{m-1}\sum_{p=0}^{\infty} a_p z^p,$$

where the coefficients a_p are inductively given by

$$\begin{aligned} &a_{mk+l} = 0 \quad (l = 0, \cdots, m), \\ &a_{mk+m+1} = \frac{a_{m(k-1)+m-1}}{(m-2)k(mk+m-1)} = \frac{\Gamma(\frac{m-1}{m}+k)}{m^2\Gamma(\frac{m-1}{m}+k+1)}a_{m(k-1)+m-1} \\ &\qquad\qquad\qquad\qquad\qquad\qquad\qquad\qquad (l \geq m+1). \end{aligned}$$

Therefore we obtain a solution of the differential equation (78):

$$z^{\frac{m-1}{2}}\sum_{k=0}^{\infty}\frac{(-1)^k}{k!\Gamma(\frac{m-1}{m}+k+1)}\left(\frac{z^{\frac{m}{2}}}{m}\right)^{2k+\frac{m-1}{m}} = z^{\frac{m-1}{2}}\,\mathrm{Bessel\,I}\left(\frac{m-1}{m}, \frac{2}{m}z^{\frac{m}{2}}\right).$$

Similarly, we obtain another independent solution as

$$z^{\frac{m-1}{2}}\sum_{k=0}^{\infty}\frac{(-1)^k}{k!\Gamma(-\frac{m-1}{m}+k+1)}\left(\frac{z^{\frac{m}{2}}}{m}\right)^{2k-\frac{m-1}{m}} = z^{\frac{m-1}{2}}\,\mathrm{Bessel\,I}\left(-\frac{m-1}{m}, \frac{2}{m}z^{\frac{m}{2}}\right).$$

So we have two independent solutions of Equation (76). Next, we find two independent solutions of Equation (77). Inserting $(g, \omega) = (z, z^{m-2})$ into Equation (77), we have

$$Y'' - \frac{m}{z}Y' - z^{m-2}Y = 0. \quad (m \in \mathbb{Z}_{\geq 2})$$

Similarly to the way we solved Equation (76), we have two independent solutions

$$z^{\frac{m+1}{2}}\,\mathrm{Bessel\,I}\left(\frac{m+1}{m}, \frac{2}{m}z^{\frac{m}{2}}\right), \quad z^{\frac{m+1}{2}}\,\mathrm{Bessel\,I}\left(-\frac{m+1}{m}, \frac{2}{m}z^{\frac{m}{2}}\right).$$

Using the initial conditions, we have the solution F as in Equations (75). □

Remark. If F is a solution of Equation (74), the surface

$$f^\sharp = (F^{-1})\overline{(F^{-1})}^t \quad \left(\text{resp. } f^\sharp = (F^{-1})\begin{pmatrix}1 & 0\\ 0 & -1\end{pmatrix}\overline{(F^{-1})}^t\right)$$

is also a CMC 1 surface in $\mathbb{H}^3$ (resp. $\mathbb{S}^{2,1}$). This was proven in [**68**] (resp. [**49**]). The surface $f^\sharp$ is called the CMC 1 dual of f. □

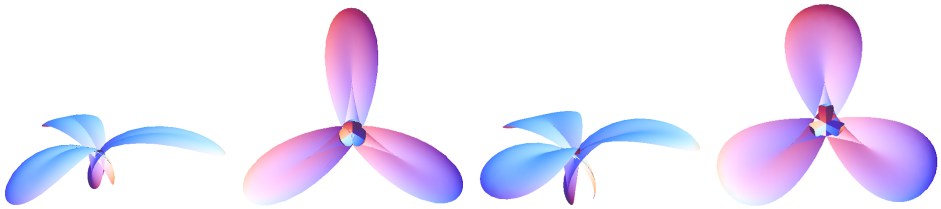

FIGURE 5. Left two pictures: $\mathfrak{B}_3$ cousin in $\mathbb{S}^{2,1}$, right two pictures: its dual cousin in $\mathbb{S}^{2,1}$

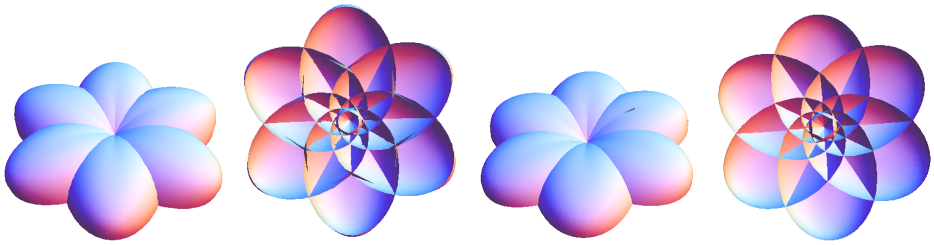

FIGURE 6. Left two pictures: $\mathfrak{B}_6$ cousin in $\mathbb{S}^{2,1}$, right two pictures: its dual cousin in $\mathbb{S}^{2,1}$

Using the explicit parametrization of the $\mathfrak{B}_m$ cousin, we can easily show the following corollary, which implies the rotational symmetric property of the $\mathfrak{B}_m$ cousins in $\mathbb{H}^3$, $\mathbb{S}^{2,1}$.

COROLLARY 1. Let $F(z) \in \mathrm{SL}_2\mathbb{C}$ be the form as in Theorem 14 with complex coordinate z. Then

$$F(\mathrm{e}^{i\frac{2\pi}{m}} \cdot z) = \begin{pmatrix} a(z) & \mathrm{e}^{i\frac{2\pi}{m}} \cdot b(z) \\ \mathrm{e}^{-i\frac{2\pi}{m}} \cdot c(z) & d(z) \end{pmatrix}.$$

Writing $\mathfrak{B}_m$ cousin in $\mathbb{H}^3$ or $\mathbb{S}^{2,1}$ as $f(z) = (x_1(z), x_2(z), x_3(z), x_0(z))^t$, given by Theorem 14, and setting $f\left(\mathrm{e}^{i\frac{2\pi}{m}} \cdot z\right) = (\hat{x}_1(z), \hat{x}_2(z), \hat{x}_3(z), \hat{x}_0(z))^t$. By Corollary 1, we have

$$\begin{aligned} \hat{x}_1(z) &= \cos\left(\frac{2\pi}{m}\right) x_1(z) - \sin\left(\frac{2\pi}{m}\right) x_2(z), \\ \hat{x}_2(z) &= \sin\left(\frac{2\pi}{m}\right) x_1(z) + \cos\left(\frac{2\pi}{m}\right) x_2(z), \\ \hat{x}_3(z) &= x_3(z),\ \ \hat{x}_0(z) = x_0(z), \end{aligned}$$

that is, by rotating z by angle $\frac{2\pi}{m}$, the first and second coordinates are also rotated by the same angle. So like in $\mathbb{R}^3$ and $\mathbb{R}^{2,1}$, $\mathfrak{B}_m$ has symmetry with respect to rotation by angle $\frac{2\pi}{m}$. Its dual $(\mathfrak{B}_m)^\sharp$ also has the same symmetry.

In order to see CMC 1 surfaces in $\mathbb{H}^3$, we use a stereographic projection. Consider the map

$$\mathbb{H}^3 \ni (x_1, x_2, x_3, x_0)^t \mapsto \left(\frac{x_1}{1+x_0}, \frac{x_2}{1+x_0}, \frac{x_3}{1+x_0}\right)^t \in \mathbb{B}^3,$$

where $\mathbb{B}^3$ denotes the 3-dimensional unit ball. This is the Poincaré ball model for $\mathbb{H}^3$. The pictures in Figures 3, 4 are two examples of $\mathfrak{B}_m$ cousins projected into $\mathbb{B}^3$.

In order to show graphics of CMC 1 surfaces in $\mathbb{S}^{2,1}$, the hollow ball model is used, see [**25**] for example. Consider the map

$$\mathbb{S}^{2,1} \ni (x_1, x_2, x_3, x_0)^t \mapsto \left(\frac{\mathrm{e}^{\arctan(x_0)} \cdot x_1}{\sqrt{1+x_0^2}}, \frac{\mathrm{e}^{\arctan(x_0)} \cdot x_2}{\sqrt{1+x_0^2}}, \frac{\mathrm{e}^{\arctan(x_0)} \cdot x_3}{\sqrt{1+x_0^2}} \right)^t \in \mathbb{B}^3_{(-\pi,\pi)},$$

where $\mathbb{B}^3_{(-\pi,\pi)} := \{(y_1, y_2, y_3)^t \in \mathbb{R}^3 \mid \mathrm{e}^{-\pi} < y_1^2 + y_2^2 + y_3^2 < \mathrm{e}^{\pi}\}$. Figures 5, 6 show two examples of $\mathfrak{B}_m$ projected into $\mathbb{B}^3_{(-\pi,\pi)}$.

5. Degree and class of Bour type surfaces in $\mathbb{R}^{2,1}$

For $\mathbb{R}^{2,1}$, the set of roots of a polynomial $Q(x, y, z) = 0$ gives an algebraic surface. An algebraic surface f is said to be of *degree* (or *order*) n when $n = \deg(f)$.

The tangent plane at a point (u, v) on a surface $f\,(u, v) = (x(u, v), y(u, v), z(u, v))$ is given by

$$Xx + Yy - Zz + P = 0, \tag{79}$$

where the Gauss map is $n = (X(u, v), Y(u, v), Z(u, v))$ and $P = P(u, v)$. We have inhomogeneous tangential coordinates $a = X/P$, $b = Y/P$, and $c = Z/P$. When we can obtain an implicit equation $\hat{Q}(a, b, c) = 0$ of $f\,(u, v)$ in tangential coordinates, the maximum degree of the equation gives the *class* of $f\,(u, v)$.

Next, using Groebner and other polynomial elimination methods (in Maple software), we calculate the implicit equations, degrees and classes of spacelike and timelike $\mathfrak{B}_2$, $\mathfrak{B}_3$ and $\mathfrak{B}_4$.

5.1. Degree and class of spacelike $\mathfrak{B}_2$, $\mathfrak{B}_3$, $\mathfrak{B}_4$ in $\mathbb{R}^{2,1}$. From (72), the parametrization of $\mathfrak{B}_2$ (maximal Enneper surface) is

$$\mathfrak{B}_2\,(u, v) = \begin{pmatrix} \frac{1}{3}u^3 - uv^2 + u \\ u^2 v - \frac{1}{3}v^3 - v \\ u^2 - v^2 \end{pmatrix} = \begin{pmatrix} x(u, v) \\ y(u, v) \\ z(u, v) \end{pmatrix},$$

where $u, v \in \mathbb{R}$. In this section, $Q_m(x, y, z) = 0$ denotes the irreducible implicit equation that spacelike or timelike $\mathfrak{B}_m$ will satisfy. Then

$$\begin{aligned} Q_2(x, y, z) = {} & -64z^9 + 432x^2z^6 - 432y^2z^6 + 1215x^4z^3 + 6318x^2y^2z^3 \\ & -3888x^2z^5 + 1215y^4z^3 - 3888y^2z^5 + 1152z^7 + 729x^6 - 2187x^4y^2 \\ & -4374x^4z^2 + 2187x^2y^4 + 6480x^2z^4 - 729y^6 + 4374y^4z^2 - 6480y^2z^4 \\ & -729x^4z + 1458x^2y^2z + 3888x^2z^3 - 729y^4z + 3888y^2z^3 - 5184z^5, \end{aligned}$$

and its degree is $\deg(\mathfrak{B}_2) = 9$. Therefore, $\mathfrak{B}_2$ is an algebraic maximal surface. To find the class of the surface $\mathfrak{B}_2$, we obtain

$$P_2(u, v) = \frac{(u^2 + v^2 - 3)(u - v)(u + v)}{3(u^2 + v^2 - 1)},$$

where $P_m(u,v)$ denotes the function as in Equation (79) for spacelike or timelike $\mathfrak{B}_m$. The inhomogeneous tangential coordinates are

$$a=\frac{6u}{\alpha(u,v)},\ b=\frac{6v}{\alpha(u,v)},\ c=\frac{6(u^2+v^2+1)}{\alpha(u,v)},$$

where $\alpha(u,v)=(u^2+v^2-3)(u-v)(u+v)$. In the tangential coordinates a,b,c,

$$\begin{aligned}\hat{Q}_2(a,b,c)&=4a^6+9a^4+9b^4+6a^2b^2c^2+12b^2c^3-3b^4c^2-18b^4c\\&-4a^4b^2+18a^4c-12a^2c^3-4a^2b^4-3a^4c^2+18a^2b^2-4a^2b^4+4b^6,\end{aligned}$$

where $\hat{Q}_m(a,b,c)=0$ denotes the irreducible implicit equation for spacelike or timelike $\mathfrak{B}_m$ in terms of tangential coordinates. Therefore, the class of the spacelike $\mathfrak{B}_2$ is $cl(\mathfrak{B}_2)=6$.

Similarly,

$$\mathfrak{B}_3(u,v)=\begin{pmatrix}\frac{u^4}{4}+\frac{v^4}{4}-\frac{3}{2}u^2v^2+\frac{u^2}{2}-\frac{v^2}{2}\\ u^3v-uv^3-uv\\ \frac{2}{3}u^3-2uv^2\end{pmatrix}=\begin{pmatrix}x(u,v)\\y(u,v)\\z(u,v)\end{pmatrix},$$

$$\mathfrak{B}_4(u,v)=\begin{pmatrix}\frac{1}{3}u^3-uv^2+\frac{1}{5}u^5-2u^3v^2+uv^4\\ -u^2v+\frac{1}{3}v^3+u^4v-2u^2v^3+\frac{1}{5}v^5\\ \frac{1}{2}u^4-3u^2v^2+\frac{1}{2}v^4\end{pmatrix}=\begin{pmatrix}x(u,v)\\y(u,v)\\z(u,v)\end{pmatrix},$$

and

$$\begin{aligned}&Q_3(x,y,z)=-43046721z^{16}+272097792x^3z^{12}-816293376xy^2z^{12}\\&+3009871872x^6z^8+14834368512x^4y^2z^8+(69\text{ other lower order terms}),\\&Q_4(x,y,z)=-1514571848868138319872z^{25}+924421294475182080000x^4z^{20}\\&-241927616557617187500000000x^4y^{12}z^5-554652776685109248000000x^2y^2z^{20}\\&-306525723266601562500000000x^{12}y^6z^2+(233\text{ other lower order terms}),\end{aligned}$$

and their degrees are $\deg(\mathfrak{B}_3)=16$, $\deg(\mathfrak{B}_4)=25$. Therefore, $\mathfrak{B}_3$ and $\mathfrak{B}_4$ are algebraic spacelike maximal surfaces. Furthermore,

$$\begin{aligned}P_3(u,v)&=\frac{u(u^2+v^2-2)(u^2-3v^2)}{(u^2+v^2-1)},\\P_4(u,v)&=\frac{(3u^2+3v^2-5)(u^2-2uv-v^2)(u^2+2uv-v^2)}{30(u^2+v^2-1)},\end{aligned}$$

and the inhomogeneous tangential coordinates are

$$\begin{aligned}a&=\frac{12}{\beta(u,v)},\ b=\frac{12v}{u\beta(u,v)},\ c=\frac{6(u^2+v^2+1)}{u\beta(u,v)}\quad(m=3),\\a&=\frac{60u}{\gamma(u,v)},\ b=\frac{60v}{\gamma(u,v)},\ c=\frac{30(u^2+v^2+1)}{\gamma(u,v)}\quad(m=4),\end{aligned}$$

where $\beta(u,v) = (u^2+v^2-2)(u^2-3v^2)$, $\gamma(u,v) = (3u^2+3v^2-5)(u^2-2uv-v^2)(u^2+2uv-v^2)$. Then

$$\begin{aligned}
&\hat{Q}_3(a,b,c) = 9a^8 + 72a^6b^2 - 8a^6c^2 + 144a^4b^4 - 168a^4b^2c^2\\
&-96a^2b^4c^2 + 96a^2b^2c^4 + 64b^6c^2 - 48b^4c^4 - 72a^7\\
&-288a^5b^2 + 288a^5c^2 + 288a^3b^2c^2 - 192a^3c^4 + 144a^6,\\
&\hat{Q}_4(a,b,c) = -16a^{10} - 8640a^2b^2c^5 - 9000a^4b^4c - 3600a^2b^6c\\
&+12000a^2b^4c^3 + 570a^4b^4c^2 - 180a^2b^6c^2 + 15b^8c^2 - 900b^8 + 1440a^4c^5\\
&+1440b^4c^5 - 5400a^4b^4 - 3600a^2b^6 + 900b^8c - 2400b^6c^3 - 416a^6b^4\\
&-416a^4b^6 + 176a^2b^8 - 16b^{10} + 12000a^4b^2c^3 - 3600a^6b^2c - 180a^6b^2c^2\\
&-3600a^6b^2 + 176a^8b^2 - 2400a^6c^3 + 900a^8c + 15a^8c^2 - 900a^8.
\end{aligned}$$

Therefore, $cl(\mathfrak{B}_3) = 8$ and $cl(\mathfrak{B}_4) = 10$.

5.2. Degree and class of timelike $\mathfrak{B}_2$, $\mathfrak{B}_3$, $\mathfrak{B}_4$ in $\mathbb{R}^{2,1}$. From (73), the parametrization of $\mathfrak{B}_2$ (timelike Enneper surface) is

$$\mathfrak{B}_2(u,v) = \begin{pmatrix} u^2+v^2 \\ u+v-\frac{1}{3}(u^3+v^3) \\ -u+v-\frac{1}{3}(u^3-v^3) \end{pmatrix} = \begin{pmatrix} x(u,v) \\ y(u,v) \\ z(u,v) \end{pmatrix}.$$

where $u, v \in \mathbb{R}$. Then

$$\begin{aligned}
&Q_2(x,y,z) = -16z^9 - 2916y^4z + 4374x^4y^2 - 6318y2x^2z^3 + 4374x^2y^4\\
&-2916x^4z - 5832x^2y^2z - 20736z^5 + 1152z^7 - 8748x^4z^2 + 8748y^4z^2\\
&+3888y^2z^5 - 3888x^2z^5 + 15552x^2z^3 + 1215x^4z^3 + 1458x^6 + 216x^2z^6\\
&+1458y^6 + 1215y^4z^3 + 216y^2z^6 + 12960y^2z^4 + 12960x^2z^4 - 15552y^2z^3.
\end{aligned}$$

Its degree is $\deg(\mathfrak{B}_2) = 9$. Hence, $\mathfrak{B}_2$ is an algebraic timelike minimal surface. To find the class of surface $\mathfrak{B}_2$ we obtain

$$P_2(u,v) = \frac{(uv+3)(u^2+v^2)}{3(uv+1)},$$

and the inhomogeneous tangential coordinates are

$$a = -\frac{(uv-1)(3uv+3)}{\hat{\alpha}(u,v)},\ b = -\frac{(u+v)(3uv+3)}{\hat{\alpha}(u,v)},\ c = -\frac{(u-v)(3uv+3)}{\hat{\alpha}(u,v)},$$

where $\hat{\alpha}(u,v) = (uv+1)(uv+3)(u^2+v^2)$. Then

$$\begin{aligned}
&\hat{Q}_2(a,b,c) = 16a^6 + 9a^4 + 36b^4c + 24a^2c^3 + 24b^2c^3 - 24a^2b^2c^2\\
&-12a^4c^2 - 16a^2b^4 - 12b^4c^2 - 36a^4c + 16a^4b^2 + 9b^4 - 16b^6 - 18a^2b^2.
\end{aligned}$$

Hence, $cl(\mathfrak{B}_2) = 6$. Similarly,

$$\mathfrak{B}_3(u,v) = \begin{pmatrix} \frac{2}{3}(u^3+v^3) \\ \frac{1}{2}(u^2+v^2) - \frac{1}{4}(u^4+v^4) \\ -\frac{1}{2}(u^2-v^2) - \frac{1}{4}(u^4-v^4) \end{pmatrix} = \begin{pmatrix} x(u,v) \\ y(u,v) \\ z(u,v) \end{pmatrix},$$

$$\mathfrak{B}_4(u,v) = \begin{pmatrix} \frac{1}{2}(u^4+v^4) \\ \frac{1}{3}(u^3+v^3) - \frac{1}{5}(u^5+v^5) \\ -\frac{1}{3}(u^3-v^3) - \frac{1}{5}(u^5-v^5) \end{pmatrix} = \begin{pmatrix} x(u,v) \\ y(u,v) \\ z(u,v) \end{pmatrix},$$

and

$$\begin{aligned} &Q_3(x,y,z) = 43046721z^{16} - 1836660096z^{14} \\ &+5435817984x^6z^4 + 602404356096x^4z^8 \\ &+165112971264x^2z^8 + (69 \text{ other lower order terms}), \\ &Q_4(x,y,z) = 311836912602146628334544598941564928z^{25} \\ &-380660293703792270916192137379840000x^4z^{20} \\ &-228396176222275362549715282427904000000x^2y^2z^{20} \\ &-380660293703792270916192137379840000y^4z^{20} \\ &-271833827901267673933071777792000000000x^8z^{15} \\ &+(233 \text{ other lower order terms}). \end{aligned}$$

So $\deg(\mathfrak{B}_3) = 16$, $\deg(\mathfrak{B}_4) = 25$. In the tangential coordinates a, b, c,

$$\begin{aligned} &\hat{Q}_3(a,b,c) = 81a^6b^2 - 27a^4b^4 - 72a^4b^2c^2 - 45a^2b^6 - 48a^2b^4c^2 - 9b^8 \\ &-8b^6c^2 - 108a^6b + 180a^4b^3 + 432a^4bc^2 - 36a^2b^5 - 288a2b^3c^2 - 288a^2bc^4 \\ &-36b^7 - 144b^5c^2 - 96b^3c^4 + 36a^6 - 108a^4b^2 + 108a^2b^4 - 36b^6, \\ &\hat{Q}_4(a,b,c) = -16a^{10} + 16b^{10} - 450a^8c + 15b^8c^2 - 225b^8 - 720a^4c^5 \\ &-1350a^4b^4 + 900a^2b^6 - 450b^8c - 1200b^6c^3 - 416a^6b^4 + 416a^4b^6 \\ &+176a^2b^8 - 4320a^2b^2c^5 + 4500a^4b^4c - 1800a^2b^6c - 6000a^2b^4c^3 \\ &+570a^4b^4c^2 + 180a^2b^6c^2 + 6000a^4b^2c^3 - 1800a^6b^2c + 180a^6b^2c^2 \\ &-225a^8 - 720b^4c^5 + 900a^6b^2 - 176a^8b^2 + 1200a^6c^3 + 15a^8c^2. \end{aligned}$$

Therefore, $cl(\mathfrak{B}_3) = 8$, $cl(\mathfrak{B}_4) = 10$.

Remark. It is clear that $\deg(x) = m$, $\deg(y) = m+1$, $\deg(z) = m+1$ for Bour's algebraic maximal and timelike $\mathfrak{B}_m$. □

CHAPTER 5

Discrete Linear Weingarten Surfaces and their Singularities in Riemannian and Lorentzian Spaceforms

1. Introduction

This is a preliminary report on recent work by the author on discrete linear Weingarten surfaces and their singularities in Riemannian and Lorentzian spaceforms.

Smooth 2-dimensional Legendre immersions in Lie sphere geometry project to surfaces in spaceforms that can have singularities. However, those surfaces considered together with their unit normal maps become immersions, and they are called fronts. The most typical singularities on fronts are cuspidal edges of 3/2 type. At such singularities, one of the principal curvatures will diverge (see [**66**]), and equivalently, one of the principal curvature spheres will become a point sphere. In this paper we use this behavior of the principal curvature spheres (the notion of principal curvature spheres in Lie sphere geometry is independent of the choice of projection to a 3-dimensional spaceform) to guide us in defining singular vertices on discrete Legendre immersions, with an emphasis on examining those discrete linear Weingarten surfaces that have Weierstrass type representations.

As just noted, typical singularities on smooth surfaces can be found by locating the points where at least one principal curvature blows up to infinity. However, on discrete surfaces the principal curvatures are discrete functions from the set of edges to the real numbers, and thus we can only identify the vertices at which a principal curvature changes sign. As a result, distinguishing between the points that are parabolic or flat (a parabolic point is one at which exactly one principal curvature becomes zero, and a flat point is one at which both principal curvatures become zero) and the points that are singular is not so immediate. This leads to our first goal below. Our goals are as follows:

(1) We will find and examine cases where the distinction between singular and parabolic or flat points is possible. Such cases include constant Gaussian curvature (CGC) which is nonzero, and some cases of discrete linear Weingarten surfaces for which Weierstrass type representations exist.
(2) We will confirm that the discrete Weierstrass type representations are compatible with other ways of defining discrete surfaces with specific curvature properties. In particular, they are compatible with the definitions in [**21**].
(3) Singular faces on projections of Legendre immersions are those that lie in non-spacelike planes, and we will find relationships between singular vertices and singular faces in particular cases.

2. Discrete Legendre immersions

First we recall smooth Legendre immersions Λ of 2-manifolds M^2 into the collection of null planes in $R^{4,2}$. By choosing two nonzero perpendicular vectors p, q in $R^{4,2}$ (p not null), we can project Λ to a surface $f : M^2 \to M^3$, where M^3 is the 3-dimensional spaceform defined by p, q via

$$M^3 = \{X \in R^{4,2} \,|\, (X, X) = (X, p) = 0, (X, q) = -1\} \,,$$

by taking $f \in \Lambda$ such that $(f, p) = 0$ and $(f, q) = -1$. Let n denote the unit normal to f in M^3, i.e. $n \in \Lambda$ and $(n, q) = 0$ and $(n, p) = -1$. The sections of $\Lambda = \text{span}\{f, n\}$ represent the sphere congruences of f, and then f, resp. n, is the point sphere, resp. tangent geodesic plane, congruence. Let s_α for $\alpha = 1, 2$ be sections of Λ that represent the principal curvature sphere congruences, which can be defined by $s_\alpha = \kappa_\alpha f + n$ using the principle curvatures κ_α of f, or equivalently by the directional derivative conditions that $D_{\vec{v}_\alpha} s_\alpha \in \Lambda$ for some tangent vector fields $\vec{v}_\alpha$ of f.

For a smooth map Λ to be a Legendre immersion, immersion and contact conditions must be satisfied. For a discrete Legendre map Λ as in Definition 24 below, discretized versions of immersion and contact conditions are again needed. We also assume the existence of "discrete curvature line coordinates", that is, we require that the four vertices of each quadrilateral be concircular, which is called a *principal net*. In this way, the properties of smooth Legendre immersions motivate the following definition of discrete Legendre immersions:

Definition 24. [**21**] A map

$$\Lambda : \mathbb{Z}^2 \text{ (or some subdomain of } \mathbb{Z}^2) \;\to \{\text{null planes in } R^{4,2}\}$$

is a *discrete Legendre immersion* if, for any quadrilateral, with vertices i, j, k, ℓ ordered counterclockwise about the quadrilateral and with i in the lower left corner in $\mathbb{Z}^2$,

(1) (principal net condition) $\dim(\text{span}\{f_i, f_j, f_k, f_\ell\}) = 3$,
(2) (first immersion condition) There exist p, q such that the difference of any two of f_i, f_j, f_k, f_ℓ is non-null,
(3) (second immersion condition) For some p, q as in item (2) above, $f_k - f_i$ and $f_\ell - f_j$ are not parallel,
(4) (contact condition) $\Lambda_i \cap \Lambda_j \neq \{\vec{0}\}$, $\Lambda_i \cap \Lambda_\ell \neq \{\vec{0}\}$.

Remark. By item (1) in Definition 24, $(f_*, q) = -1$ implies that f_i, f_j, f_k, f_ℓ all lie in some 2-dimensional plane. By item (3), it follows that any two or three vertices amongst f_i, f_j, f_k, f_ℓ span a 2 or 3 dimensional subspace of $R^{4,2}$, respectively, with nondegenerate induced metric $(+, -)$ or $(+, +, -)$. □

3. FPS vertices of projections of discrete Legendre immersions

Generically, a smooth surface (section) $f \in \Lambda$ will have a singularity when one of the principal curvature spheres s_α becomes a point sphere, i.e. when $s_\alpha \perp p$ for

$\alpha = 1$ or 2. Also, where f does not have a singularity, it will have a parabolic or flat point if one of the s_α becomes a tangent geodesic plane, i.e. $s_\alpha \perp q$.

In the case of discrete Legendre immersions, the domain becomes $\mathbb{Z}^2$, or some subdomain of $\mathbb{Z}^2$, rather than M^2. We define the curvature spheres as those spheres represented by nonzero vectors

$$s_1 \in \Lambda_i \cap \Lambda_j \neq \{\vec{0}\} \quad \text{and} \quad s_2 \in \Lambda_i \cap \Lambda_\ell \neq \{\vec{0}\} \ .$$

Thus we have spheres in M^3, associated to edges, that lie in both of the sphere pencils defined at the two endpoints of the edges. In particular the normal geodesics (i.e. the geodesics through the vertices and perpendicular to the spheres in the sphere pencils) emanating from the adjacent vertices, when they do intersect, will intersect at equal distances from the two vertices.

Thus, $s_1 = s_{(m,n),(,m+1,n)}$ will be defined on horizontal edges from vertex $i = (m,n) \in \mathbb{Z}^2$ to vertex $j = (m+1,n) \in \mathbb{Z}^2$ as the representative (for a sphere) that is common to both the null planes $\Lambda(i)$ and $\Lambda(j)$, and $s_2 = s_{(m,n),(m,,n+1)}$ is defined analogously on vertical edges from i to $\ell = (m,n+1)$. We then define the principal curvatures by

$$\kappa_{ij} = \frac{(s_1,q)}{(s_1,p)} \ , \quad \kappa_{i\ell} = \frac{(s_2,q)}{(s_2,p)} \ . \tag{80}$$

As the principal curvature spheres s_α and principal curvatures $\kappa_{\alpha\beta}$ are defined on edges, not vertices, we lose the ability to look for points in the domain where s_α is exactly perpendicular to p or q. Thus we reformulate the conditions for singularities and parabolic or flat points by finding vertices in the domain at which the $\kappa_{\alpha\beta}$ change sign in at least one direction:

Definition 25. For a Λ as in Definition 24, together with a choice of spaceform determined by choosing p and q, we say that (m,n) is a *flat-or-parabolic-or-singular (FPS) vertex* if

$$\kappa_{(m-1,n),(m,n)} \cdot \kappa_{(m,n),(m+1,n)} \leq 0 \quad \text{or} \quad \kappa_{(m,n-1),(m,n)} \cdot \kappa_{(m,n),(m,n+1)} \leq 0 \ .$$

When both p and q are non-null, switching p and q will result in the projected surface f changing to its Gauss map n. In the smooth case, generically, a parabolic or flat point on one of the two surfaces corresponds to a singular point on the other, thus it is not surprising that these notions appear together in the above definition of FPS vertices.

In certain special cases, we can distinguish the singular points from the parabolic or flat points, as we will see in upcoming sections.

As another approach for considering singularities on discrete surfaces, motivated by the work [**70**], we define singular faces as follows:

Definition 26. For a Λ as in Definition 24, together with a choice of spaceform determined by choosing p and q, we say that a face with vertices f_i, f_j, f_k, f_ℓ is *singular* if those four vertices lie in a non-spacelike plane.

We will later examine criteria for singular faces, and also their relationships with singular vertices in some special cases.

4. Smooth linear Weingarten surfaces of Bryant and Bianchi type

We include this section to motivate the discretizations in the next section.

In $\mathbb{R}^{3,1}$ with metric $(-,+,+,+)$, with points $(x_0,x_1,x_2,x_3)\in\mathbb{R}^{3,1}$ described in matrix form as

$$X=\begin{pmatrix} x_0+x_3 & x_1-ix_2\\ x_1+ix_2 & x_0-x_3\end{pmatrix}\ ,$$

the metric is

$$\langle X,Y\rangle=\tfrac{-1}{2}\left(X\sigma_2 Y^t\sigma_2\right)\ ,\quad \sigma_2:=\begin{pmatrix}0 & -i\\ i & 0\end{pmatrix}\ .$$

Solving

$$dE=E\begin{pmatrix}0 & g'\\ (g')^{-1} & 0\end{pmatrix}dz$$

for $E\in \mathrm{SL}_2(\mathbb{C})$, where g is a holomorphic function with nonzero derivative $g'=\partial_z g$ on a Riemann surface with local coordinate z, we take, for any constant $t\in\mathbb{R}$,

$$L=\begin{pmatrix}0 & \sqrt{1+tg\bar g}\\ \frac{-1}{\sqrt{1+tg\bar g}} & \frac{-t\bar g}{\sqrt{1+tg\bar g}}\end{pmatrix}\ ,\quad \hat f=EL\overline{EL}^t\ ,\quad \hat n=EL\begin{pmatrix}1 & 0\\ 0 & -1\end{pmatrix}\overline{EL}^t\ , \tag{81}$$

making the genericity assumption

$$\mathcal{T}:=1+tg\bar g\neq 0\ .$$

The choice of sign of $\sqrt{\mathcal{T}}$ will not affect $\hat f$, $\hat n$.

Then $\hat f$ is a linear Weingarten surface of Bryant type (following the notation in [**28**] and [**45**], and we abbreviate this to "BrLW surface") in $\mathbb{H}^3$ with normal $\hat n$ in $\mathbb{S}^{2,1}$, since $\langle d\hat f,\hat n\rangle=0$, and $\hat n$ is called a linear Weingarten surface of Bianchi type (following the notation in [**7**], abbreviated to "BiLW surface"). The surface $\hat f$ satisfies

$$2t(H_{\hat f}-1)+(1-t)(K_{ext,\hat f}-1)=0\ , \tag{82}$$

where H_* and $K_{ext,*}$ are the mean curvature and extrinsic Gaussian curvature of $*=\hat f$ or $\hat n$, respectively.

The three fundamental forms of $\hat f$ become, with $h:=|g'|^{-2}\mathcal{T}^{-2}$,

$$I=\langle d\hat f,d\hat f\rangle=h\left\{((1-t)|g'|^2+\mathcal{T}^2)^2dx^2+((1-t)|g'|^2-\mathcal{T}^2)^2dy^2\right\}\ ,$$

$$II=-\langle d\hat f,d\hat n\rangle=-h\left\{(|g'|^4-(t|g'|^2-\mathcal{T}^2)^2)dx^2+(|g'|^4-(t|g'|^2+\mathcal{T}^2)^2)dy^2\right\}\ ,$$

$$III=\langle d\hat n,d\hat n\rangle=h\left\{((1+t)|g'|^2-\mathcal{T}^2)^2dx^2+((1+t)|g'|^2+\mathcal{T}^2)^2dy^2\right\}\ .$$

The principal curvatures of $\hat f$ and $\hat n$ are then

$$k_{1,\hat f}=-\frac{(1+t)|g'|^2-\mathcal{T}^2}{(1-t)|g'|^2+\mathcal{T}^2}\ ,\quad k_{2,\hat f}=-\frac{(1+t)|g'|^2+\mathcal{T}^2}{(1-t)|g'|^2-\mathcal{T}^2}\ ,\quad k_{1,\hat n}=\frac{1}{k_{1,\hat f}}\ ,\quad k_{2,\hat n}=\frac{1}{k_{2,\hat f}}\ .$$

and

$$H_{\hat f}=\frac{H_{\hat n}}{K_{ext,\hat n}}\quad\text{and}\quad K_{ext,\hat f}=\frac{1}{K_{ext,\hat n}}\ ,$$

and so $\hat{n}$ satisfies

$$2t(H_{\hat{n}} - 1) - (1+t)(K_{ext,\hat{n}} - 1) = 0 \,. \tag{83}$$

In fact, all BrLW and BiLW surfaces without umbilics (g' would be zero at umbilics) can be constructed this way, using holomorphic functions g.

Thus sufficient conditions for $\hat{f}$ and $\hat{n}$, respectively, to have singularities are

$$\mathcal{T}^4 = (1-t)^2|g'|^4 \,, \quad \mathcal{T}^4 = (1+t)^2|g'|^4 \,,$$

respectively. For certain special values of t these conditions simplify:

$$\begin{aligned} \hat{f} \text{ with } t = 0: &\quad |g'| = 1 \,, \\ \hat{n} \text{ with } t = 0: &\quad |g'| = 1 \,, \\ \hat{f} \text{ with } t = 1: &\quad \text{null condition} \,, \\ \hat{n} \text{ with } t = -1: &\quad |g| = 1 \,. \end{aligned}$$

We can lift to Lie sphere geometry with (see [**62**], for example)

$$f = (\hat{f}, 1, 0)^t \,, \quad n = (\hat{n}, 0, 1)^t$$

determined by

$$p = (0,0,0,0,0,1)^t \,, \quad q = (0,0,0,0,-1,0)^t \,.$$

For a BrLW surface $\hat{f} \in \mathbb{H}^3$ with BiLW normal $\hat{n} \in \mathbb{S}^{2,1}$, we can define the Legendre lift $\Lambda = \operatorname{span}\{s_+, s_-\}$ for

$$s_\pm = b_\pm f + n \quad \text{with} \quad b_+ = 1 \quad \text{and} \quad b_- = \frac{t+1}{t-1} \,,$$

and then $s_\pm$ have constant conserved quantities in the sense that $(s_\pm, q_\pm) = 0$, equivalently (see [**20**], [**62**])

$$\Gamma^\pm q_\pm = 0 \quad \text{for} \quad q_+ = (0,0,0,0,1,1)^t \,, \quad q_- = (0,0,0,0,t-1,t+1)^t \,.$$

Furthermore, because $b_\pm$ are constant and because

$$\frac{\sqrt{g_{11}}}{\sqrt{g_{22}}} = \frac{1-\kappa_2}{1-\kappa_1} = \frac{-t-1+(t-1)\kappa_2}{t+1-(t-1)\kappa_1} \,,$$

all of Equations (4.5) and (4.10) and (4.11) in [**62**] hold, and so $s_\pm$ are isothermic sphere congruences. Thus Λ is an Ω surface with a pair of constant conserved quantities.

Conversely, if we start with an Ω surface with constant conserved quantities $q_\pm$ for isothermic sphere congruences $s_\pm = b_\pm f + n$ respectively, we can reverse the above arguments to see that we obtain a BrLW surface $\hat{f}$ with BiLW normal $\hat{n}$ in the spaceforms created from p and q as above.

We conclude the following lemma, which as already understood in [**20**]:

Lemma 9. [**20**] All smooth BrLW and BiLW surfaces are projections of Ω surfaces with constant conserved quantities, at least one of which is lightlike. Conversely, for any smooth Ω surface with constant quantities $q_\pm$, at least one of which is lightlike, its projections f and n given by choosing $p, q \in \operatorname{span}\{q_\pm\}$ are BrLW and BiLW surfaces, respectively.

The same result holds for general linear Weingarten $\hat{f}$ and $\hat{n}$, but without the condition that at least one of the $q_\pm$ is lightlike, again see [**20**]. However, it is only the cases given in Lemma 9 that we will consider later.

5. Discrete BrLW and BiLW surfaces

First we give the representation for these surfaces using the more symmetric form of the base equation as in Section 6 of [**38**]. Let g be a discrete holomorphic function as defined in [**17**] (Chapter 8, called "circle pattern" there), [**38**], for example, with cross ratio factorizing functions α_{ij}, $\alpha_{i\ell}$. We assume the discrete version of $g' \neq 0$, i.e. $dg_{ij} := g_j - g_i \neq 0$ and $dg_{i\ell} \neq 0$ for all quadrilaterals. We again make the genericity assumption

$$1 + tg_i\overline{g_i} \neq 0$$

for all vertices i, for the chosen constant $t \in \mathbb{R}$. Take $\lambda \in \mathbb{R}$ to be any non-zero constant. Solving

$$E_i^{-1}E_j = \frac{1}{\sqrt{1-\lambda\alpha_{ij}}}\begin{pmatrix} 1 & dg_{ij} \\ \frac{\lambda\alpha_{ij}}{dg_{ij}} & 1 \end{pmatrix}$$

and the similar equation with j replaced by ℓ, for $E \in \mathrm{SL}_2\mathbb{C}$, and defining

$$L_i = \begin{pmatrix} 0 & \sqrt{1+tg_i\overline{g_i}} \\ \frac{-1}{\sqrt{1+tg_i\overline{g_i}}} & \frac{-t\overline{g_i}}{\sqrt{1+tg_i\overline{g_i}}} \end{pmatrix} ,$$

the surface $\hat{f}$ and its normal $\hat{n}$

$$\hat{f}_i = E_iL_i\overline{E_iL_i}^t , \quad \hat{n}_i = E_iL_i\begin{pmatrix} 1 & 0 \\ 0 & -1 \end{pmatrix}\overline{E_iL_i}^t$$

are called discrete BrLW surfaces and BiLW surfaces in $\mathbb{H}^3$ and $\mathbb{S}^{2,1}$, respectively. Direct computations confirm the following lemma:

Lemma 10. For any choice of t, we have the following:

- $d\hat{f}_{ij} || d\hat{n}_{ij}$, $d\hat{f}_{i\ell} || d\hat{n}_{i\ell}$ in $\mathbb{R}^{3,1}$ for all edges ij, $i\ell$.
- $1 + t|g_i|^2 > 0$, resp. $1 + t|g_i|^2 < 0$, if and only if $\hat{f}_i$ lies in the upper, resp. lower, sheet of $\mathbb{H}^3$.
- $\hat{f}_i$, $\hat{f}_j$, $\hat{f}_k$, $\hat{f}_\ell$ lie in a plane in $\mathbb{R}^{3,1}$, and thus are concircular in $\mathbb{H}^3$.

Corollary 2. For any choice of t, the parallel surfaces $\cosh\theta \cdot \hat{f} + \sinh\theta \cdot \hat{n}$ are concircular for all $\theta \in \mathbb{R}$.

Proof. $d\hat{f}_{i*} || d\hat{n}_{i*}$ and the fact that f and n lie in parallel planes imply that $\cosh\theta \cdot f + \sinh\theta \cdot n$ also lies in a parallel plane, proving the corollary. □

Like in the previous section, we can lift $\hat{f}$ and $\hat{n}$ to $f, n \in \mathbb{R}^{4,2}$. This produce a discrete Legendre immersion $\Lambda = \mathrm{span}\{f, n\}$. We define

$$\mathcal{A}(f,f)_{ijk\ell} := \tfrac{1}{2}df_{ik} \wedge df_{j\ell} ,$$

and we can define real-valued functions $H = \mathcal{H}_{ijk\ell}$ and $K = \mathcal{K}_{ijk\ell}$ on faces by

$$\mathcal{A}(f,n)_{ijk\ell} := \tfrac{1}{4}\{df_{ik} \wedge dn_{j\ell} + dn_{ik} \wedge df_{j\ell}\} = -H \cdot \mathcal{A}(f,f)_{ijk\ell} , \tag{84}$$

$$\mathcal{A}(n,n)_{ijk\ell} = \tfrac{1}{2} dn_{ik} \wedge dn_{j\ell} = K \cdot \mathcal{A}(X,X)_{ijk\ell} \ . \tag{85}$$

We have the following definition:

Definition 27. [**21**] We call K and H the *Gauss* and *mean curvature* of the projection $\hat{f}$ of Λ to the spaceform given by p, q.

Proposition 12. [**21**] All discrete BLW surfaces are projections of discrete Ω surfaces with constant conserved quantities, at least one of which is lightlike. Conversely, for any discrete Ω surface with constant quantities $q_\pm$, at least one of which is lightlike, its projections f and n given by choosing $p, q \in \operatorname{span}\{q_\pm\}$ are discrete BrLW and BiLW surfaces, respectively. Furthermore, the mean and Gauss curvatures H_f and K_f of f satisfy

$$2t(H_f - 1) + (1-t)(K_f - 1) = 0 \ ,$$

and the mean and Gauss curvatures H_n and K_n of n satisfy

$$2t(H_n - 1) - (1+t)(K_n - 1) = 0 \ .$$

Lemma 11. The definition $\kappa_{i*} = \coth \theta_{i*}$ as in [**38**] is compatible with $dn_{i*} = -\kappa_{i*} df_{i*}$, and also with (80) in the case of flat surfaces in $\mathbb{H}^3$ (t=0), and furthermore

$$\kappa_{i*} = \frac{-|dg_{i*}|^2(1+t) + (1+t|g_i|^2)(1+t|g_*|^2)\lambda\alpha_{i*}}{-|dg_{i*}|^2(-1+t) + (1+t|g_i|^2)(1+t|g_*|^2)\lambda\alpha_{i*}} \ , \tag{86}$$

for $* = j, \ell$.

Proven similarly to the corresponding result for $\mathbb{R}^3$ in [**15**], we have:

Lemma 12. For all choices of spaceforms, we have

$$H = \frac{\kappa_{i\ell}\kappa_{jk} - \kappa_{ij}\kappa_{k\ell}}{\kappa_{ij} - \kappa_{i\ell} - \kappa_{jk} + \kappa_{k\ell}} \ , \quad K = \frac{\kappa_{ij}(\kappa_{jk}\kappa_{k\ell} + \kappa_{i\ell}(-\kappa_{jk} + \kappa_{k\ell})) - \kappa_{i\ell}\kappa_{jk}\kappa_{k\ell}}{\kappa_{ij} - \kappa_{i\ell} - \kappa_{jk} + \kappa_{k\ell}} \ .$$

6. Singular vertices on discrete nonzero CGC surfaces in M^3

When a smooth surface has CGC $K = \kappa_1\kappa_2 \neq 0$, then when one of the κ_α passes through zero, the other passes through infinity, and we can always call this a singular point. This is precisely what allowed for the definition of singularities of discrete flat (i.e. $K \equiv 1$) surfaces in hyperbolic 3-space $\mathbb{H}^3$ as given in [**38**]. Here we give that same definition without reliance on a Weierstrass type representation, extending it to all discrete surfaces in $\mathbb{H}^3$ with nonzero constant Gauss curvature, and also extending it to the same types of surfaces in de Sitter 3-space $\mathbb{S}^{2,1}$.

Definition 28. Consider Λ as in Definition 24, together with a choice of spaceform determined by choosing p and q, that has projection $\hat{f}$ with nonzero constant discrete Gauss curvature K_f. We say that (m,n) is a *singular vertex* of $\hat{f}$ if

$$\kappa_{(m-1,n),(m,n)} \cdot \kappa_{(m,n),(m+1,n)} \leq 0 \quad \text{or} \quad \kappa_{(m,n-1),(m,n)} \cdot \kappa_{(m,n),(m,n+1)} \leq 0 \ .$$

Lemma 13. In the Bryant type case (in $\mathbb{H}^3$ with $K \equiv 1$), Definition 28 is equivalent to the definition of singular vertices for discrete flat surfaces in $\mathbb{H}^3$ as given in [**38**].

Proof. By Lemma 11, for $t = 0$ we have

$$\kappa_{i*} = \frac{-|dg_{i*}|^2 + \lambda\alpha_{i*}}{|dg_{i*}|^2 + \lambda\alpha_{i*}} \, .$$

Let p_-, p and p_+ be three consequtive vertices in one direction in the lattice domain. We can define singularities on discrete flat surfaces in $\mathbb{H}^3$, now without referring to caustics as in [**38**], by simply using the condition

$$\frac{-|dg_{p_-p}|^2 + \lambda\alpha_{p_-p}}{|dg_{p_-p}|^2 + \lambda\alpha_{p_-p}} \cdot \frac{-|dg_{pp_+}|^2 + \lambda\alpha_{pp_+}}{|dg_{pp_+}|^2 + \lambda\alpha_{p_+p}} < 0 \, ,$$

as understood in [**38**]. □

7. Singular faces on discrete CMC 1 surfaces in $\mathbb{S}^{2,1}$

By Definition 26, we know that a quadrilateral of a discrete CMC 1 surface $\hat{n}$ in $\mathbb{S}^{2,1}$ is *singular* if it does not lie in a spacelike plane, and this mimics the notion of singular faces of discrete CMC 0 surfaces (maximal surfaces) in $\mathbb{R}^{2,1}$ [**70**]. We give a geometric condition for when a quadrilateral of $\hat{n}$ is singular, analogous to a condition in the case of discrete CMC 0 surfaces in $\mathbb{R}^{2,1}$ (again see [**70**]). We then prove a relation between FPS vertices and singular faces on discrete CMC 1 faces in $\mathbb{S}^{2,1}$, a relation that helps indicate which of the FPS vertices are actually singular. The condition for a singular face to occur is

$$(d\hat{f}_{ij}, d\hat{f}_{ij})(d\hat{f}_{i\ell}, d\hat{f}_{i\ell}) - (d\hat{f}_{ij}, d\hat{f}_{i\ell})^2 \leq 0 \, . \tag{87}$$

In the smooth CMC 1 case, when using the potential matrix

$$\begin{pmatrix} 0 & g' \\ (g')^{-1} & 0 \end{pmatrix} \, ,$$

the singularities occur exactly where $|g| = 1$. However, by a change of coordinate $z \to \sqrt{\lambda\alpha}z$ that potential matrix becomes, analogous to the discrete case,

$$\begin{pmatrix} 0 & g' \\ \lambda\alpha(g')^{-1} & 0 \end{pmatrix} \, ,$$

so again the singularities still occur exactly where $|g| = 1$. The next proposition and theorem are the corresponding condition in the discrete case to $|g| = 1$, and can be proven by computationally spelling out Equation (87). We define

$$h_1 = (1 - |g_j|^2)|dg_{i\ell}|^2(1 - \lambda\alpha_{ij}) \, ,$$

$$h_2 = (1 - |g_\ell|^2)|dg_{ij}|^2(1 - \lambda\alpha_{i\ell}) \, ,$$

$$h_3 = (1 - |g_i|^2)|dg_{j\ell}|^2 \, .$$

Proposition 13. A face of a discrete CMC 1 surface $\hat{n}$ in $\mathbb{S}^{2,1}$ is singular if and only if

$$h_1^2 + h_2^2 + h_3^2 - (h_2 - h_1)^2 - (h_3 - h_1)^2 - (h_3 - h_2)^2 \geq 0 \, .$$

THEOREM 15. A quadrilateral of $\hat{n}$ as in Proposition 13 is singular for all λ sufficiently close to zero if and only if the corresponding circumcircle of g intersects $\mathbb{S}^1$ transversally.

COROLLARY 3. Let p_-, p and p_+ be three consequtive vertices in one direction in the lattice domain of a CMC 1 surface in $\mathbb{S}^{2,1}$, with corresponding values g_-, g and g_+ for the discrete holomorphic function in the Weierstrass type representation. Then $\kappa_{p_-p} \cdot \kappa_{pp_+} < 0$ for all λ sufficient close to zero if and only if exactly one of $|g_-|^2$ and $|g_+|^2$ has value less than 1 and the other has value greater than 1.

Proof. Because the surface is CMC 1 in $\mathbb{S}^{2,1}$, we have $t = -1$. Then Equation (86) implies the result. □

This corollary tells us that we will find FPS vertices roughly where g (discretely) crosses $\mathbb{S}^1$. Because of Proposition 13, philosophically, we can now regard these points as singular vertices and not flat points. The following rigorous statement is immediate:

COROLLARY 4. For all λ sufficiently close to zero, the pair of faces adjacent to the edge p_-p are singular, or the pair of faces adjacent to the edge pp_+ are singular, including the possibility that all four of those faces are singular.

The converse of this corollary does not hold, that is, it is possible to have two edge-adjacent singular faces (for all λ sufficiently close to 0) so that their two common vertices are non-singular for all λ sufficiently close to 0.

Bibliography

[1] R. Aiyama, K. Akutagawa, Kenmotsu-Bryant type representation formulas for constant mean curvature surfaces in $\mathbb{H}^3(-c^2)$ and $\mathbb{S}^3_1(c^2)$, Ann. Global Anal. Geom. 17, 1 (1998), 49-75.

[2] R. Aiyama and K. Akutagawa, Kenmotsu-Bryant type representation formula for constant mean curvature spacelike surfaces in $\mathbb{H}^3_1(-c^2)$, Diff. Geom. Appl. 9 (1998), 251–272.

[3] R. Aiyama and K. Akutagawa, Kenmotsu type representation formula for spacelike surfaces in the de Sitter 3-space, Tsukuba J. Math. 24 (2000), 189–196.

[4] R. Aiyama and K. Akutagawa, Kenmotsu type representation formula for surfaces with prescribed mean curvature in the hyperbolic 3-space, J. Math. Soc. Japan 52 (2000), 877–898.

[5] R. Aiyama and K. Akutagawa, Kenmotsu type representation formula for surfaces with prescribed mean curvature in the 3-sphere, Tohoku Math. J. 52 (2000), 95–105.

[6] K. Akutagawa and S. Nishikawa, The Gauss map and spacelike surfaces with prescribed mean curvature in Minkowski 3-space, Tohoku Math. J. 42, (1990), 67-82.

[7] J. A. Aledo and J. M. Espinar, A conformal representation for linear Weingarten surfaces in the de Sitter space, Journal of geom. and phys., 57 (2007), 16691677.

[8] E. Bour, Théorie de la déformation des surfaces, Journal de l'Êcole Imperiale Polytechnique, 22, Cahier 39 (1862), 1-148.

[9] A. I. Bobenko, Constant mean curvature surfaces and integrable equations, Russian Math. Surveys 46:4, 145 (1991).

[10] A. I. Bobenko, Discrete conformal maps and surfaces, Symmetry and integrability of difference equations, Cambridge Univ. Press, London Math. Soc. Lect. Note Series 255 (1999), 97-108.

[11] A. I. Bobenko, Surfaces in terms of 2 by 2 matrices. Old and new integrable cases, Harmonic maps and integrable systems, 83127, Aspects Math., E23, Vieweg, Braunschweig, 1994.

[12] A.I. Bobenko, U. Pinkall, Discrete Surfaces with Constant Negative Gaussian Curvature and the Hirota Equation, J. Differ. Geom. 43 (1996), 527-611,

[13] A. I. Bobenko and U. Pinkall, Discrete isothermic surfaces, J. Reine Angew. Math., 475 (1996), 187-208.

[14] A. I. Bobenko and U. Pinkall, Discretization of surfaces and integrable systems, Oxford Lecture Ser. Math. Appl., 16. Oxford Univ. Press (1998). 3-58.

[15] A. I. Bobenko, H. Pottmann, and J. Wallner, A curvature theory for discrete surfaces based on mesh parallelity, Math. Annalen 348 (2010), 1-24.

[16] R. Bryant, Surfaces of mean curvature one in hyperbolic space, Astérisque 154-155 (1987), 321-347.

[17] A. I. Bobenko and Y. Suris, Discrete differential geometry, integrable structure, Graduate Textbooks in Mathematics 98, A.M.S., 2008.

[18] A.I. Bobenko, Y. Suris, Discrete Koenigs nets and discrete isothermic surfaces, Internat. Math. Research Notices (2009), 1976-2012.

[19] F. E. Burstall, U. Hertrich-Jeromin and W. Rossman, Lie geometry of flat fronts in hyperbolic space, C. R. Acad. Sci. Paris, Ser. I 348 (2010), 661-664.

[20] F. E. Burstall, U. Hertrich-Jeromin and W. Rossman, Lie geometry of linear Weingarten surfaces, C. R. Acad. Sci. Paris, Ser. I 350 (2012), 413-416.

[21] F. E. Burstall, U. Hertrich-Jeromin and W. Rossman, Discrete linear Weingarten surfaces, submitted.

[22] F. E. Burstall, U. Hertrich-Jeromin, W. Rossman and S. Santos, Discrete special isothermic surfaces, to appear in Geometriae Dedicata.
[23] F. E. Burstall, U. Hertrich-Jeromin, W. Rossman and S. Santos, Discrete surfaces of constant mean curvature, RIMS Kokyuroku, 1880 (2013), 133-179.
[24] J. Dorfmeister, F. Pedit and H. Wu, Weierstrass type representation of harmonic maps into symmetric spaces, Comm. Anal. Geom. **6(4)** (1998), 633-668.
[25] S. Fujimori, Spacelike CMC 1 surfaces with elliptic ends in de Sitter 3-Space, Hokkaido Math. J. 35 (2006), 289-320.
[26] S. Fujimori, W. Rossman, M. Umehara, K. Yamada, S.D. Yang, Spacelike mean curvature one surfaces in de Sitter 3-space, Comm. Anal. Geom. 17, 3 (2009), 383-427.
[27] S. Fujimori, K. Saji, M. Umehara, K. Yamada, Singularities of maximal surfaces, Math. Z. 259 (2008), 827-848.
[28] J. A. Gálvez, A. Mártinez and F. Mìlan, Complete linear Weingarten surfaces of Bryant type, a Plateau problem at infinity, Trans. A.M.S. 356 (2004), 3405-3428.
[29] J. A. Gálvez, A. Mártinez and F. Mìlan, Flat surfaces in hyperbolic 3-space, Math. Ann. 316 (2000), 419-435.
[30] A. Gray, Modern differential geometry of curves and surfaces with Mathematica. Second edition, CRC Press, Boca Raton, FL, 1998.
[31] E. Güler, Bour ' s spacelike maximal and timelike minimal surfaces in the three dimensional Lorentz-Minkowski space, submitted.
[32] E. Güler, S. Konnai and M. Yasumoto, Bour surface companions in non-Euclidean space forms, submitted.
[33] U. Hertrich-Jeromin, Transformations of discrete isothermic nets and discrete cmc-1 surfaces in hyperbolic space, Manusc. Math. 102 (2000), 465-486.
[34] U. Hertrich-Jeromin, T. Hoffmann and U. Pinkall, A discrete version of the Darboux transform for isothermic surfaces, Oxford Lecture Ser. Math. Appl., 16. Oxford Univ. Press (1998). 59-81.
[35] T. Hoffmann, Discrete cmc surfaces and discrete holomorphic maps, Discrete integrable geometry and physics (Vienna, 1996), 83-96, Oxford Lecture Ser. Math. Appl., 16, Oxford Univ. Press, New York, 1999.
[36] T. Hoffmann, Discrete curves and surfaces, doctoral thesis, TU Berlin (2000).
[37] T. Hoffmann, Discrete differential geometry of curves and surfaces, MI Lecture Note 18, 2009.
[38] T. Hoffmann, W. Rossman, T. Sasaki and M. Yoshida, Discrete flat surfaces and linear Weingarten surfaces in hyperbolic 3-space, Trans. A.M.S. 364 (2012), 5605-5644.
[39] E. L. Ince, Ordinary Differential Equations, Dover Publications, 1956.
[40] J. Inoguchi, S. Lee, Null curves in Minkowski 3-space, Int. Electron. J. Geom., 1, 2 (2008), 40-83.
[41] S. Izumiya and K. Saji, The mandala of Legendrian dualities for pseudo-spheres in Lorentz-Minkowski space and " flat " spacelike surfaces, Journal of Singularities Volume 2 (2010), 92-127
[42] O. Karpenkov and J. Wallner. On offsets and curvatures for discrete and semidiscrete surfaces. Beitr. Algebra Geom. 55 (2014), 207-228.
[43] K. Kenmotsu, Weierstrass formula for surfaces of prescribed mean curvature, Math. Annalen 245 (1979), 89-99.
[44] M. Kokubu, W. Rossman, K. Saji, M. Umehara and K. Yamada, Singularities of flat fronts in hyperbolic space, Pacific J. Math. 221 (2005), 303-351.
[45] M. Kokubu and M. Umehara, Orientability of linear Weingarten surfaces, spacelike CMC- 1 surfaces and maximal surfaces, Math. Nachr. 284, 14- 15 (2011), 1903-1918.
[46] Y. Kinoshita and W. Rossman, Isothermicity of discrete surfaces in the Euclidean and Minkowski 3-space, OCAMI publications 3, 2010.
[47] O. Kobayashi, Maximal surfaces in the 3-dimensional Minkowski space $\mathbb{L}^3$, Tokyo J. Math. 6 (1983), 297-309.
[48] H. B. Lawson Jr., Complete minimal surfaces in $\mathbb{S}^3$, Ann. of Math. 92 (1960), 335-374.

[49] S. Lee, Spacelike surfaces of constant mean curvature ± 1 in de Sitter 3-space $\mathbb{S}^3_1(1)$, Illinois J. Math. 49 (2005), 63-98.
[50] Y. Machigashira, Piecewise truncated conical minimal surfaces and the Gauss hypergeometric functions, J. Math-for-Ind. 4A (2012) 25-33.
[51] M. Magid, Timelike surfaces in Lorentz 3-space with prescribed mean curvature and Gauss map, Hokkaido Math. J. 20, 3 (1991), 447-464.
[52] C. Mueller, Semi-discrete constant mean curvature surfaces, to appear in Math. Z.
[53] C. Mueller and J. Wallner, Oriented mixed area and discrete minimal surfaces, Discrete Comput. Geom. 43 (2010), 303-320.
[54] C. Mueller and J. Wallner, Semi-discrete isothermic surfaces, Results Math. 63 (2013), 3-4, 1395-1407.
[55] J.C.C. Nitsche, Lectures on minimal surfaces. Vol. 1. Introduction, fundamentals, geometry and basic boundary value problems, Cambridge University Press, Cambridge, 1989.
[56] Y. Ogata and M. Yasumoto, *The DPW method for discrete constant mean curvature surfaces in Riemannian spaceforms*, in preparation.
[57] R. Palais, The principle of symmetric criticality, Comm. Math. Physics 69 (1979), 19-30.
[58] B. Palmer, Spacelike constant mean curvature surfaces in pseudo-Riemannian space forms, Ann. Glob. Anal. Geom. 8, 3 (1990), 217-226.
[59] U. Pinkall and K. Polthier, Computing discrete minimal surfaces and their conjugates, Exp. Math. 2 (1993), 15-36.
[60] K. Polthier and W. Rossman, Discrete constant mean curvature surfaces and their index, J. Reine. U. Angew. Math. 549 (2002), 47-77.
[61] W. Rossman, Discrete constant mean curvature surfaces via conserved quantities, MI Lecture Note 25, (2010).
[62] W. Rossman, Isothermic surfaces in Möbius and Lie sphere geometries, Rokko Lec. Series Math. 22 (2014), 1–138.
[63] W. Rossman and M. Yasumoto, Discrete linear Weingarten surfaces and their singularities in Riemannian and Lorentzian spaceforms, in preparation.
[64] W. Rossman and M. Yasumoto, Weierstrass representation for semi-discrete minimal surfaces, and comparison of various discretized catenoids, J. Math-for-Ind. 4B (2012) 109-118.
[65] H.A. Schwarz, Miscellen aus dem gebiete der minimalflächen, Journal de Crelle, vol. 80, 1875, (published also in Gesammelte Mathematische Abhandlungen).
[66] K. Teramoto, Parallel and dual surfaces of cuspidal edges, preprint.
[67] M. Umehara, K. Yamada, Complete surfaces of constant mean curvature 1 in the hyperbolic 3-space, Annals of Math. 137 (1993), 611638.
[68] M. Umehara, K. Yamada, A duality on CMC-1 surfaces in hyperbolic space, and a hyperbolic analogue of the Osserman ineqality, Tsukuba J. Math. 21 (1997), 229-237.
[69] M. Umehara, K. Yamada, Maximal surfaces with singularities in Minkowski space, Hokkaido Math. J. 35 (2006), 13-40.
[70] M. Yasumoto, Discrete maximal surfaces with singularities in Minkowski space, submitted.
[71] M. Yasumoto, Semi-discrete maximal surfaces with singularities in Minkowski space, submitted.
[72] J. Wallner, On the semidiscrete differential geometry of A-surfaces and K-surfaces. J. Geometry 103 (2012), 161-176.
[73] J.K. Whittemore, Minimal surfaces applicable to surfaces of revolution, Ann. of Math. (2) 19, 1 (1917), 1-20.

APPENDIX A

Discrete constant mean curvature surfaces in Riemannian space forms

We apply the discrete analogue of the DPW method, which is a generalized Weierstrass representation, to Riemannian spaceforms (i.e. the Euclidean 3-space $\mathbb{R}^3$, spherical 3-space $\mathbb{S}^3$ and hyperbolic 3-space $\mathbb{H}^3$.) See [**56**].

Here we define some notations related to the fundamental theory of discrete differential geometry, as in [**13**], [**14**], [**23**], [**33**], [**35**], [**36**]. To define discrete constant mean curvature (CMC) surfaces, we need to use the cross-ratio of a quadrilateral.

DEFINITION 29 ([**23**], [**33**]). Let X_1, X_2, X_3 and X_4 be in $su_2 \approx \mathbb{R}^3$ ($\mathrm{SU}_2 \approx \mathbb{S}^3$ or $\left\{F\bar{F}^t \,|F \in \mathrm{SL}_2(\mathbb{C})\right\} \approx \mathbb{H}^3$). Then

$$\mathrm{cr}(X_1, X_2, X_3, X_4) := (X_1 - X_2)(X_2 - X_3)^{-1}(X_3 - X_4)(X_4 - X_1)^{-1}$$

is called the *cross-ratio* of X_1, X_2, X_3 and X_4.

Remark. [[**23**], [**33**]] The cross-ratio $\mathrm{cr}(X_1, X_2, X_3, X_4)$ is a scalar function multiple of the identity matrix if and only if the four points X_1, X_2, X_3 and X_4 lie in a circle. □

DEFINITION 30 ([**23**], [**33**]). A *discrete isothermic surface* is a map $f : \mathbb{Z}^2 \longrightarrow \mathbb{R}^3$ (resp. $\mathbb{S}^3$ and $\mathbb{H}^3$) for which all elementary quadrilaterals satisfy

$$\mathrm{cr}(f_{m,n}, f_{m+1,n}, f_{m+1,n+1}, f_{m,n+1}) = -\frac{\beta_n^2}{\alpha_m^2} I \quad \text{for all } (m,n) \in \mathbb{Z}^2,$$

where α_m, $\beta_n \in \mathbb{R}\backslash\{0\}$ are functions depending only on m or n, respectively. Then α_m, β_n are called the cross-ratio factorizing functions.

DEFINITION 31 ([**13**], [**14**], [**35**], [**36**]). $\mathcal{Z} : \mathbb{Z}^2 \longrightarrow \mathbb{C}$ is a *discrete holomorphic map* if

$$\mathrm{cr}(\mathcal{Z}_{m,n}, \mathcal{Z}_{m+1,n}, \mathcal{Z}_{m+1,n+1}, \mathcal{Z}_{m,n+1}) = -\frac{\beta_n^2}{\alpha_m^2} \quad \text{for all } (m,n) \in \mathbb{Z}^2,$$

where α_m, β_n are like in Definition 30.

DEFINITION 32 ([**13**], [**14**], [**35**], [**36**]). Let $f : \mathbb{Z}^2 \longrightarrow \mathbb{R}^3$ (resp. $\mathbb{S}^3$ and $\mathbb{H}^3$) be a discrete isothermic surface. Then the *dual surface* f^* of f is given by the following

equations:

$$f^*_{m+1,n} - f^*_{m,n} = \frac{1}{\alpha_m^2} \frac{f_{m+1,n} - f_{m,n}}{\|f_{m+1,n} - f_{m,n}\|^2},$$
$$f^*_{m,n+1} - f^*_{m,n} = -\frac{1}{\beta_m^2} \frac{f_{m,n+1} - f_{m,n}}{\|f_{m,n+1} - f_{m,n}\|^2},$$

where $\|\cdot\|^2 := \langle \cdot, \cdot \rangle$ is the norm in $\mathbb{R}^3$ (resp. $\mathbb{R}^4$ and $\mathbb{R}^{3,1}$).

Remark. The dual surface f^* of f is also a discrete isothermic surface, with the same cross-ratios as f. □

Definition 33 ([**23**], [**33**]). A discrete isothermic surface $f : \mathbb{Z}^2 \longrightarrow \mathbb{R}^3$ (resp. $\mathbb{S}^3$ and $\mathbb{H}^3$) is called a discrete CMC surface with constant mean curvature H if there is a dual surface f^* at constant squared distance $\frac{1}{H^2}$ from f, i.e.

$$\|f_{m,n} - f^*_{m,n}\|^2 = \frac{1}{H^2}.$$

The discrete Lax pair. Here we introduce the concept of the moving frame correponding to a discrete CMC surface: First we recall the twisted Lax pair for smooth surfaces $f : \Sigma \longrightarrow \mathbb{R}^3$ (resp. $\mathbb{S}^3$ and $\mathbb{H}^3$), and in order to discretize it, we will change the conformal coordinates to isothermic ones. As is well known, isothermic surfaces have real constant Hopf differentials Q. (See [**14**].) Without loss of generality, we can normalize the mean curvature $H = \frac{1}{2}$ and Hopf differential $Q = 1$, and then the Lax pair becomes

$$F_z = FU, \quad F_{\bar{z}} = FV,$$

where

$$U = \frac{1}{2} \begin{pmatrix} u_z & -\lambda^{-1} e^u \\ \lambda^{-1} e^{-u} & -u_z \end{pmatrix}, \quad V = \frac{1}{2} \begin{pmatrix} -u_{\bar{z}} & -\lambda e^{-u} \\ \lambda e^u & u_{\bar{z}} \end{pmatrix}$$

by using the metric function u in $ds_f^2 = 4e^{2u} dz d\bar{z}$. Thus, as a natural choice, we can define the *discrete Lax pair* as follows:

$$F_{m+1,n} = F_{m,n} U_{m,n}, \quad F_{m,n+1} = F_{m,n} V_{m,n}, \tag{88}$$

where

$$U_{m,n} = \begin{pmatrix} a_{m,n} & \lambda b_{m,n} + \frac{1}{\lambda b_{m,n}} \\ -\frac{\bar{b}_{m,n}}{\lambda} - \frac{\lambda}{b_{m,n}} & \bar{a}_{m,n} \end{pmatrix}, \; V_{m,n} = \begin{pmatrix} d_{m,n} & \lambda e_{m,n} + \frac{1}{\lambda e_{m,n}} \\ -\frac{\bar{e}_{m,n}}{\lambda} - \frac{\lambda}{\bar{e}_{m,n}} & \bar{d}_{m,n} \end{pmatrix}, \tag{89}$$

where $a_{m,n}, b_{m,n}, d_{m,n}, e_{m,n} \in \mathbb{C}$. Our goal is to find such $U_{m,n}$ and $V_{m,n}$ to obtain a discrete CMC surface.

As in [**24**], certain matrix splittings play an important role in the DPW method for constructing CMC surfaces in the smooth case. Here we consider the discrete version of Birkhoff splitting and SU_2-Iwasawa splitting. However, we use the projectivization of loop groups, instead of ordinary loop goups. These groups are considered, as in [**35**], [**36**].

DEFINITION 34 ([**35**], [**36**]). For $\lambda_0 \in \mathbb{R}\backslash\{\pm 1\}$ and $\lambda_1 \in i\mathbb{R}\backslash\{\pm i\}$, the set $\mathrm{P}\Lambda\mathrm{SL}_2(\mathbb{C})$, the projectivization of $\Lambda\mathrm{SL}_2(\mathbb{C})$, is defined by the following conditions: $C(\lambda) \in \mathrm{P}\Lambda\mathrm{SL}_2(\mathbb{C})$ if

(1) $C(\lambda)$ is a Laurent polynomial in λ.
(2) $C(\lambda)$ is twisted: $C(-\lambda) = \sigma_3 C(-\lambda)\sigma_3$.
(3) $\det(C(-\lambda)) = (1-\frac{\lambda_0^2}{\lambda^2})^i(1-\frac{\lambda_1^2}{\lambda^2})^j(1-\lambda_0^2\lambda^2)^k(1-\lambda_1^2\lambda^2)^l$ for some $i,j,k,l \in \mathbb{N}$.

Remark. We can identify $F \in \mathrm{P}\Lambda\mathrm{SL}_2(\mathbb{C})$ with $\tilde{F} \in \mathrm{SL}_2(\mathbb{C})$ projectively up to some scalar function $\alpha : \mathbb{S}^1 \longrightarrow \mathbb{C}$, i.e. we can write $\tilde{F} = \alpha(\lambda)F$. □

We introduce the *discrete Birkhoff splitting* in the following proposition, as in [**35**], [**36**].

PROPOSITION 14 ([**35**], [**36**]). Let $C \in \mathrm{P}\Lambda\mathrm{SL}_2(\mathbb{C})$. Then there exist matrices X, $\tilde{C} \in \mathrm{P}\Lambda\mathrm{SL}_2(\mathbb{C})$ such that

$$\begin{cases} C = X\tilde{C} \\ X(\lambda) \overset{\lambda\to\infty}{\longrightarrow} I \\ \det(\tilde{C}(\lambda)) = \frac{\det(C(\lambda))}{1-\frac{\lambda_l^2}{\lambda^2}}, \end{cases}$$

where $l = 0$ or 1.

In Proposition 14, X lies in the set corresponding to what would be the minus group, and $\tilde{C}$ lies in the set corresponding to what would be the plus group, in the smooth case. We denote these groups by $\mathrm{P}\Lambda^-\mathrm{SL}_2(\mathbb{C})$ and $\mathrm{P}\Lambda^+\mathrm{SL}_2(\mathbb{C})$.

Next we introduce the *discrete* SU_2*-Iwasawa splitting* as follows:

PROPOSITION 15 (discrete SU_2-Iwasawa splitting [**35**], [**36**]). Let $L^-_{l,m,n} \in \mathrm{P}\Lambda^-\mathrm{SL}_2(\mathbb{C})$ be of the form

$$L^-_{l,m,n}(\lambda) = \begin{pmatrix} 1 & \frac{p_{l,m,n}}{\lambda} \\ \frac{\lambda_l^2}{p_{l,m,n}\lambda} & 1 \end{pmatrix} \quad (l = 0, 1).$$

Then there exist a matrix $L_{l,m,n}(\lambda)$ of the form

$$L_{l,m,n}(\lambda) = \begin{pmatrix} a_{l,m,n} & \lambda b_{l,m,n} + \frac{1}{\lambda b_{l,m,n}} \\ -\frac{\bar{b}_{l,m,n}}{\lambda} - \frac{\lambda}{b_{l,m,n}} & \bar{a}_{l,m,n} \end{pmatrix}$$

with $\left(L^-_{l,m,n}(\lambda_l)\right)^{-1} \cdot L_{l,m,n}(\lambda_l) = \mathbf{0}$ and $\det(L_{l,m,n}(\lambda)) = \frac{1}{|\lambda_l|^2}\left(1-\frac{\lambda_l^2}{\lambda^2}\right)(1-\lambda_l^2\lambda^2)$, and this $L^-_{l,m,n}(\lambda)$ is unique up to sign.

In Proposition 15, $L_{l,m,n}(\lambda)$ lies in the set corresponding to what would be SU_2, and $(L_{l,m,n})^{-1} \cdot L^-_{l,m,n}$ lies in the set corresponding to what would be the plus group, in the smooth case. We denote these groups by $\mathrm{P}\Lambda\mathrm{SU}_2$ and $\mathrm{P}\Lambda^+\mathrm{SL}_2(\mathbb{C})$.

First we introduce the discrete DPW method for discrete CMC $H \neq 0$ surfaces in $\mathbb{R}^3$, studied in [**35**], [**36**]. After that, we give the main result here, which is a discrete analogue of the DPW method for CMC surfaces in $\mathbb{S}^3$ with any constant mean curvature H and CMC surfaces in $\mathbb{H}^3$ with $|H| > 1$, by using discrete holomorphic potentials. (See Theorem 16.)

PROPOSITION 16 ([**35**], [**36**]). Any discrete CMC surface $f : \mathbb{Z}^2 \longrightarrow \mathbb{R}^3$ can be constructed by the following Steps 1∼4:

- Step 1: Choose $\lambda_0 \in \mathbb{R}\backslash\{\pm 1\}$ and $\lambda_1 \in i\mathbb{R}\backslash\{\pm i\}$. Let $\mathcal{Z} : \mathbb{Z}^2 \longrightarrow \mathbb{C}$ be a discrete holomorphic map with $\mathrm{cr}(\mathcal{Z}_{m,n}, \mathcal{Z}_{m+1,n}, \mathcal{Z}_{m+1,n+1}, \mathcal{Z}_{m,n+1}) = \frac{\lambda_0^2}{\lambda_1^2}$ and set

$$\begin{cases} L^-_{m,n} = \begin{pmatrix} 1 & \frac{p_{m,n}}{\lambda} \\ \frac{\lambda_0^2}{\lambda p_{m,n}} & 1 \end{pmatrix} \\ M^-_{m,n} = \begin{pmatrix} 1 & \frac{q_{m,n}}{\lambda} \\ \frac{\lambda_1^2}{\lambda q_{m,n}} & 1 \end{pmatrix} \end{cases} \tag{90}$$

  for $p_{m,n} := \mathcal{Z}_{m+1,n} - \mathcal{Z}_{m,n}$ and $q_{m,n} := \mathcal{Z}_{m,n+1} - \mathcal{Z}_{m,n}$.
- Step 2: Solve

$$\begin{cases} \phi_{m+1,n} = \phi_{m,n} L^-_{m,n} \\ \phi_{m,n+1} = \phi_{m,n} M^-_{m,n} \end{cases} \tag{91}$$

  with the initial condition $\phi_{0,0} = I$.
- Step 3: Split

$$\phi_{m,n} = F_{m,n} B_{m,n} \quad (F_{m,n} \in \mathrm{P\Lambda SU}_2, B_{m,n} \in \mathrm{P\Lambda^+ SL}_2(\mathbb{C})). \tag{92}$$

- Step 4: Input $F_{m,n}$ to the Sym-Bobenko formula

$$\begin{aligned} f_{m,n} &= \mathrm{Sym}_{\mathbb{R}^3}(F_{m,n}) \\ &= \mathrm{Im}\left[\frac{1}{2}\left(\frac{-1}{2} F_{m,n} i\sigma_3 F_{m,n}^{-1} - i\lambda(\partial_\lambda F_{m,n}) F_{m,n}^{-1}\right)\right]\Big|_{\lambda=1}, \end{aligned} \tag{93}$$

  where

$$\begin{array}{ccccc} \mathrm{Im}: & \mathbb{H} & \longrightarrow & \mathrm{Im}(\mathbb{H}) \\ & \cup & & \cup \\ & \begin{pmatrix} a+ib & c+id \\ -c+id & a-ib \end{pmatrix} & \longmapsto & \begin{pmatrix} ib & c+id \\ -c+id & -ib \end{pmatrix}. \end{array}$$

THEOREM 16. Any discrete CMC surface $f : \mathbb{Z}^2 \longrightarrow \mathbb{S}^3$ (resp. $\mathbb{H}^3$) with any mean curvature H (resp. $|H| > 1$) can be constructed by the same Steps 1∼3 in Proposition 16 and the following Step 4' or 4", respectively:

- Step 4': Set $F^1_{m,n} = F_{m,n}|_{\lambda=t_1:=e^{i\gamma_1}}$ and $F^2_{m,n} = F_{m,n}|_{\lambda=t_1^{-1}}$ for $\gamma_1 \in \mathbb{R}$ and $2\gamma_1 \neq n\pi$ $(n \in \mathbb{Z})$. We define the following Sym-Bobenko type formula

$$f_{m,n} = \mathrm{Sym}_{\mathbb{S}^3}(F_{m,n}) = F^1_{m,n} \begin{pmatrix} t_1 & 0 \\ 0 & t_1^{-1} \end{pmatrix} (F^2_{m,n})^{-1}. \tag{94}$$

  Then, f is a discrete CMC $H = \cot(2\gamma_1)$ surface in $\mathbb{S}^3$.
- Step 4": Set $F^0_{m,n} = F|_{\lambda=t_0:=e^{\frac{q}{2}}}$ for $q \in \mathbb{R}$, $q \neq 0$. We define the following Sym-Bobenko type formula

$$f_{m,n} = \mathrm{Sym}_{\mathbb{H}^3}(F_{m,n}) = \Pi\left[F^0_{m,n} \begin{pmatrix} t_0 & 0 \\ 0 & t_0^{-1} \end{pmatrix} \overline{F^0_{m,n}}^t\right], \tag{95}$$

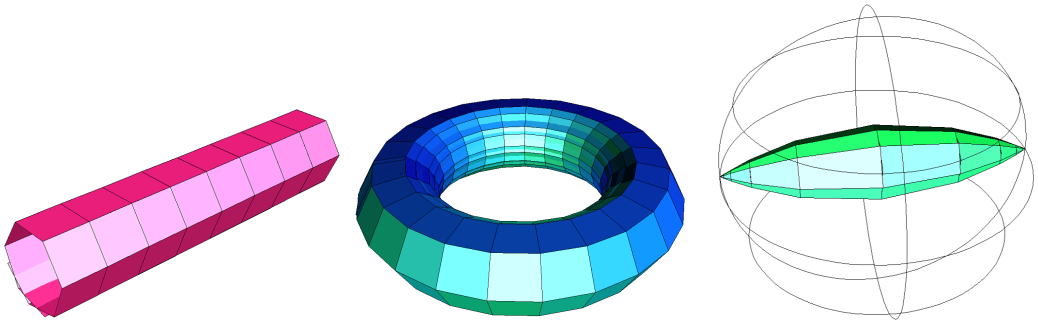

FIGURE 1. Cylinders in $\mathbb{R}^3$, $\mathbb{S}^3$ and $\mathbb{H}^3$ (left to right).

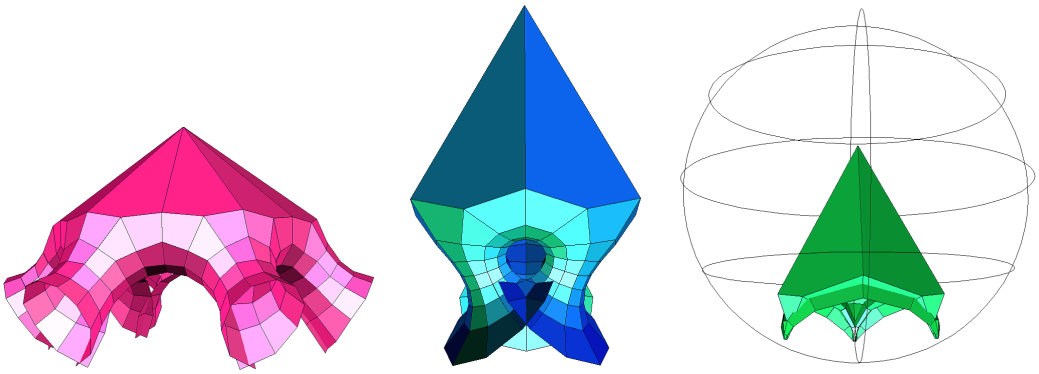

FIGURE 2. Smyth surfaces in $\mathbb{R}^3$, $\mathbb{S}^3$ and $\mathbb{H}^3$ (left to right).

where

$$\begin{array}{rccc} \Pi: & \mathrm{PSL}_2(\mathbb{C}) & \longrightarrow & \mathrm{SL}_2(\mathbb{C}) \\ & \cup & & \cup \\ & X & \longmapsto & \frac{1}{\sqrt{\det(X)}} X. \end{array}$$

Then, f is a discrete CMC $H = \coth(-q)$ surface in $\mathbb{H}^3$.

Finally, we introduce some examples of discrete CMC surfaces in $\mathbb{R}^3$, $\mathbb{S}^3$ and $\mathbb{R}^3$, using the discrete DPW method.

EXAMPLE 9 (Round cylinders). Let $\mathcal{Z}_{m,n} = m + in$. Then we have the discrete round cylinders, as in Figure 1.

EXAMPLE 10 (Smyth surfaces). Let $\mathcal{Z}_{m,n}$ be the discrete power function with order $\frac{2}{k+2}$ for $k \in \mathbb{N}$, as in [**35**], [**36**]. Then we have the discrete $(k+2)$-legged Smyth surfaces, as in Figure 2.